

BIODEGRADABLE POLYMER - HYDROXYAPATITE NANOCOMPOSITES
FOR BONE PLATE APPLICATIONS

A THESIS SUBMITTED TO
THE GRADUATE SCHOOL OF NATURAL AND APPLIED SCIENCES
OF
MIDDLE EAST TECHNICAL UNIVERSITY

BY

ERKİN AYDIN

IN PARTIAL FULFILLMENT OF THE REQUIREMENTS
FOR
THE DEGREE OF DOCTOR OF PHILOSOPHY
IN
BIOTECHNOLOGY

JULY 2010

Approval of the thesis:

**BIODEGRADABLE POLYMER - HYDROXYAPATITE
NANOCOMPOSITES FOR BONE PLATE APPLICATIONS**

submitted by **ERKİN AYDIN** in partial fulfillment of the requirements for the degree of **Doctor of Philosophy in Biotechnology Department, Middle East Technical University** by,

Prof. Dr. Canan Özgen
Dean, Graduate School of **Natural and Applied Sciences** _____

Prof. Dr. İnci Eroğlu
Head of Department, **Biotechnology** _____

Prof. Dr. Vasif Hasırcı
Supervisor, **Biological Sciences Dept., METU** _____

Prof. Dr. Josep A. Planell
Co-Supervisor, **Materials Science and Metallurgy Dept., UPC, Spain** _____

Examining Committee Members:

Prof. Dr. Mesude İşcan
Biological Sciences Dept., METU _____

Prof. Dr. Nazmi Özer
Biochemistry Dept., Faculty of Medicine, Hacettepe Univ. _____

Prof. Dr. Vasif Hasırcı
Biological Sciences Dept., METU _____

Prof. Dr. Levent Toppare
Chemistry Dept., METU _____

Assoc. Prof. Dr. Caner Durucan
Metallurgical and Materials Engineering Dept., METU _____

Date: 15.07.2010

I hereby declare that all information in this document has been obtained and presented in accordance with academic rules and ethical conduct. I also declare that, as required by these rules and conduct, I have fully cited and referenced all material and results that are not original to this work.

Name, Last name : Erkin, Aydın

Signature :

ABSTRACT

BIODEGRADABLE POLYMER - HYDROXYAPATITE NANOCOMPOSITES FOR BONE PLATE APPLICATIONS

Aydın, Erkin

Ph.D., Department of Biotechnology

Supervisor : Prof. Dr. Vasif Hasircı

Co-Supervisor: Prof. Dr. Josep A. Planell

July 2010, 115 pages

Long bone fractures are fixed with bone plates to restrain movement of bone fragments. Fracture site must experience some pressure for proper healing. Bone plates are mostly made up of metals having 5 - 10 times higher elastic modulus than bones and most of the load is carried by them, leading to stress shielding and a bony tissue with low mineral density and strength. To avoid these problems, biodegradable polymer-based composite plates were designed and tested in this study.

Poly(L-lactide) and Poly(3-hydroxybutyrate-co-3-hydroxyvalerate) biodegradable polymer composite fibers containing hydroxyapatite (HAP) nanoparticles were produced by extrusion and spinning techniques to reinforce the polymeric bone plates. The composite fibers were expected to mimic the natural organization of bone so that HAP nanorods aligned parallel to the loading axis of bone plate. Also,

lactic acid was grafted on HAP surfaces and had a positive effect on the mechanical properties of the PLLA composites.

A 50% (w/w) HAP nanoparticle content was found to increase tensile modulus value (4.12 GPa) ca. 2.35 times compared to the pure polymeric fiber with a reduction to one third of the original UTS (to 50.4 MPa). The fibers prepared were introduced to polymeric plates with their long axes parallel. Fiber reinforced bone plates were compression tested longitudinally and up to a 4% increase in the Young's Modulus was observed. Although this increase was not high was not high probably due to the low fiber content in the final plates, this approach was found to be promising for the production of biodegradable polymeric bone plates with mechanical values closer to that of cortical bones.

Biological compatibility of fibers was validated with in vitro testing. The osteoblasts attached and spread on the fibers indicating that bone fractures fixed with these could attract of bone forming osteoblasts into defect area and help speed up healing.

Keywords: Biodegradable bone plate, stress-shielding, nanocomposite, hydroxyapatite.

ÖZ

KEMİK PLAKASI UYGULAMALARI İÇİN BİYOBOZUNUR POLİMER-HİDROKSİAPATİT NANOKOMPOZİTLERİ

Aydın, Erkin

Doktora, Biyoteknoloji Bölümü

Tez Yöneticisi : Prof. Dr. Vasıf Hasırcı

Ortak Tez Yöneticisi : Prof. Dr. Josep A. Planell

Temmuz 2010, 115 sayfa

Uzun kemik kırıklarında kırılan parçalar kemik plakası ile sabitlenir ve bunlar genellikle çeşitli metallere yapılır. Doğru bir iyileşme için kırılan bölgenin belli bir yüke maruz kalması gereklidir. Metallerin elastik modülleri kemiğe göre 5-10 kat fazladır ve bu yüzden yükün büyük bir kısmı metal plakalarca taşınır. Bu durum stres izolasyonu olarak bilinir ve kemiğin gerekli mineral yoğunluğuna ulaşmasını engelleyerek sağlığını düşürür.

Polimerik kemik plakalarının mekanik özelliklerini iyileştirmek üzere Poli(L-laktid) PLLA ve Poli(3-hidroksibutirat-co-3-hidroksivalerat) (PHBV) biyobozunur polimerlerinden hidroksiapatit (HAP) nanoparçacıkları içeren kompozit lifler ekstrüzyon ve spinning yöntemleriyle üretilmiştir. HAP nanoçubuklar normal kemik dokusundakine benzer şekilde üretim eksenine paralel olması sağlanmıştır. Ayrıca kompozit yapımında kullanılan HAP nanoparçacıklarının, PLLA'nın

monomeri olan laktik asit ile kimyasal kaplanmasının mekanik özellikleri iyileştirdiği görülmüştür.

Çalışmada ağırlıkça %50 HAP nanoparçacıkları içeren kompozit liflerin çekme modülü saf polimerden üretilenlere göre 2.35 kat daha fazla olurken (4.12 GPa) en yüksek çekme dayanımlarının (50.4 MPa) üçte bir oranında azaldığı görülmüştür. Elde edilen lifler üretilen polimerik kemik plakalarına uzun eksenleri paralel olacak şekilde gömülmüştür. Eklenen lifler miktarca az olmasına karşın, elde edilen fiber güçlendirilmiş kemik plakalarının basma modülleri %4 oranında artmıştır. Bu yaklaşımın, kemik plakalarının basma değerlerini kortikal kemik düzeyine çıkarmada umut vaad ettiği görülmüştür.

Üretilen lifler doku kültürü ortamında denenmiş ve osteoblast hücrelerine iyi bir yapışma yüzeyi sağladıkları görülmüştür. Bu durum kemik yapıcı osteoblast hücrelerinin kırık bölgesine çekilmesinde de bir avantaj yaratabilir.

Anahtar kelimeler: Biyobozunur kemik plağı, stres izolasyonu, nanokompozit, hidroksiapatit.

To my wife Aysun and my son Yağız Eray

ACKNOWLEDGEMENTS

I would like to express my gratitude to people who were with me during this work.

I would like to express my sincere gratitude to my supervisor, Prof. Dr. Vasif Hasırcı, for his understanding, support, and advices which drove my motivation not only through this thesis but in all respects of my life. I am honored to find the opportunity to work with such an excellent scientist and exceptional person.

I would like to thank all my labmates in METU – BIOMAT family who were always joyful and supportive during my time in the group and helped me one way or the other: Dr. Pınar Yılgör, Dr. Halime Kenar, Dr. Deniz Yücel, Aysel Kızıltay, Tuğba Endoğan, Hayriye Özçelik, Albana Ndreu, Beste Kınıkoğlu, Gökhan Bahçecioğlu, Birsen Demirbağ, Özge Karadaş, Sinem Kardeşler, Gizem Altay, Gözde Eke, Aysu Küçükürhan. I would like to thank Mr. Zeynel Akın for his practical solutions to my unforeseen technical needs.

My special thanks goes to Arda Büyüksungur especially for being an invaluable friend and colleague and also for his enormous help in my journey to the tissue lab.

My dear wife Aysun Cebeci Aydın always supported me with love, and her presence is very valuable to me. She always held a candle when I was lost in darkness. This thesis would not be possible without her. My deepest admiration and love belongs to my son Yağız Eray, who always experienced a busy father and showed a great patience at long days, weekends and holidays I could not be with him. He is my source of happiness and joy.

TABLE OF CONTENTS

ABSTRACT	iv
ÖZ	vi
ACKNOWLEDGEMENTS	ix
TABLE OF CONTENTS	x
LIST OF ABBREVIATIONS	xiv
CHAPTERS	
1. INTRODUCTION	1
1.1. Bone	1
1.1.1. Physical Characteristics of Bone	2
1.1.2. Mechanical Properties of Bone	4
1.1.3. Bone Healing	6
1.2. Hard Tissue Implants	7
1.2.1. Prosthetic Implants	8
1.2.2. Temporary Implants.....	9
1.2.3. Current Biomaterials in Hard Tissue Implants.....	9
1.3. Bone Plates	10
1.3.1. Metallic Bone Plates	11
1.3.1.1. A Problem Associated with Stiff Metallic Bone Plates: Stress Shielding.....	13
1.4. Polymers	14
1.4.1. Nondegradable Polymers	15

1.4.2. Biodegradable Polymers	15
1.4.2.1. Polyhydroxyacids	16
1.4.2.1.1. Degradation of Lactide and Glycolide Polymers.....	16
1.4.2.2. Polyhydroxyalkanoates.....	18
1.5. Polymer Ceramic Composites	20
1.5.1. Collagen-HAP Composites	21
1.5.2. PHBV-HAP Composites.....	23
1.5.3. Polylactide-HAP Composites.....	23
1.6. Biodegradable Implants.....	24
1.6.1. Biodegradable Polymeric Implants.....	25
1.6.1.1. Biodegradable Bone Plates for Oral and Maxillofacial Surgery.	28
1.6.1.2. Biodegradable Interference Screws.....	29
1.7. Bone Tissue Engineering.....	31
1.8. Aim and Novelty of the Study	33
2. MATERIALS AND METHODS	35
2.1. Materials.....	35
2.2. Preparation of HAP Nanocrystals	35
2.2.1. Method 1: Synthesis of HAP Nanofibers in Simulated Body Fluid ..	36
2.2.2. Method 2: Production of HAP nanorods by recrystallization	37
2.2.3. Method 3: Preparation of Nanograde Osteoapatite-like Rod Crystals	
.....	38
2.3. Grafting of HAP Surface with Lactic Acid	38
2.4. Production of Polymer – HAP Nanorod Composite Fibers	39
2.4.1. Spinnability Tests of Polymers.....	40
2.4.2. Melt Spinning of Polymers	40
2.4.3. Wet Spinning of Polymers	41

2.4.4. Extrusion of Polymers at Sub-Melting Temperatures	42
2.4.5. Mixing PLLA and HAP Nanorods for capillary rheometer extrusion	42
2.4.6. Polymer Fiber Production with Capillary Rheometer	43
2.5. Production of Fiber Reinforced PLLA Bone Plates.....	45
2.6. Mechanical Characterization	45
2.7. Microscopic Characterization	47
2.7.1. Scanning Electron Microscopy.....	47
2.7.2. Transmission Electron Microscopy	47
2.7.3. Confocal Laser Scanning Microscopy	48
2.8. Chemical Characterization	48
2.8.1. Attenuated Total Reflectance - Fourier Transform Infrared Spectrometry (ATR-FTIR) of LA Coated HAP	48
2.8.2. Elemental Analysis of LA Coated HAP	48
2.9. <i>In Situ</i> Degradation Studies	48
2.10. <i>In Vitro</i> Evaluation of Composite Fibers.....	49
2.10.1. Production of Polymeric Plates for <i>In Vitro</i> Evaluation	49
2.10.2. Isolation of Rat Mesenchymal Osteoprogenitor Cells	50
2.10.3. Seeding Rat Mesenchymal Osteoprogenitor Cells on Polymeric Plates.....	50
2.10.4. Determination of Cell Proliferation	50
2.10.5. Microscopic examination of the Bone Plates in the <i>In Vitro</i> Medium	52
3. RESULTS AND DISCUSSION	53
3.1. Synthesis of HAP Nanorods	53
3.1.1. Method 1: Synthesis of HAP Nanofibers in Simulated Body Fluid .53	
3.1.2. Method 2: Production of HAP Nanorods by Recrystallization.....	53

3.1.3. Method 3: Preparation of Nanograde Osteoapatite-Like Rods	55
3.2. Grafting of Lactic Acid on HAP Surface	59
3.3. Spinnability Tests of Polymers	62
3.4. Production of Polymer – HAP Nanorod Composite Fibers	62
3.4.1. Melt Spinning of Polymers	62
3.4.2. Wet Spinning of Polymers	63
3.4.2.1. Wet Spinning of PHBV	63
3.4.2.2. Wet Spinning of PLLA	64
3.4.2. Extrusion of Polymers at Sub-Melting Temperatures	66
3.4.3. Composite Fiber Production with Capillary Rheometer.....	70
3.4.3.1. PHBV – HAP Composite Fiber Production with Capillary Rheometer	70
3.4.3.2. PLLA – HAP Composite Fiber Production with Capillary Rheometer	72
3.4.3.3. SEM Investigation of the HAP Nanoparticles	78
3.4.3.4. SEM Investigation of the Produced PLLA-sHAP Nanocomposite Fibers.....	80
3.5. In situ degradation of PLLA – HAP composite fibers	85
3.6. Production of Fiber Reinforced PLLA Bone Plates.....	88
3.7. <i>In Vitro</i> Evaluation of the Composite Fibers	91
4. CONCLUSIONS	99
REFERENCES	102
APPENDICES	
A. CALIBRATION CURVE FOR CELL NUMBER DETERMINATION	113
CURRICULUM VITAE	114

LIST OF ABBREVIATIONS

ACL	Anterior Cruciate Ligament
ASTM	American Society for Testing and Materials
ATR-FTIR	Attenuated Total Reflectance - Fourier Transform Infrared Spectrometry
BMP	Bone Morphogenic Protein
BSA	Bovine Serum Albumin
CLSM	Confocal Laser Scanning Microscopy
DCP	Dynamic Compression Plate
DMEM	Dulbecco's Modified Eagle Medium
DMSO	Dimethyl Sulfoxide
EDS (EDX)	Energy Dispersive X-ray Spectroscopy
FCS	Fetal Calf Serum
FGF	Fibroblast Growth Factor
GPa	Gigapascal
HA	Calcined Hydroxyapatite
HAP	Hydroxyapatite
HDPE	High Density Polyethylene
LA	Lactic Acid
LA-sHAP	LA Coated Synthesized HAP Nanorod
LC-DCP	Low Contact-Dynamic Compression Plate
LDPE	Low Density Polyethylene
LLDPE	Linear Low Density Polyethylene
MPa	Megapascal
MSC	Mesenchymal Stem Cell
nmHAP	HAP nano-microrods
PBS	Phosphate Buffered Saline

PCL	Poly(ϵ -caprolactone)
PDLA	Poly(D-lactide)
PDLLA	Poly(D,L-lactide)
PE	Polyethylene
PGA	Poly(glycolide)
pHAP	Commercial Amorphous HAP
PHB	Polyhydroxybutyrate
PHBV	Poly(3-hydroxybutyrate-co-3-hydroxyvalerate)
PHEMA	Poly(2-hydroxyethyl methacrylate)
PLA	Poly(lactide)
PLGA	Poly(lactide-co-glycolide)
PLLA	Poly(L-lactide)
PMMA	Polymethylmetacrylate
PP	Polypropylene
PPF	Poly(propylene) Fumarate
PTFE	Polytetrafluoroethylene
PVC	Polyvynylchloride
SEM	Scanning Electron Microscope
sHAP	non-coated Synthesized HAP nanorod
SMF	Simulated Body Fluid
TEM	Transmission Electron Microscopy
T _g	Glass Transition Temperature
THF	Tetrahydrofuran
T _m	Temperature Melting Point
UHMWPE	Ultra High Molecular Weight Polyethylene
UTS	Ultimate Tensile Strength
VLDPE	Very Low Density Polyethylene
YM	Young's Modulus
α -TCP	α -Tricalcium Phosphate
β -TCP	β -Tricalcium Phosphate

CHAPTER 1

INTRODUCTION

1.1. Bone

Bone is a mineralized hard tissue that forms the endoskeleton of vertebrates and there are 206 bones in adult humans (Steele *et al.*, 1998). Bone is composed of two major phases: organic and inorganic. The organic phase is comprised mainly of the protein collagen while the inorganic phase is dominated by hydroxyapatite (HAP) and water (20%, 60% and 9% of total mass of bone, respectively) (Murugan and Ramakrishna, 2005). It has three distinct classes of functions: Mechanical, synthetic, and metabolic. Mechanical functions include giving the body its shape, protecting internal organs, and enabling body movement in conjunction with muscles. Production of blood cells within the marrow cavity is its synthetic function. It has important metabolic functions, too, including storage of calcium and phosphate ions, buffering the blood, and acting like an endocrine organ by secretion of osteocalcin (helps maintain blood sugar concentration by increasing insulin secretion and sensitivity of cells to insulin) and fibroblast growth factor – 23 (FGF-23 acts on kidneys to stop phosphate reabsorption).

There are two distinct structural classes of bones in the adult skeleton. Cortical (compact) bone is a dense and low porosity (5 – 10%) tissue. It occurs mostly in the shaft of long bones and is responsible for the mechanical properties of bone (Buckwalter *et al.*, 1995). Cancellous (trabecular) bone is found in the ends of long bones and is composed of a network of rod- and plate-like elements with plenty of

empty space in between (30 – 90% porosity) which is inhabited by blood vessels and bone marrow.

1.1.1. Physical Characteristics of Bone

Bone is made up of various levels of hierarchical structural organizations (Figure 1.1). These levels and structures are: (1) the macrostructure: cancellous and cortical bone, (2) the microstructure (10 to 500 μm): Haversian systems, osteons, single trabeculae, (3) the sub-microstructure (1 to 10 μm): lamellae, (4) the nanostructure (a few 100's nanometers to 1 μm): fibrillar collagen and embedded mineral, and (5) the subnanostructure: molecular structure of constituent elements, such as mineral, collagen, and non-collagenous organic proteins. This hierarchically organized structure has an irregular but optimized arrangement and orientation of the components makes bone heterogeneous and anisotropic (Rho *et al.*, 1998).

Collagen of bone is a fibrous molecule with 100 to 2000 nm length and has longitudinally aligned HAP crystals within the discrete spaces between the collagen fibrils (Figure 1.2). The HAP crystals are plate shaped with the dimensions of 3 nm x 25 nm x 50 nm (Weiner and Traub, 1992). The issue of exact orientation of HAP crystals in relation to collagen fibers is still controversial, though. Studies by Danilchenko and coworkers in 2006 who heated HAP from both synthetic and natural sources up to 500°C or 1300°C and checking the X-ray diffraction patterns support the idea that bone mineral is not a discrete aggregation of crystals, rather a continuous mineral phase with direct crystal-crystal bonding.

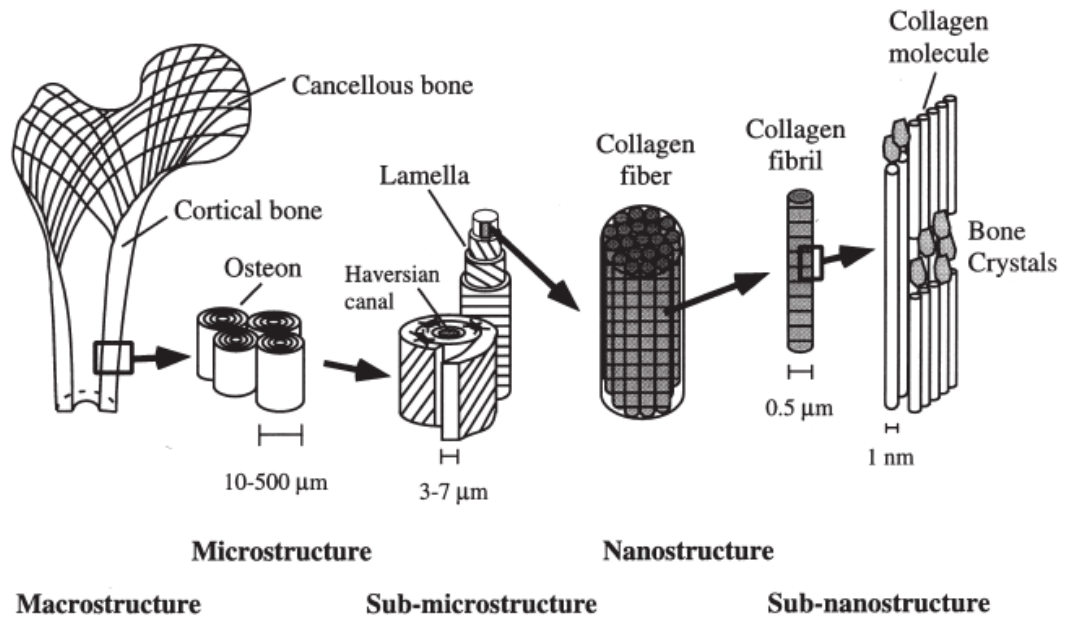


Figure 1.1. Hierarchical structural organization of bone. Macrostructure: cortical and cancellous bone, microstructure: osteons with Haversian systems, sub-microstructure: lamellae; nanostructure: collagen fiber assemblies of collagen fibrils, sub-nanostructure: bone mineral crystals (hydroxyapatite, HAP), collagen molecules, and non-collagenous proteins (Figure adapted from Rho *et al.*, 1998).

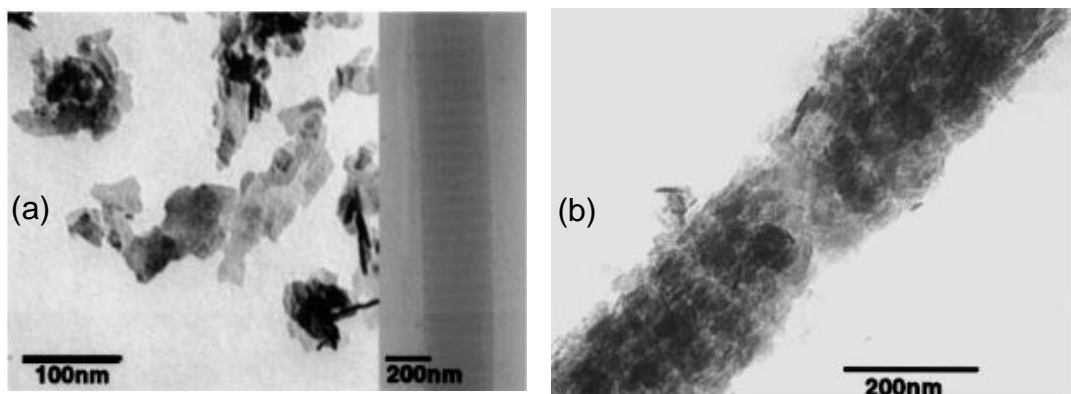


Figure 1.2. TEM micrographs of bone mineral: (a) hydroxyapatite nanoplates (left) and demineralized collagen (right); (b) mineralized collagen fiber with attached hydroxyapatite nanoplates (Adapted from Weiner and Wagner, 1998).

The basic structural unit of collagen fibrils is a tropocollagen fiber which is composed mainly of three intertwined polypeptides. Those polypeptides mainly consist of the aminoacids; glycine, proline and hydroxyproline and the polypeptides are held together by steric forces caused by proline and hydroxyproline molecules, in contrast to α -helices where the peptide bonds are held together by hydrogen bonding (Meisenberg and Simmons, 2006).

1.1.2. Mechanical Properties of Bone

In view of materials science, bone is actually a mineralized polymer composite, where collagen is the polymer component and HAP is the ceramic component. Here, HAP is in the form of plate-like crystals with several tens of nanometers length and several nanometers width. The collagen fibers are 15 μm in length and 40-70 nm in diameter. Both constituents are aligned in parallel to the long axis of the bone, giving the bone a special mechanical anisotropy.

Demineralized bone can be obtained by removal of calcium phosphate minerals by acid dissolution (eg. HAP) and is a very flexible material. Bone without collagen (obtained after pyrolysis) on the other hand is very brittle. Therefore, collagen provides elasticity and toughness to the bone while HAP gives the bone stiffness and hardness (Weiner and Wagner, 1998). The amount of energy absorbable (toughness) by bone before fracture occurs is decreased in both clinical cases of hypo- and hypermineralized bone (Currey *et al.*, 1996). As it is, bone is a mechanically ideal composite which has a high loading and bending capacity without being fragile. It responds to excessive forces by its high fracture and fatigue resistance. Therefore, in designing composites, and mimicking the nature, the best solution might be to search for bone substitutes to be mechanically, chemically, and physically compatible with bone. The mechanical properties of bone are shown in a stress – strain graph in Figure 1.3.

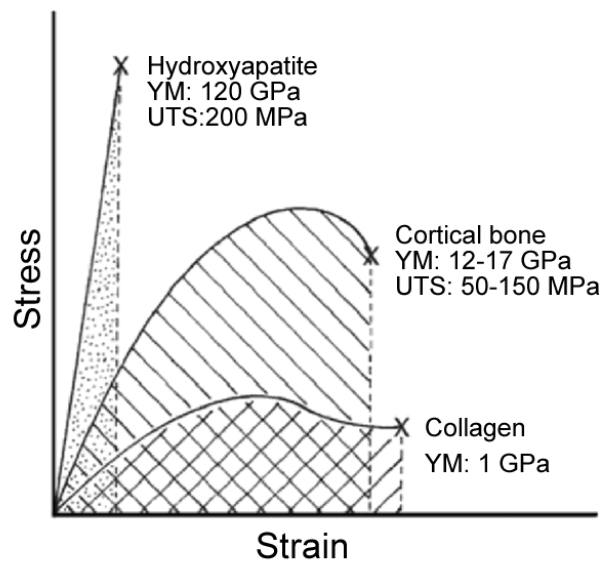


Figure 1.3. Stress – strain plot of bone (wet sample) and comparison of collagen, HAP and bone. YM: Young’s Modulus -measure of the stiffness of an isotropic elastic material, and defined as the ratio of stress over strain, UTS: Ultimate Tensile Strength - the maximum stress a material can withstand when subjected to tension.

Stiffness and hardness are the most important properties of bone for the supporting and protecting functions. The protein phase is about 3 orders of magnitudes softer than the mineral; however, stiffness of bone is not significantly reduced by the presence of protein. The presence of this protein phase actually is the reason why modulus of elasticity is much lower than a monolithic ceramic material, although bone contains 60 to 70% of this ceramic material. There are different calcified tissues in human body and their organizations and mechanical properties are distinctly different. In all of these, however, the protein matrix component, collagen and the inorganic, ceramic-like content, HAP are in common. These two components have organizations in nano-scale and therefore, bone itself is a true nanocomposite. Ji and Gao, in 2004, studied the reasons of the superior strengths of natural nanocomposites from different origins like bone and tooth, all of which

are nanocomposites of hard mineral plates or needles within a soft protein matrix, and compared them with an equivalent sized monolithic structure of the same mineral. They searched the reason why repeating subunits in these natural structures are all nano-sized. They assumed the proteins are, in practice, equivalent to cracks in a monolithic mineral crystal and deduced from their studies that there exists a critical length below which the fracture strength of a cracked crystal is the same as that of a perfect crystal. This length is roughly 30 nm, the lengths of mineral constituents of most hard tissues are either around this number or up to 10 times of this number (probably because of some other design concerns).

The liquid crystal model states that collagen fibers respond to tensile stress, applied in parallel to long axis, by tilting some of the aminoacids within the collagen structure to distort their side to side arrangements. In bone, packing of the collagen fibrils with rigid hydroxyapatite crystals, which are in contact with each other, prevents this tilting of intrafibril molecules and side to side arrangement is maintained. This explains the fact that collagen fibrils in bone are stiffer than those in unmineralized tissues, making the bone superior in mechanical properties, especially the compressive strength (Hukins, 1978).

1.1.3. Bone Healing

Bone healing is a complicated but controlled process, and is regenerative instead of simple repair. The process includes three distinct but overlapping stages; namely, inflammatory, repair, and remodeling stage (Burchardt and Enneking, 1978). A bone fracture results in immediate hemorrhage, followed by hematoma (fibrin clot) formation, and inflammation at the fracture site due to disruption of blood vessels at and nearby sites. The damaged tissues release cytokines and growth factors that induce migration of osteoprogenitor cells to the fracture site. Repair process starts with removal of blood clot, tissue and cell debris. Then fibroblasts residing in the inner layer of periostum migrate and proliferate towards the injured site, and lay down a fibrous collagen matrix. This collagen matrix is called fracture callus and happens to be at both ends of fractured bone segments,

bridging these ends. Cartilage then forms at the sites of the callus where there is not enough blood supply and calcification is started by the osteoblasts, by the action of chondroblasts (Allori et. al., 2008). Cartilage is then transformed into trabecular bone and finally into compact bone.

The early inflammation period lasts several days to weeks, followed by a repair period in which new vascularization takes place. If the fracture site is not properly fixed (stabilized), the newly formed vessels could be destroyed and the calcification of the callus may not occur, resulting in the formation of only a fibrous callus (a scar instead of a calcified tissue). Most of the original mechanical strength is regained after 3-4 months. A bone implant should, therefore, maintain its integrity during this period (Gu and Zheng, 2010). The original shape and mechanical properties of bone is regained through the remodeling stage, which may take several months to years (Kalfas, 2001). A proper remodeling is dependent on the mechanical stimulus the healing bone experiences during this period.

During the bone healing process, several growth factors, including some from the transforming growth factor-beta (TGF- β) superfamily (bone morphogenetic proteins (BMPs), insulin-like growth factor (IGF), fibroblast growth factor (FGF), platelet derived growth factor (PDGF) and vascular endothelial growth factor (VEGF)) function in a spatial and concentration dependent way to regulate different phases of the repair process (Hauschka et. al., 1986).

1.2. Hard Tissue Implants

It is very important to rigidly fix the fracture site for early vascularization and ossification to take place and the current gold standard of fixation devices are metals. Their inherent strength and stiffness easily supports the initial high mechanical requirement. Biodegradable fracture fixation implants, mostly of polymeric origin, cannot meet this criterion due to the intrinsic low mechanical properties of the polymers. This is the reason why such biodegradable implants

cannot be employed in the fixation of fractures of weight bearing bones in the body at the moment. This also is the reason for the fact that polymeric implants usually cannot be produced in compact geometries, unlike their metal counterparts, causing problems in fixation sites with restricted access or small surfaces.

Bone is a dynamic tissue in that bone formation and resorption occurs repeatedly by the action of osteoblasts and osteoclasts, respectively. The balance between these two processes is maintained by the current state of the body and the physical activity of the patient. This is also true in the healing and remodeling when there is a fracture, only here more parameters are involved; mechanical stimulus, and condition and location of the fracture site. Similarly, a too rigid fixation causes problems at the later stages of healing process. If there is not enough load transfer to the newly forming tissue due to load being borne by the implant, then new bone formation stops but bone resorption continues, leading to an osteoporotic and mechanically weak bone (Paavolainen *et al.*, 1978). Therefore, the early advantages of standard metallic fixation devices turn to be a problem in the later stages of bone healing process. At this point, strong biodegradable implants would be very well suited to satisfy the loading requirements. By tailoring the degradation rate, and thus the loss of intrinsic stiffness of the implant, polymeric materials could match the load transfer requirements of the newly forming bone.

1.2.1. Prosthetic Implants

Orthopedic implants, such as hip, spine, shoulder, and knee prostheses are mostly used in cases of loss of function due to degenerative joint diseases. The rate of orthopedic implantation surgeries is experiencing a rapid growth. For example, the number of hip replacements has shown a 33% increase from 1990 to 2000 (Webster, 2003). Ten to 15 years of service life is the average for a total hip implant (Emery *et al.*, 1997). This obviously is not enough especially for young people and is also a cause for concern when the increased life expectancy in modern countries is considered. Additionally, it is predicted that the percentage of people over 50 years of age affected by bone diseases will double by 2020

(Navarro *et al.*, 2008). These implants are meant to substitute the mechanical function of the tissues they replace and, therefore, their service life must be long, implying them not to be manufactured from biodegradable polymeric materials.

1.2.2. Temporary Implants

There are also temporary implants which augment healing of fractured bones both by keeping the fractured fragments in proper geometries and by helping to carry the body's weight which cannot be done by the fractured bone due to the physical discontinuity. Fracture fixation is a significant research area due to high number of cases encountered: 6.2 million fractures occur in the United States alone each year (Sutherland and Bostrom, 2005). Fracture fixation implants e.g. plates, intramedullary nails, pins and screws are all in this category. In order not to interfere with the normal state and functioning of the surrounding tissues continuously and for patient comfort, it is best that they are eliminated from the body soon after tissue healing is completed. This is because foreign materials, like metals or polymers, always have the potential to cause inflammation and delayed infection problems due to their degradation or corrosion products (Bayston *et al.*, 2007), and also accumulation of material wear debris at the injury site (Kim *et al.*, 1997, Mine *et al.*, 2010). Therefore, if the implant cannot be eliminated biologically, this should be done with surgery, which causes another trauma for the injury site that leads to increased risk of infection, further cost, loss of work days and patient discomfort (pain). In order to avoid these problems, sometimes surgeons allow implants to remain in the body for the lifetime of the patient if a permanent implant is not foreseen to constitute a major problem. However, even this is not an option for pediatric patients whose skeletal growth would be retarded due to the presence of fixed dimension implants.

1.2.3. Current Biomaterials in Hard Tissue Implants

Currently, bone, cartilage, and joint augmentation or replacement, and fixation of fractures of the load-bearing bones are achieved by using metals (e.g. stainless

steel, titanium) and metal alloys (e.g. nickel/titanium, zirconium, cobalt/chromium) (Niinomi, 2008, D’Antonio and Sutton, 2009, Fleck and Eifler, 2009), polymers (e.g. polyetheretherketone) (Moon *et al.*, 2009), or ceramics (e.g. aluminum oxide, glass-ceramics) (Thomas *et al.*, 2005, D’Antonio and Sutton, 2009). All of these materials are essentially nondegradable and are chosen primarily due to their ability to withstand the stress and strain to which the bone is exposed during normal physical activities. Mechanical properties of bone and typical bone implants are presented in Table 1.1.

Table 1.1. Mechanical properties of bone and typical bone implant materials (adapted from Ramakrishna *et al.*, 2001).

Material	Ultimate Tensile Strength (MPa)	Young’s Modulus (GPa)
Cancellous bone (wet)	7.4	0.4
Cortical bone (wet) (longitudinal direction)	133	17.7
Cortical bone (wet) (transverse direction)	52	12.8
Titanium alloys	140-370	116
Stainless steel	414	171
Aluminum	40-50	70
HDPE	23-40	0.4-1.2

1.3. Bone Plates

Diaphyseal fractures are those that are through the shaft of long bone. These are common fracture patterns of the long bones, and the usual strategy to treat them is to fix the fracture site with a bone plate in order to restrain the movement of the fragments. Bone plate transfers the compression force between the bone

fragments, thus support the body and protect the fracture area by maintaining proper alignment of the fragments throughout the healing process.

1.3.1. Metallic Bone Plates

Use of bone plates for fixation of fractured bone fragments dates back to late 1800's. The idea basically was to hold the bone fragments aligned in the correct plane because it was known that if such an alignment is not supported, the union does not take place in the normal geometry of the bone, if occurs at all, causing bends and other anomalies (called malunion). In order to support the high loads the bones normally faced with, these plates were made of metals. However, early plates suffered from corrosion and failure. With the advances in the materials science, these initial problems have mostly been overcome by the 1950's and only then the design issues have been extensively dealt with. During this period, it was discovered that it was not enough to hold the fractured fragments in position, but the fragments must be compressed towards each other. This caused the development of compression bone plates, which still are the standard in bone plate applications. The compression of fractured fragments towards each other is achieved with the presence of special oval drill holes on the bone plate, which cause the compression of the two ends of the fragmented bone together during screw tightening.

The advantages of this design, shown in Figure 1.4, known as dynamic compression plate (DCP), are low incidence of malunion, stable internal fixation, and no need for external immobilization which allow immediate capability of the neighboring joints to move. Despite these advantages, they have important drawbacks, too. The healthy cortical bone under the plate is lost to a large extent, leaving a very large medullary space that is weakened and therefore unable to carry the load which the bone is exposed to. Another problem is the lack of observations that disappearance of fracture gap and occurrence of an external bridging callus, which are accepted as the proof of bone healing. In such cases, a refracture is frequently observed after plate removal (Uthhoff *et al.*, 2006).

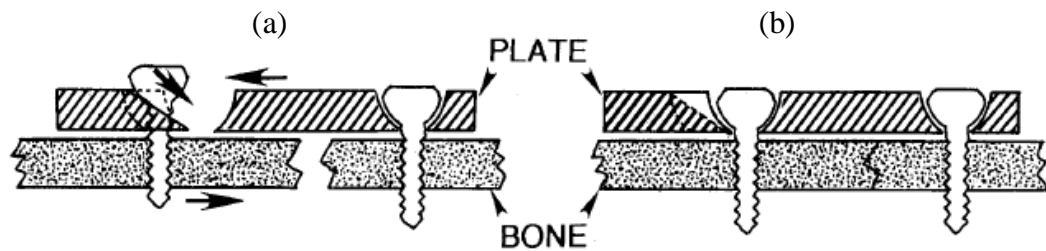


Figure 1.4. Schematic representation of a dynamic compression plate. (a) Before, and (b) after fixation. The screw on the right is fixed first, after which, fixing the screw on the left in place pushes the left bone fragment towards the right (arrow shows the direction of bone movement relative to the plate) (Adapted from Park *et al.*, 2003).

Figures 1.5 a and b show radiographs of a fractured humerus – one of the lower arm bones – before and after fixation with a titanium bone plate. Figures 1.5 c and d show titanium bone plates in different geometries.

The absence of disappearance of fracture gap and occurrence of external bridging callus was thought to be due to the inability of only one plate to fix the fractured fragments with enough stability. The suggested solution to this was to double plate the fracture site, however, this did not reduce the incidence of refractures.

The other major problem of loss of cortical bone under the plate was suggested to be due to the lack of perfusion through the region that is in touch with the plate. Therefore, some design modifications have been made on DCPs in order to decrease the contact area of the plate with bone, giving rise to low contact-dynamic compression plates (LC-DCP). However LC-DCP did not prove to be better than conventional DCPs in reducing the amount of bone lost (Jain *et al.*, 1999).

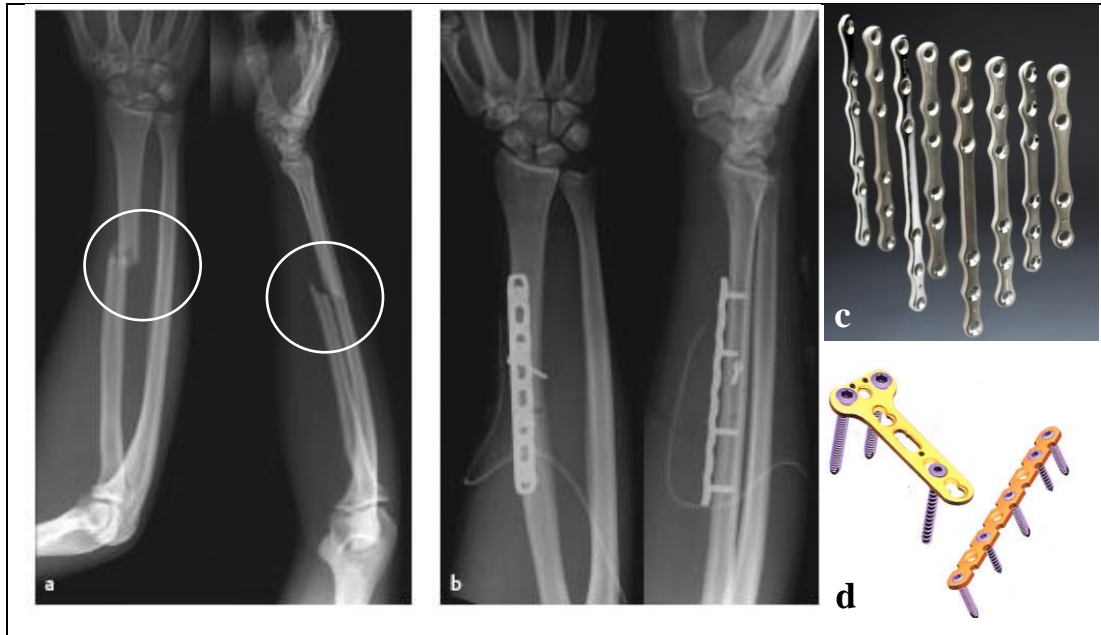


Figure 1.5. X-ray radiographs of fractures of humerus (a) fracture site before operation, (b) fragments after being stabilized by a titanium bone plate (Adapted from <http://emedicine.medscape.com/article/1239870-overview>, last visited on July 2010). (c and d) titanium bone plates with different geometries (Adapted from www.sciencemuseum.org.uk/broughttolife/objects/display.aspx?id=5826 and www.indiamart.com/anantaortho/orthopedic-instruments.html, respectively, both last visited on July 2010).

The conventional compression plates are made of metals, including stainless steel, titanium, and alloys like Co-Cr and Ti-Al-V. A problem with the use of metals as an implant is corrosion and/or accumulation of metallic particles at implant vicinity that may alter osteoblast behavior even at sub toxic levels (Sun *et al.*, 1997), or at distant body parts including draining lymph nodes, spleen and liver.

1.3.1.1. A Problem Associated with Stiff Metallic Bone Plates: Stress Shielding

Bone healing is strongly influenced by mechanical forces acting on the bone during the remodeling stage. In 1892, Wolff introduced the concept of structural

adaptation of bone, who observed that bone under compressive or tensile stress is remodeled and it is resorbed when no stress is applied to it (Wolff, 1892).

Elastic modulus of human cortical bone is in the range of 15–26 GPa, however, that of metals are 5 to 10 times higher than this value. This material modulus mismatch leads to a phenomenon, so called as "stress-shielding effect" - in which the metal plates provoke the decrease of bone mineral mass and occasionally cause bone refracture after the plate removal.

Observations of successful plating that result in unsuccessful bone healing led scientists to seek other sources for the problem. One of the first indications of stress-shielding phenomenon caused by orthopedic implants was presented in the study of Brown and Mayor in 1978. They compared the performances of intramedullary rods made of steel, titanium, polyacetal and polyamide on rabbit tibia. Their study revealed that fracture remodeling was adversely impaired in animals that were implanted with metal rods and cortical bone resorption had occurred at fracture site. Cortical bone resorption was negligible at fracture sites that carried the polymeric rod implants. An interesting observation was the formation of new bone at the ends of the metallic rods, which is practically the only location that experiences loading due to body's weight. Torsion tests of tibia after sacrificing the animals at 16 weeks showed that the fractures treated with polymeric rods had higher strength and toughness than the fractures treated with metallic rods. They deduced from these observations that transfer of mechanical stress to metallic rods causes stress shielding and impaired healing of the fracture site. The stress shielding was much less in the case of polymeric rods and healing was better. It is now accepted that mechanics of bone healing obeys Wolff's Law.

1.4. Polymers

Polymers are long-chain molecules composed of small repeating units. There are natural (DNA, proteins, cellulose and starch) and synthetic (PVC, PE, PP, PMMA, etc.) polymers. Synthetic polymeric materials draw attention in biomedical

science, since they can be easily manufactured and attain many forms as fibers, textiles, films, rods, and viscous liquids (Park and Lake, 2007).

1.4.1. Nondegradable Polymers

Polyethylene (PE) has been used in different densities (low density PE, high density PE, linear low density PE, very low density PE and ultra high molecular weight PE) (Lee *et al.*, 2003). UHMWPE is preferred in biomedical applications, not only because it can withstand high temperatures in the sterilization process but also being resistant load-bearing applications of orthopedic implants, eg. acetabular cup of total hip and the tibial plateau and patellar surfaces of knee joints (Park and Lake, 2007). Polypropylene (PP) is structurally similar to PE, making them having similar physical properties. PP is mainly used in sutures and artificial vascular grafts. Polymethylmetacrylate (PMMA) is glassy at room temperature and especially used in intraocular lenses and hard contact lenses. PMMA is also used in maxillofacial prostheses and bone cement for joint prostheses fixation (Lee *et al.*, 2003). Polytetrafluoroethylene (PTFE), is commonly known as Teflon[®] (DuPont), and is a very stable polymer. It is used in microporous form (Gore-Tex) in making vascular grafts (Visser *et al.*, 1996). Polyamides (Nylons) are commonly used as sutures, and polyesters (e.g. PET) are used in artificial vascular grafts and sutures (Visser *et al.*, 1996, Lee *et al.*, 2003).

1.4.2. Biodegradable Polymers

There are a number of synthetic or natural origin biodegradable polymers studied in the context of biomaterials research, e.g. poly(lactide) (PLA), poly(glycolide) (PGA), poly(lactide-co-glycolide) (PLGA), poly(ϵ -caprolactone) (PCL), polyhydroxybutyrate (PHB), poly(3-hydroxybutyrate-co-3-hydroxyvalerate) (PHBV), chitosan, poly(2-hydroxyethyl methacrylate) (PHEMA), collagen, and hyaluronic acid). However, only a few of them are suitable as implant materials to be used in hard tissue regeneration requiring high mechanical properties. Most important ones among the eligible ones are PLA, PLGA family, PHBV, and PCL.

1.4.2.1. Polyhydroxyacids

Historically, the most extensively studied biodegradable polymer group as a biomaterial is poly- α -hydroxyacids, namely lactide and glycolide family of polymers and these efforts has resulted in a number of FDA approved devices. Different formulations of PGA, PLA and PLGA were extensively studied in this context. PGA is the simplest member of the linear aliphatic polyester family and was used to produce the first completely absorbable synthetic suture in the 1960's (Middleton and Tipton, 2000). The monomer glycolide is synthesized by dimerization of glycolic acid and then PGA is synthesized via ring opening polymerization (Figure 1.6). It is a highly crystalline polymer (45-55%), and therefore, it is not soluble in most organic solvents. PGA fibers have high tensile strength (70 – 138 MPa) and modulus (6.9 GPa), and their high stiffness prevents easy processing and interferes with the properties of resulting product (Perrin and English, 1997). Therefore, only a small number of products were prepared using PGA. Their copolymers with lactic acid with lower stiffness values are more suitable for orthopedic applications, and therefore, are used instead of PGA.

Poly lactide is obtained through ring opening polymerization of lactide (Figure 1.6); there are two lactide isomers, namely D- and L- forms. The stereopolymer PLLA is semicrystalline, with a crystallinity of around 37%, and has the highest inherent tensile strength and modulus (2.7 GPa) among the polylactides. PDLA on the other hand, is an amorphous polymer with lower tensile strength and modulus (2.0 GPa). As a result of this crystallinity difference, PLLA requires a much longer time for degradation in the body than does PDLA.

1.4.2.1.1. Degradation of Lactide and Glycolide Polymers

In vitro and *in vivo* degradation of PLGA polymers were studied by numerous researchers (Lee *et al.*, 2003, Ruhe *et al.*, 2005, Lim *et al.*, 2009). Nonspecific hydrolytic scission and enzymatic action by esterase are the predominant mechanism of degradation in these polymers (Lee *et al.*, 2003). Semicrystalline

polymers have repeating units that go into tight associations with each other, producing dense regions throughout the polymer backbone, called crystallites. Although these are due to steric effects, these crystalline regions are tightly held together so that they act like chemical crosslinks and increase the tensile strength and stiffness.

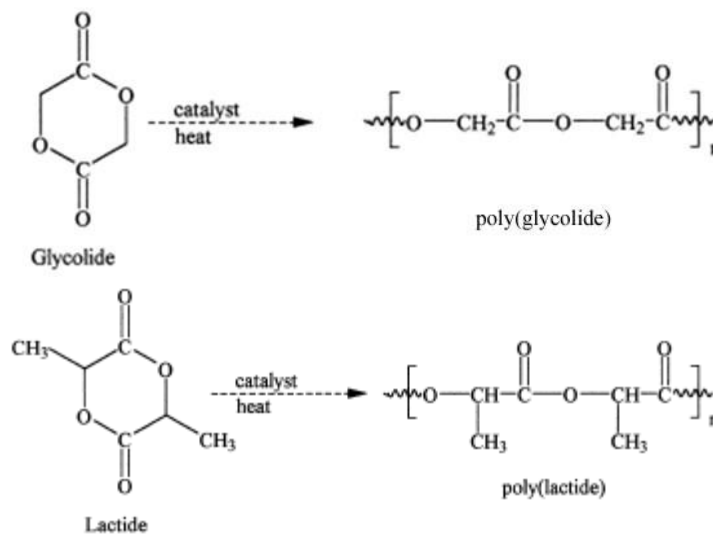


Figure 1.6. Synthesis of PGA and PLA via ring opening polymerization.

In semicrystalline polymers, water penetrates the amorphous phase and attacks the chemical bonds. Backbone is continuously fragmented into smaller chains until those oligomers are soluble in aqueous media and are eliminated from the device and then the body by the excretory system. This causes an initial reduction in the molecular weight without a loss of physical integrity of the device due to the fact that the device matrix is held together by the crystalline regions. After further fragmentation of the implant, physical properties are lost. The water penetration into the crystalline phase is very limited and so is the hydrolytic degradation at crystalline regions. The result is large amounts of independent small and rough,

highly crystalline and resistant remnants. Such particles are known to be highly inflammatory and may cause post implantation responses (Bergsma *et al.*, 1995).

Bergsma *et al.* (1995) conducted a study on patients with zygomatic (cheek bone) fractures that received PLLA plates and screws for up to 5.7 years; even after that duration, highly crystalline PLLA particles internalized by various cells and remnants of degraded PLLA material surrounded by a dense fibrous capsule were observed. Those particles do not cause irritation or injury to cells but there were swellings at the implantation sites in some of the patients. These give some ideas about the fate of those materials within the body.

Crystallinity, degradation rate and mechanical properties of the polymers can be adjusted to particular needs of the patient through production of PLA with different ratios of chiral lactides or their copolymers with glycolide.

1.4.2.2. Polyhydroxyalkanoates

Synthetic polymer PLGA has a high degradation rate leading to local acidity around the biomaterial. PLLA, on the other hand, has a low degradation rate due to its high crystallinity and leaves crystalline particulates behind even after several years leading to incomplete healing. Owing to those disadvantages, alternative biodegradable polymers were introduced. For example, poly(hydroxybutyrate-*co*-hydroxyvalerate) (PHBV) has a degradation rate in between PLLA and PLGA, therefore it does not rise local acidity and still does not leave crystalline remnants behind (Kose *et al.*, 2005). Furthermore, PHBV has recently gained FDA approval to be used as a polymer to be used in a number of biomaterials applications. PHBV has a UTS of ca. 27 MPa and Young's Modulus of ca. 1 GPa (Bhardjaw, *et al.*, 2005).

Polyhydroxyalkanoates are natural polymers synthesized by some bacteria under certain culture conditions. Polyhydroxybutyrate (PHB) is the first example of this family. It has relatively poor impact strength for biomaterials applications, but this

problem may be eased by incorporation of different ratios of hydroxyvalerate monomers into the polymer to produce polyhydroxybutyrate-co-valerate (PHBV). PHBV is metabolized to the same final products, carbon dioxide and water, with PHB under aerobic conditions (Hankermeyer and Tjeerdema, 1999). It is biodegradable (Koosha *et al.*, 1989), biocompatible (Fukada and Ando, 1986), and non-toxic (Pouton and Akhtar, 1996). The molecular representation of PHBV is shown in Figure 1.7.

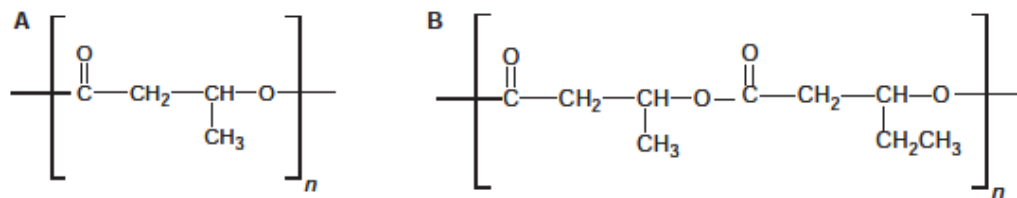


Figure 1.7. The molecular representation of A) PHB and B) PHBV (Adapted from Hasirci and Yucel, 2008)

Though, an important disadvantage of PHB and its copolymers like PHBV is their poor thermal stability during high temperature processing and relatively low impact resistance. The small difference between melting and thermal degradation temperature of them hinders their thermal processability. Melting point of PHBV (8% hydroxyvalerate, w/w) is ca. 165°. Molecular weight of PHBV starts to degrade above 170°C and this thermal degradation is accompanied with random scission of the ester bonds (Mohanty *et al.*, 2005). However, processing of polymers at elevated temperatures (and pressures) in order to improve the mechanical properties to be used in hard tissue implants is common. Therefore, these may be the reasons for the fact that use of polyhydroxyalkanoates in the area of hard tissue implants is not as well studied as in the other biomaterial fields like controlled release and tissue engineering scaffolds.

1.5. Polymer Ceramic Composites

Composites contain two or more distinct phases of materials in that one constitutes the continuous phase, or the matrix, while the other is the discontinuous phase; such as a filler within a matrix. Due to the distinct mechanical properties of metals or alloys, composites produced by coating metals with bioactive compounds are extensively studied in order to achieve osteointegration, the direct bonding of implant to the bone tissue (De Jonge *et al.*, 2008).

Bone has excellent mechanical properties originating from its composite nature. In general, ca. 60–70% of bone matrix is inorganic or mineral, which consists mainly of flat crystal plates of hydroxyapatite ($\text{Ca}_{10}(\text{PO}_4)_6\text{OH}_2$) (HAP), and the rest is primarily collagen. The rigidity of HAP and the toughness of the collagen give the bone its unique strength. Thus, it is logical to try to mimic this structure in the production of a bone substitute or an implant material.

Use of calcium phosphate polymer composites creates a highly biocompatible product - by increasing cell-material interactions compared to the polymer alone (Rizzi *et al.*, 2001). Furthermore, the sustained release of calcium and phosphate from those composites, where the two ions serve as substrates in the remodeling reactions of mineralized tissues is an added benefit (Skrtic *et al.*, 2003).

However, both solid and porous monolithic implants produced using calcium phosphate ceramics have certain mechanical disadvantages, such as a high level of brittleness and a decrease of the tensile strength.

With a number of biodegradable polymers available, biodegradable polymer – calcium phosphate composites constitute the most important group. Polymers bring in a high viscoelastic behavior and ease of fabrication into a variety of geometries, i.e. sheets, sponges, gels, and complex structures with and without high porosity (Thomson *et al.*, 2000). Although some of the properties can be improved by blending using copolymers with different monomers or adjusting

chain lengths, the most important disadvantage of polymer presence in a composite of load bearing applications is the lack of rigidity and low ultimate tensile and compressive stress values.

Most important calcium phosphate derivatives that have been used in composites with polymers are HAP or calcium deficient HAP, and α - and β -tricalcium phosphates (TCP). HAP is the first choice due to its similarity to bone's own ceramic material, while TCP finds use due to its faster degradation *in vitro* and *in vivo*.

The recent awareness and advances in nanotechnology already influenced the biomaterials field and helped designing of the composites that employ nano-scale components. Nanocomposite materials are the subject of a popular research area on the production of implants for bone augmentation.

1.5.1. Collagen-HAP Composites

Collagen is a biopolymer and is magnetically anisotropic and the natural osteogenesis process is assisted by this piezoelectric property of the collagen fibers. Piezoelectric materials have the ability to translate mechanical force into electric forces and vice versa; application of mechanical stress on collagen causes the liberation of electrons on the surface of the molecule. This not only guides the mineralization process of collagen fibers, but also helps collagens own deposition. (Ficai *et al.*, 2010). Thus, collagen appears to be a proper polymer to have in a bone substitute.

Homogenous distribution of the particles in the matrix is a critical issue in composite systems. Distribution of calcium phosphate particles, especially in nano size, in polymer matrices is such an example. A number of approaches have been reported by Mathieu *et al.* (2006), including mechanical blending of the polymer and ceramic in dry state, mixing calcium phosphate particles with polymer solution, and mixing the ceramic with molten polymer. It was found that mixing

the calcium phosphate particles in the polymer solution or in the melt result in a more homogenous dispersion than obtained by dry mechanical mixing.

Composites of collagen and HAP are very attractive due to presence of these two materials in the bone itself because their integration with the host tissue would be smoother with the already available osteogenetic process. Different approaches were used to achieve this by mixing the components (Bakos *et al.*, 1999, Chang *et al.*, 2001), by devising methods to obtain self organization (Kikuchi *et al.*, 2001), or by using a high magnetic field to obtain unidirectional orientation (Wu *et al.*, 2007). Bakos *et al.*, (1999) prepared a HAP-collagen-hyaluronic acid composite by preparing first a HAP-hyaluronic acid suspension by simple mixing of the components and then added bovine tendon atelocollagen (dispersed in deionized water) to the suspension and mixed further to obtain a complex precipitate. The resultant structure was not homogeneous in appearance due to agglomeration of HAP crystals and the weak bonding between them and the collagen fibrils. Besides, the mechanical properties of the composite were low (bending strength ca. 5.4 kPa), indicating a poor level of biomimicry.

Kikuchi *et al.* (2001) synthesized a HAP-collagen composite by simultaneous titration and precipitation using calcium and phosphate solutions and porcine atelocollagen. In this way, a self-assembled nanostructure with chemical interaction between the newly formed HAP and collagen was obtained. The cylindrical shaped constructs produced in this way had very high three point bending strengths (ca. 40 MPa) and moduli (2.5 GPa); and the values were almost equal to that of cancellous bone. These composite materials were tested *in vivo*, in 20 mm long tibial defects in beagles, and were shown to be involved in the remodeling process; they were resorbed by osteoclasts and new bone was formed by osteoblasts after resorption.

1.5.2. PHBV-HAP Composites

Coskun *et al.*, in 2005, produced composite bone plates of PHBV's of different valerate contents with commercial HAP, which was in the form of short rods with dimensions of 2-4 μm in diameter and 20-30 μm in length. They used injection molding to produce the bone plates and the highest tensile of 18.99 MPa was obtained with the homopolymer PHB that contained 15% (w/w) HAP. The micrometer-scaled crystals are obviously much larger than the plate-shaped crystals found in the natural bone (3 nm thickness x 25 nm width x 50 nm length). This size scale does not exactly mimic the nature but it provided improved mechanical properties. Still the nanometer scale is supposed to be the main reason for superior mechanical properties of bone (Ji and Gao, 2004).

1.5.3. Polylactide-HAP Composites

Due to the extensive use of PLAs in the biomedical field, their composites with HAP or TCP constitute the most common materials in the literature about biodegradable hard tissue implants. For example, PLGA is known to support osteoblast proliferation and migration well (Ishaug *et al.*, 1996), and therefore, it is frequently chosen as the polymer constituent in the composites.

Polymer-ceramic composites designed as bone grafts are proposed for several orthopedic applications. HAP, when blended with PLLA, not only improved the bending strength of the composite but also had an active role in new bone formation (Furukawa *et al.*, 2000). The HAP surface was found to be highly reactive and led to favorable attachment to tissue and bioactivity in bone repair (Ducheyne and Qiu, 1999). Due to this bioactivity it is preferred in bone fixation applications where tissue bonding to implant is desirable.

Poly (D, L-lactide) (PDLLA) and hydroxyapatite (HAP) composites are prepared by Zhang *et al.*, (2006). The authors observed that the composites have the advantages of biodegradation and biocompatibility, along with easy availability of

PDLLA, osteoconductivity of HAP, and excellent shape memory, which, when considered in total, may increase the composite's potential for application in minimally invasive surgery and bone and tissue repair. Liao *et al.* (2004) used PLA to obtain a nano HAP-collagen-PLA composite in order to overcome the mechanical disadvantages of the previously reported HAP-collagen composites found in literature. They obtained a composite that is similar to bone in terms of hierarchical microstructure and collagen composition. Moreover, it had 80% interconnected porosity at the macro level of the composite, similar to that of spongy bone, which *in vivo* led to complete healing of critical size defects (15 mm) when implanted into the radius of rabbit. However, mechanical properties of these materials were very weak to be implantable to humans; a maximum compressive strength of 1.9 MPa and elastic modulus of 43 MPa, where these values were reported to be 167 MPa and 17.2 GPa for femur, respectively (Park and Lakes, 2007). This was due to non-continuous distribution of mineralized collagen particles within the PLA matrix.

1.6. Biodegradable Implants

To avoid the stress-shielding phenomenon, it is desirable to use plates made of materials whose mechanical properties are close to those of the bones. For this, the most frequently evaluated materials in the literature are polymers, especially the fully biodegradable ones that would not cause foreign particle accumulation within the body and would eliminate the cost and discomfort of a removal surgical operation. Therefore, applications of such biodegradable polymeric osteofixation devices have been under investigation for the last forty years. However the common problem of those devices is their insufficient load bearing capability. A variety of biodegradable polymeric biomaterials were tested successfully in orthopedic applications that require no or low levels of stress. The devices used included cylindrical rods, screws, tacks, plugs, arrows, and wires (Rokkanen *et al.*, 2000). Such materials were tested in applications such as mandibular fractures (Yerit *et al.*, 2002), orthognathic (jaw) surgeries (Cheung *et al.*, 2004), facial and mandibular fractures (Bell and Kindsfater, 2006), pediatric craniofacial surgeries

(Eppley *et al.*, 2004), plating in degenerative or traumatic disruptions of cervical spine (Vaccaro *et al.*, 2002) and in internal fixation of both cartilaginous and ossified parts of the larynx (Sasaki *et al.*, 2003). Recently, there are studies on the biodegradable metals which inherent mechanical properties of metals and with the advantage of being degradable within the body (Song and Atrens, 2003, Windhagen, 2005, Staiger *et al.*, 2006, Gu and Zheng, 2010).

1.6.1. Biodegradable Polymeric Implants

Despite a large number of synthetic or natural biodegradable polymers are studied in the context of biomaterials research, e.g. polylactide, polyglycolide, poly(lactic acid-co-glycolic acid), poly(ϵ -caprolactone), polyhydroxybutyrate, PHBV, chitosan, poly(2-hydroxyethyl methacrylate), collagen, and hyaluronic acid, only a few of them, are suitable as implant materials for use in hard tissue regeneration.

The current theory of bone healing accepts that the bone needs to experience some stress for proper healing, though not as high as to cause its refracture. In theory, polymers can prevent overloading and simultaneously transfer appropriate levels of load from plate to bone during healing since their elastic moduli are closer to bone than metals. Modulus of elasticity values are; 17.2 GPa for femur, 2.2 GPa for UHMWPE, 1.55 GPa for PP and 193 GPa for 316L stainless steel (Katz, 1996, Park and Lakes 2007). Figure 1.8 shows the load transfer behavior of an ideal bone plate during the bone healing process. If the polymer is biodegradable, it might be possible to adjust its physical and/or chemical characteristics so that the degradation rate (and decrease of the strength of the material) is synchronous with the recovery of the broken bone.

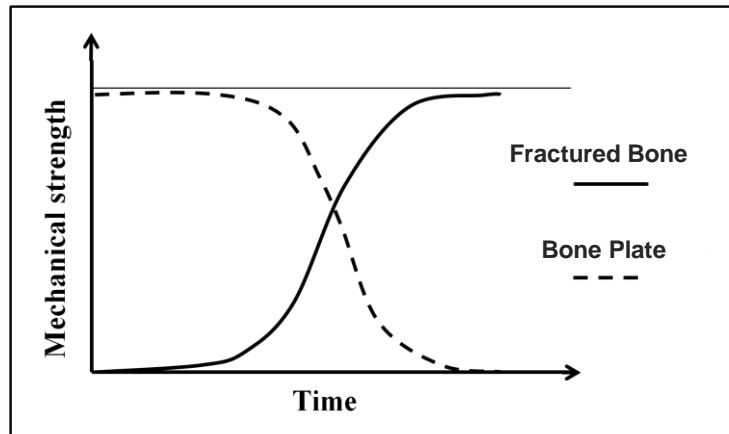


Figure 1.8. Load transfer characteristics of an ideal degradable bone plate in which the collective mechanical strength of the healing bone and bone plate complex is constant throughout the healing process.

Several biodegradable polymeric or polymer-ceramic composite bone plate systems are commercially available; these are all designed for fixation of fractures in the non-load bearing bones (Table 1.2).

Despite the presence of these orthopedic fixation devices made of biodegradable polymers, there are no examples of load bearing devices (e.g. for fixation of fractures at tibia and femur). For example there are commercially available miniplates (e.g. Inion miniplates made of highly oriented PGA and PLA fibers) (Wood, 2005), but their main function is to stabilize the site of application, not to carry the load. An example is represented in Figure 1.9, where a commercially available craniofacial bone plate system is used to stabilize the fractures.

Table 1.2. Examples of commercial biodegradable bone plate systems.

Bone plate system	Site of use	Chemical composition
Inion S1 (Inion Ltd, Finland)	Anterior Cervical Fusion System / Graft Containment System	Poly(L-lactide) and poly(D,L-lactide)
Inion S2 (Inion Ltd, Finland)	Anterior Thoraco-Lumbar Fusion System / Graft Containment System	Poly(L-lactide) and poly(D,L-lactide)
Inion OTPS (Inion Ltd, Finland)	Many parts in skeleton including hand, fingers, ankle	Poly(L-lactide) and poly(D,L-lactide), and trimethylene carbonate
RapidSorb (Synthes Inc, USA)	Cranio-maxillofacial plating applications	Poly(L-lactide-co-glycolide)
LactoSorb (Walter Lorenz Surgical Inc, USA)	Cranio-maxillofacial plating applications	Poly(L-lactide-co-glycolide) / polyglycolide blend
Delta Resorbables (Stryker Corp, USA)	Craniofacial and mid-facial plating applications	Poly(L-lactide), poly(D-lactide), and glycolide tripolymer blend

In Finland the technology of biodegradable biomaterials for use in orthopedic surgery is highly developed. According to a survey, between 1984 and 2000, in 3200 clinical cases at the Department of Orthopaedics and Traumatology at Helsinki University Hospital, surgeons used biodegradable, self-reinforced PGA and PLLA cylindrical rods, screws, tacks, plugs, arrows, and wires with a high success rate (Rokkanen *et al.*, 2000). The fact that this list of devices does not contain bone plates can be attributed to the inability of the biodegradable bone plates being not of appropriate strength.

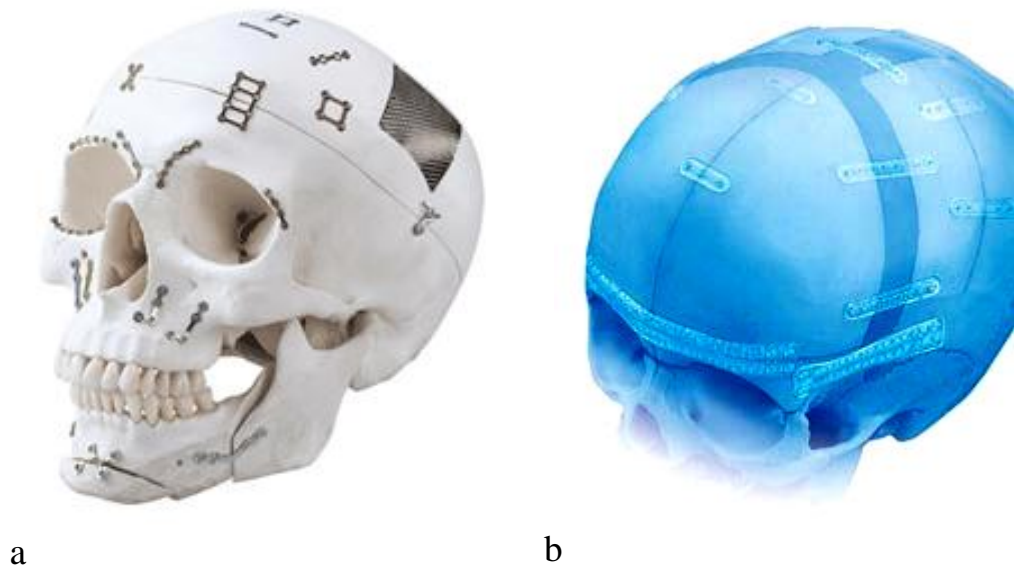


Figure 1.9. Craniofacial bone plate systems (a) conventional titanium miniplates (Adapted from <http://jeilmed.en.ec21.com/GC00673860/CA01767811/LeforteSystem.html>), (b) resorbable fixation system made of PLGA (Adapted from <http://us.synthes.com/Products/Biomaterials/Resorbable+Fixation/>).

1.6.1.1. Biodegradable Bone Plates for Oral and Maxillofacial Surgery

Fixation of osteotomized and fractured bone segments are achieved using internal rigid fixation devices including plates and screws, and the gold standard material for these is titanium (Hasirci *et al.*, 2000, Cheung *et al.*, 2004) due to its inherent stiffness and biocompatibility. However, this ever lasting stiffness may cause the aforementioned stress shielding phenomenon and resulting osteoporotic bone and skeletal growth retardation in pediatric patients (Yaremchuk and Posnick, 1995). Therefore, a number of polymer-based biodegradable plates, screw, rods, and pins are already available with some clinical experience (Park *et al.*, 2003). In a canine femoral pilot study, Uthoff *et al.*, (2006) used PLA bone plates to evaluate their applicability in cortical bone fractures. They hypothesized that PLA bone plates would eliminate the stress shielding and achieve load transfer to the bone as the

bone plates degrade. However, early failure of plates occurred due to poor mechanical properties and/or early degradation. Nevertheless the plates showed a decrease in stress shielding compared to their metallic counterparts (dynamic compression plates) used in the study.

1.6.1.2. Biodegradable Interference Screws

In anterior cruciate ligament (ACL) reconstruction surgeries, one end of the ligament to be grafted is fixed to the lower femoral head while the other end is to the upper tibial head, with one screw for each site fixing the ligament in place. Along with the classical metal screws, there are commercially available biodegradable screws, and they are nowadays popular in knee surgeries (Alan *et al.*, 1995, Keading *et al.*, 2005) (Figure 1.10).

According to a randomized clinical trial on patients having arthroscopic patellar tendon autografts (Alan *et al.*, 1995), commercial PLLA interference screws showed essentially no difference in terms of ease of application or patient's healing period when compared to metal screws produced for the same application during a 12 months follow up of 85 patients. In another study, PLLA and titanium interference screws yielded comparable results in 97 patients having patellar tendon autograft reconstruction of ACL (Keading *et al.*, 2005).



Figure 1.10. Interference screw used in the fixation of cruciate ligaments in the knee. Screw materials are poly lactide (a), hydroxyapatite (b), and stainless steel (c) (Adapted from http://news.cnet.com/8301-27083_3-10461572-247.html?tag=mncol;title)

A study in 2004 by Ma *et al.* showed that after interference screw fixation of hamstring reconstruction on two groups of 15 patients with 24 to 40 months follow up, 83% of all implanted PLLA screws were found to be intact or only partially degraded.

Following successful results obtained with PLLA screws, Macarini *et al.*, (2009) produced PLLA-HAP interference screws for tibial graft fixation. The composite screws were quite stable and had superior osteoconduction and biocompatibility when compared to plain PLLA screws.

1.7. Bone Tissue Engineering

The traditional methods to repair bone defects include autografts and allografts, and although these techniques have been fairly successful, they also have disadvantages. In the case of autografts, the disadvantages include insufficient supply of donor tissue, the long operation time required to harvest the cells, and morbidity at the donor site -due to infection, pain and hematoma-. In case of allografts, the risk of disease transfer and rejection of the foreign tissue are the main disadvantages (Laurencin *et al.*, 1999, Burg *et al.*, 2000). In order to avoid these problems, tissue engineering can be used. Tissue engineering is a multidisciplinary field and applies engineering, biology and chemistry to solve problems associated with organ transplantations (Laurencin *et al.*, 1999).

In bone tissue engineering, common strategy is to isolate appropriate cells, usually bone marrow mesenchymal progenitor cells, culture these cells *in vitro* and seed on biodegradable polymer scaffold to promote growth and remodelling. Addition of growth factors onto this medium creates a temporary ECM, which will later be degraded and absorbed by the body (Sabir *et al.*, 2009).

Bone tissue engineering is especially attractive in complex bone fracture scenes, where there is loss of bone material and the gap between fragments is so large to be united by the body. The limit that the body can heal itself is called critical sized bone defect, and above this limit, healing can be obtained through some porous filling material that is osteoconductive and/or osteoinductive in order to allow bone-forming osteoblasts to colonize in and synthesize new bone material that will unite with the original bone. For optimal remodeling of the newly formed tissue, the implant needs to be replaced with the regenerating tissue, thus necessitating use of biodegradable materials for this approach. In some applications only porous implants that allow osteoblasts to migrate in, proliferate and deposit their extracellular material (Hutchens *et al.*, 2009) are used while in others tissue engineering is used where the patient's own mesenchymal stem cells are seeded in the constructs which are, *ex vivo*, differentiated into osteoblasts within the

constructs and are ready to form new bone tissue right after implantation. Controlled delivery systems of bone morphogenic proteins (BMPs) or other growth factors can be introduced to facilitate bone formation and/or remodeling (Basmanav *et al.*, 2008, Yilgor *et al.*, 2009).

Tissue engineering scaffolds must have an inherent high porosity with interconnected pores to facilitate fluid drain and cell entrance, attachment, and proliferation for later tissue remodeling. Excessive porosity conversely affects the mechanical properties of materials, and is especially important for a tissue like bone, which is under continuous cyclic loading. Designing highly porous yet mechanically bone compatible scaffolds is a particular challenge if the inventory is limited to biodegradable materials. Ramay and Zhang (2004) suggested the use of a biodegradable composite scaffold composed of β -tricalcium phosphate (β -TCP) matrix and calcined hydroxyapatite (HA) nanofibers for load bearing bone applications. A high porosity (ca. 73%) composite was obtained with a technique that is a combination of gel casting and polymer sponge with following heating up to 600 °C to completely burn out the polymer and sintering. A maximum compressive strength of ca. 10 MPa was obtained with use of 5 w/w % HA nanofibers, which is comparable to the mechanical properties of the cancellous bone. Thus such a material needs to be implanted with other parallel supportive structure, such as a bone plate or intramedullary rod to be mechanically satisfactory.

An *in vivo* study by Chu *et al.* (2007) demonstrates applicability of a polymer/ceramic composite, made of poly(propylene) fumarate (PPF) and tricalcium phosphate (TCP), that was designed as a temporary bone support during rhBMP-2 release from an endogenous porous dicalcium phosphate dehydrate carrier system in a rat femoral segmental defect model. The implant is a hollow tube made from non-porous polymer/ceramic composite, to be placed in the intramedullary cavity of the damaged rat femur, and the porous BMP-2 carrier is inserted into a hole drilled in the implant. The initial compressive strength of the implant was 23 MPa, which decreased to 12 MPa after 12 weeks in phosphate

buffered solution at 37 °C. Although the authors state that there is no need for bone plate or other means of stabilizing due to sufficient inherent strength of the implant, they placed a (nondegradable) stainless steel K wire passing through the internal cavity of the hollow tube-shaped implant in order to obtain sharing of load by the implant and by friction between the wire and contact areas of intramedullary canal. Therefore, even a nonporous ceramic implant does not have sufficient mechanical strength for bone fixation applications.

1.8. Aim and Novelty of the Study

Bone plate transfers the compressive forces between fractured bone fragments to support the body and protect the fracture area with proper alignment of the fragments throughout the healing process. The aim of this project was to develop a design strategy for the production of a PHBV or PLLA based, nanohydroxyapatite containing biodegradable bone plate reinforcement structures with enhanced strength and modulus properties for use in the fixation of long bone fractures in the body.

Although biodegradable polymers are in use in several fracture fixation bone plate applications, they are used solely for the fixation of low or non-load bearing bones. This is mainly due to their low mechanical properties that results in material failure under body's normal physical activity. In this study, a composite approach was applied in order to enhance the mechanical properties of polymeric plates which itself cannot solely have a load bearing capacity that is comparable to load bearing bones in human body.

There are numerous studies in the literature that use hydroxyapatite or polymer fibers as reinforcement for the production of bone plates with the purpose of increasing the mechanical properties of them. Unique to this study, instead of directly incorporate hydroxyapatite particles into the final construct, nanorods of hydroxyapatite were first prepared and incorporated into polymeric fibers with the aim of obtaining fibers with HAP nanorod aligned in them to achieve higher

mechanical properties. These nanocomposite fibers were then used to construct the composite bone plates.

Use of capillary rheometer for production of the composite fibers was found to be a successful approach in that composites produced with this instrument showed a degree of alignment of hydroxyapatite nanorods towards the longitudinal axis of composite fibers. Furthermore, tensile and compressive mechanical tests showed that the fibers produced with this method had the best mechanical properties obtained throughout the study with different fiber production methods.

CHAPTER 2

MATERIALS AND METHODS

2.1. Materials

Poly(L-lactide) (ResomerTM L210, i.v. 3.3 – 4.3 dL/g) was purchased from Boehringer-Ingelheim (Germany). Poly(3-hydroxybutyrate-co-3-hydroxyvalerate) (PHBV) with 8% (w/w) valerate content, dexamethasone, β -glycerophosphate disodium salt, L-ascorbic acid, and $MgCl_2$ were purchased from Sigma-Aldrich (Germany). Dulbecco's Modified Eagle Medium (DMEM, high glucose) and fetal calf serum (FCS) were obtained from Hyclone (USA). Alamar Blue cell proliferation assay was from Biosource (USA). Lactic acid (90%), KCl, $Ca(NO_3)_2 \cdot 4H_2O$, and hydroxyapatite (random crystals) were obtained from Fluka, Switzerland. $CaCl_2$, NaCl, $NaHCO_3$, K_2HPO_4 , tetrahydrofuran, toluene, ethylacetate, ethanol, acetone, KH_2PO_4 , NaCl, and KOH were supplied by Merck, Germany. Ammonia solution (25%) was purchased from Riedel de Haen, Germany. K_2HPO_4 was purchased from BDH chemicals, England. Chloroform was supplied from J.T. Baker, Netherlands. Triton X-100 was obtained from Applichem, Germany.

2.2. Preparation of HAP Nanocrystals

Hydroxyapatite (HAP) ($Ca_{10}(PO_4)_6(OH)_2$) was not commercially available in the form of nanorods, therefore, several methods were used to produce the nano crystalline HAP, either by direct synthesis from Ca^{+2} and PO_4^{-3} sources or by recrystallization of other commercial HAP sources.

2.2.1. Method 1: Synthesis of HAP Nanofibers in Simulated Body Fluid

According to Wang *et al.* (2006), HAP crystals are formed in a reaction between CaCl_2 and K_2HPO_4 in a simulated body fluid (SMF) environment at 37°C with no pH control. The formed hydroxyapatite crystals were stated to be in nanorod form with 50-100 nm length and 3-5 nm diameter. Various temperatures ($37 - 50^\circ\text{C}$) had been tried and only HAP microrods of different lengths and thicknesses were obtained.

Preparation of Simulated Body Fluid (SBF)

The following solution is called the simulated body fluid (Wang *et al.*, 2006) and was prepared in a glass bottle in deionized water under continuous stirring in the given order. During this, it was ensured that each chemical is dissolved before adding the next.

Composition of Simulated Body Fluid

- NaCl, 136.8 mM
- NaHCO_3 , 4.2 mM
- KCl, 5 mM
- K_2HPO_4 , 1 mM
- MgCl_2 , 1.5 mM
- CaCl_2 , 2.5 mM
- Na_2SO_4 , 0.5 mM

Preparation of Hydroxyapatite Nanorods

In order to prepare the nanorods, 5 mM CaCl_2 was added to 50 mL SBF while continuously stirring. Then 3 mM K_2HPO_4 was added. The suspension was stirred for a further 10 minutes. The bottle was tightly capped and incubated in a 37°C water bath for 24 h.

The content was filtered under vacuum, washed three times with absolute ethyl alcohol and then poured in a petri plate as a thick slurry. Then it was dried at 50°C for 24 h under vacuum. A small amount of the dry powder obtained was dispersed in methanol and ultrasonicated at 25 W for 2 min with a probe tip ultrasonicator (4710 series, Cole-Palmer Instruments, USA) for microscopic evaluation.

2.2.2. Method 2: Production of HAP nanorods by recrystallization

In the literature, HAP crystals in the form of nanorods (20 nm x 100-400 nm) were reported to form using this procedure (Chen *et al.*, 2005). It is based on dissolving a commercial HAP and then recrystallizing it under appropriate conditions to obtain nanocrystals. The experimental conditions published were in the form of a wide range of parameters and values. Therefore, different process conditions were tried in order to obtain HAP crystals with shape and dimensions suitable for the purposes of this study. Table 2.1 shows the parameters and the values tested.

Table 2.1. Conditions tested in method 2 for production of the HAP nanorods.

Temperature range (°C)	pH range	Incubation time
25, 50, 75	5.8, 6.5, 7.0, 7.5, 8.0	18 h, 3 d, 7 d

Commercial HAP powder (2.5 g) of irregular particles was placed into a beaker and 500 mL distilled water is added. The suspension were stirred continuously and HNO₃ was added until the powder was dissolved. The pH was then adjusted to 2 by further HNO₃ addition to ensure complete dissolution. The resulting solution was expected to contain both Ca⁺² and PO₄⁻³ species in the same theoretical molar Ca/P ratio of HAP (Ca/P = 1.67). Ammonium hydroxide was then added dropwise to 20 ml of the above solution with continuous stirring until the desired pH (5.8,

6.5, 7.0, 7.5, or 8.0) was reached. It was expected that the HAP nanorods would grow from this supersaturated aqueous solution upon increase of pH to 5.8 - 8.0. The resulting suspension was sealed in a tube and kept incubated at 25 to 70°C for 18 h to 7 days. Following centrifugation (5000 rpm, 10 min.), the suspension was filtered and the remnants were washed 3 times with distilled water. The resulting pellets dispersed in methanol and ultrasonicated at 25 W for 2 min with a probe tip ultrasonicator (4710 series, Cole-Palmer Instruments, USA) before examining under scanning electron microscope (SEM).

2.2.3. Method 3: Preparation of Nanograde Osteoapatite-like Rod Crystals

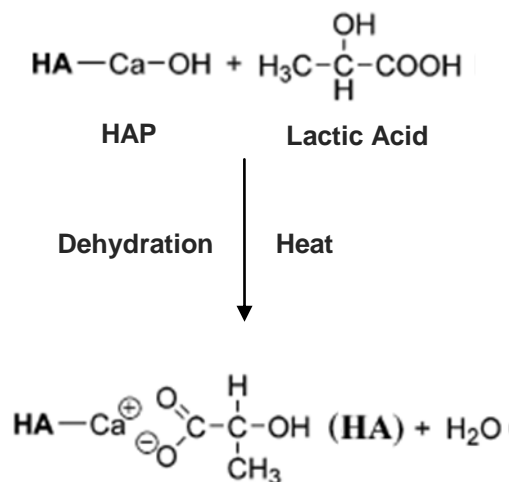
HAP nanorods of 15 - 150 nm length and ca. 20 nm diameter were reported by Yubao *et al.*, (1995). The following is a modified version of that procedure to obtain HAP nano crystals in this study.

Ca(NO₃)₂ (aq) (0.5 M) and (NH₄)₂HPO₄(aq) (0.3 M) solutions were prepared and pH was adjusted to 11 with ammonia addition. (NH₄)₂HPO₄ (100 mL) was added dropwise onto 100 mL of Ca(NO₃)₂ solution under continuous stirring. The solution was divided into two portions where one was allowed to stand at room temperature and the other at 70°C in an incubator, for 2 h. The final solution was washed 3 times with distilled water with centrifugation at 5000 rpm for 10 min after each wash. Distilled water (200 mL) was added to the pellet and incubated at 140°C for 2 h. The product was washed with distilled water, then with absolute ethyl alcohol, finally with acetone and was dried overnight at 50°C under vacuum. The resulting pellet was dispersed in methanol with ultrasonication at 25 W for 2 min with a probe tip ultrasonicator (4710 series, Cole-Palmer Instruments, USA) before studying under scanning electron microscope (SEM).

2.3. Grafting of HAP Surface with Lactic Acid

In order to achieve a higher chemical compatibility between HAP and the PLLA bulk of the bone plate and have a more homogenous distribution of rods within the

polymer, a chemical modification procedure for HAP nanoparticle surface was applied (Qiu *et al.* (2005). According to the following mechanism:



The procedure applied was as follows: HAP (1 g) nanorod aggregates were disintegrated with an agate mortar, placed in a test tube containing tetrahydrofuran (THF) (5 mL), dispersed with a probe tip ultrasonicator for 1 min. at 25 W. After ultrasonication, the content of the tube was stirred in a round bottom flask, and 1.2 or 2.2 mL of 90 % lactic acid (LA) aqueous solution was added drop wise into the suspension. More THF was added to bring its volume to 30 mL. The flask was heated at 60°C for 30 min, 45 mL toluene was added, the flask was tightly fitted to a reflux system and heated in an oil bath at 150°C for 10 h. The HAP particles were washed 5 times with THF, then 5 times with ethyl acetate using repeated centrifugation and resuspension in order to remove any ungrafted lactic acid present in the medium. The particles were dried in a petri plate for 24 h at 60°C under vacuum.

2.4. Production of Polymer – HAP Nanorod Composite Fibers

A variety of methods were tested to determine the best approach for producing polymer or polymer-HAP composites to incorporate in the bone plate.

2.4.1. Spinnability Tests of Polymers

Ability of a polymer to form spins depends on a number of factors, including its molecular weight and molecular weight distribution. Specifically for PLLA, it is also highly dependent on the quality of the source (Zhang H. *et al.*, 2009). PLLA and PHBV were tested for their spinnabilities. A small amount of polymer was put in a test tube with a nitrogen gas inlet (to prevent thermal degradation) and heated in a silicone oil bath just above the melting point of the polymer (T_m 165°C and 175°C for PHBV and PLLA, respectively), a wire with a hook on its tip was inserted in the tube and drawn out rapidly. A thin thread of polymer forms. A long polymer spin without break implies a proper processibility with melt spinning techniques.

2.4.2. Melt Spinning of Polymers

Melt spinning is a technique for production of small diameter polymer fibers (spins) where molten polymer is forced through a number of very narrow orifice (called spinnerets, 50 – 100 μm diameter) under high pressure to form continuous spins. This is actually the technique that textile fibers are produced by. If the filler (HAP, in this case) is mixed with the polymer beforehand, a composite of these two can be obtained. It was hypothesized that the shear force could also help alignment of HAP nanorods parallel to the spinning direction.

Polymer powder or pellets (3-4 g) with or without HAP nanorods was placed in the heating chamber of a custom made melt spinning device (Figure 2.1). Ram was placed into the heating chamber over the loaded polymer, the gas-proof cap was placed, and heater is set to T_m of the particular polymer. After the desired temperature was obtained, nitrogen influx was started to apply the pressure on the ram. Spun polymer fibers were collected from the spinneret.

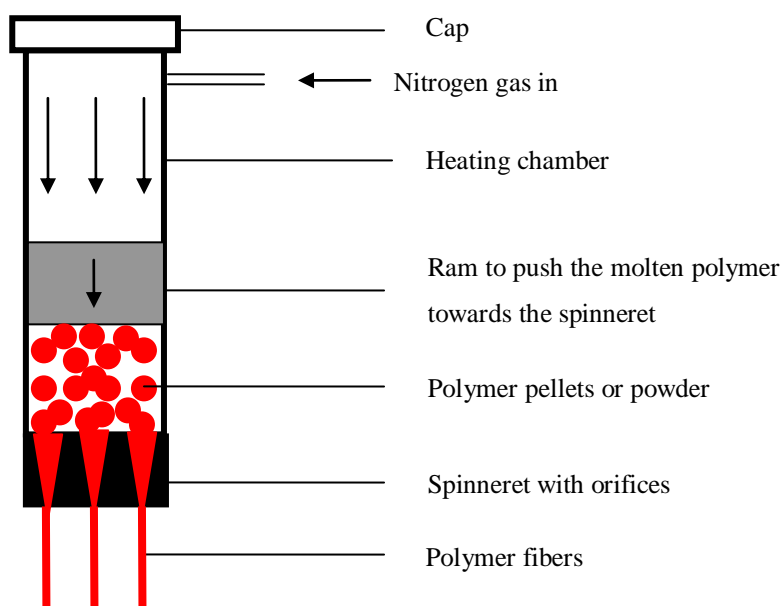


Figure 2.1. Scheme of the custom made melt spinning device.

2.4.3. Wet Spinning of Polymers

Wet spinning is a technique in which a polymer is dissolved in a good solvent and then injected by a syringe into a non-solvent that is miscible with the solvent. As soon as the polymer solution comes in contact with the non-solvent, solvent diffuses into non-solvent and polymer dries, forming fibers of different dimensions depending on the injection rate, solution concentration, and diameter of the orifice of the needle.

For wet spinning of PHBV or PLLA, they were dissolved in chloroform, HAP nanorods were added into the solution, the suspension was stirred on a magnetic stirrer, and filled in a syringe fitted with a needle having an internal diameter of ca. 90 μm . This was then placed in an automatic syringe pump (World Precision Instruments, UK) and different combinations of parameters including injection rate (5 - 500 $\mu\text{L}/\text{min}$), polymer concentration (0.05 - 0.15 g/L), and HAP content (20 %

w/w) were applied. The polymer spins were injected into a test tube containing ethanol, which were then collected and dried at room temperature.

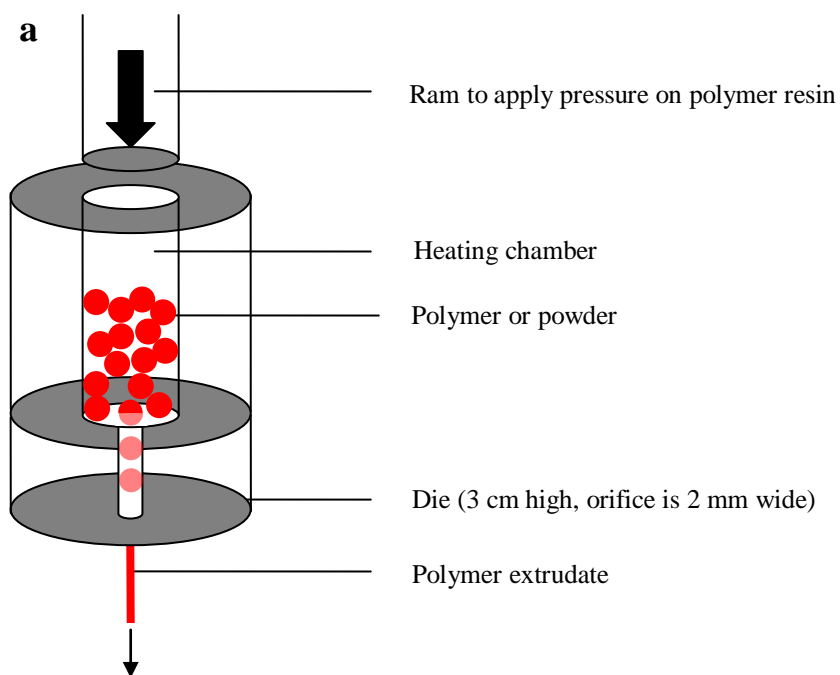
2.4.4. Extrusion of Polymers at Sub-Melting Temperatures

In this application, polymer is forced through a small orifice after increasing its fluidity by heating to sub-melting temperatures and then applying pressure. Thus, the polymer takes the form and the dimension of the orifice when it leaves the extruder. If a filler material is mixed with the polymer before extrusion, a blend of these two is obtained.

Polymer powder or pellets (2 g) (with or without HAP nanorod content) was placed in the heating chamber of custom made spinning device (Figure 2.2). Ram was placed into the heating chamber that was set to 5°C below the melting point of the polymer. After the desired temperature was obtained, pressure is applied with hydraulic press (custom made). Polymer fibers that were spun from the nozzle were collected. The diameter of the nozzle was 2 mm and path length was 3 cm.

2.4.5. Mixing PLLA and HAP Nanorods for capillary rheometer extrusion

PLLA polymer powder (1 – 2 g) was dissolved in chloroform to obtain a 5% (w/v) polymer solution, which was stirred overnight using magnetic stirrer. Necessary amount of HAP (0 – 50%, w/w, so as to obtain a total 2 g of PLLA or PLLA – HAP mixture) was placed in a test tube, 3 – 4 mL of chloroform was added, and the suspension was ultrasonicated at 25 W for 2 min with a probe tip ultrasonicator (4710 series, Cole-Palmer Instruments, USA) for 2 to 3 min. The tube content was added to the polymer solution and the final mixture was placed in an ultrasonic bath (Branson, 2200) at 60 W for 6 h. Then the content was poured in a petri plate and allowed to dry overnight. After drying, a thick polymer slab was obtained, which was then cut into about 0.5 cm x 0.5 cm chips and further dried in a vacuum oven at 50°C for 8 h.



b



Figure 2.2. Scheme (a) and photo (b) of the custom-made extruder

2.4.6. Polymer Fiber Production with Capillary Rheometer

Capillary rheometer (Dynisco, LCR-7001, USA, nozzle diameter 0.508 mm, 20 mm path length) is a computer-controlled instrument consisting of a heated barrel and a piston that drives molten polymer through a die. Its normal use is for

measuring the flow properties of polymer melts with a shear stress versus shear rate graph at a defined constant temperature. It has a capillary tube of specified diameter and length for measuring differential pressures and flow rates. The polymer melt is extruded through the die at the bottom of the instrument as a fiber. Figure 2.3 shows a photograph and a schematic drawing of the capillary rheometer. Polymer chips (total 2 g) containing 0% to 50% (w/w) amounts of HAP nanoparticles were placed in heating barrel of capillary rheometer. After a temperature above T_m was reached, the electronically controlled ram was used to apply pressure on the polymer at a fixed rate. Polymer fibers spun from the die at temperatures between 165 to 240°C were mechanically evaluated afterwards.

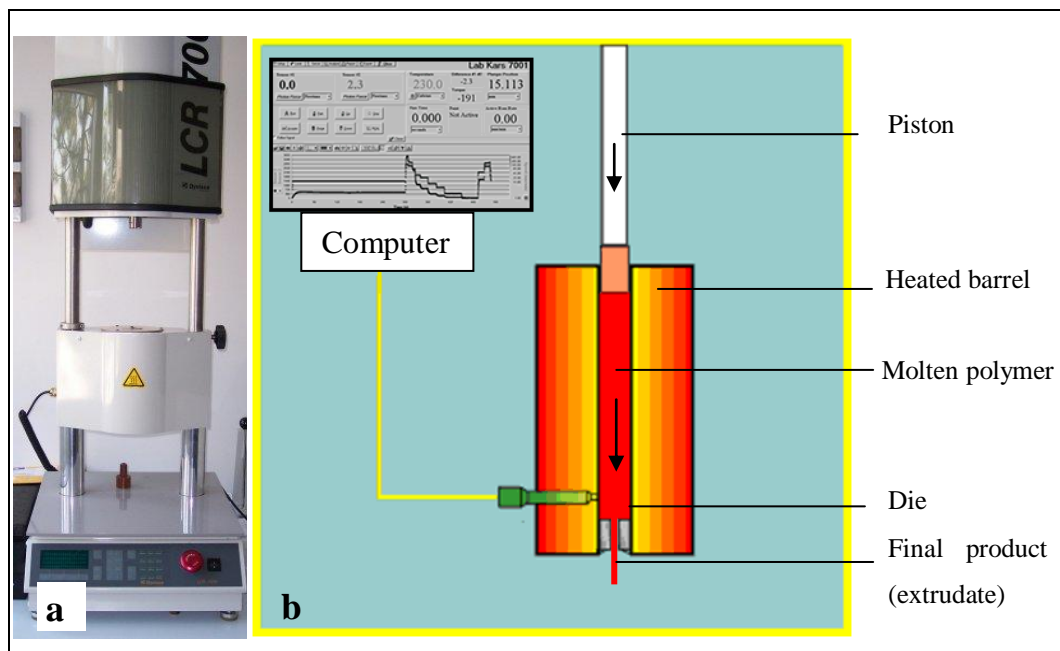


Figure 2.3. Dynisco, LCR-7001 capillary rheometer. a) Photograph where the heating chamber is behind the white-colored protecting panel in the middle. b) Schematic presentation (Adapted from <http://www.celsum.com/eta2100.htm>).

2.5. Production of Fiber Reinforced PLLA Bone Plates

A custom made steel mold with a moving pressure applying element was used to produce bone plate samples (Figure 2.4). When the moving upper compresses the mold, a rectangular prism shaped product is obtained with dimensions of 50 mm x 10 mm x 3 mm. Bone plates were produced as follows: PLLA powder (1 g) is put in the mold and evenly distributed. When PLLA or PLLA-HAP composite fibers are used, they are cut into 5 cm long pieces and 8 or 16 such fibers are placed on top of the PLLA layer. Then, another 1 g of PLLA was placed and evenly distributed on the fiber layer. Upper moving element is placed on top and the mold is wrapped with an electronically controlled heating jacket and a temperature sensing probe was attached. The mold was put under hydraulic pressure and a pressure of 2 bars is applied while maintaining the temperature for 1 h at 178°C. The mold was then allowed to cool to room temperature before disassembling it to remove the plate.

2.6. Mechanical Characterization

Ultimate tensile strength (UTS) is the maximum stress that the sample can withstand when subjected to a tensile force, while, ultimate compressive strength is the highest compressive stress that it can resist before failure. Young's Modulus is a measure of the stiffness (resistance to elastic deformation) of the sample. These are the properties of the samples that are expected to approximate those of real bones.

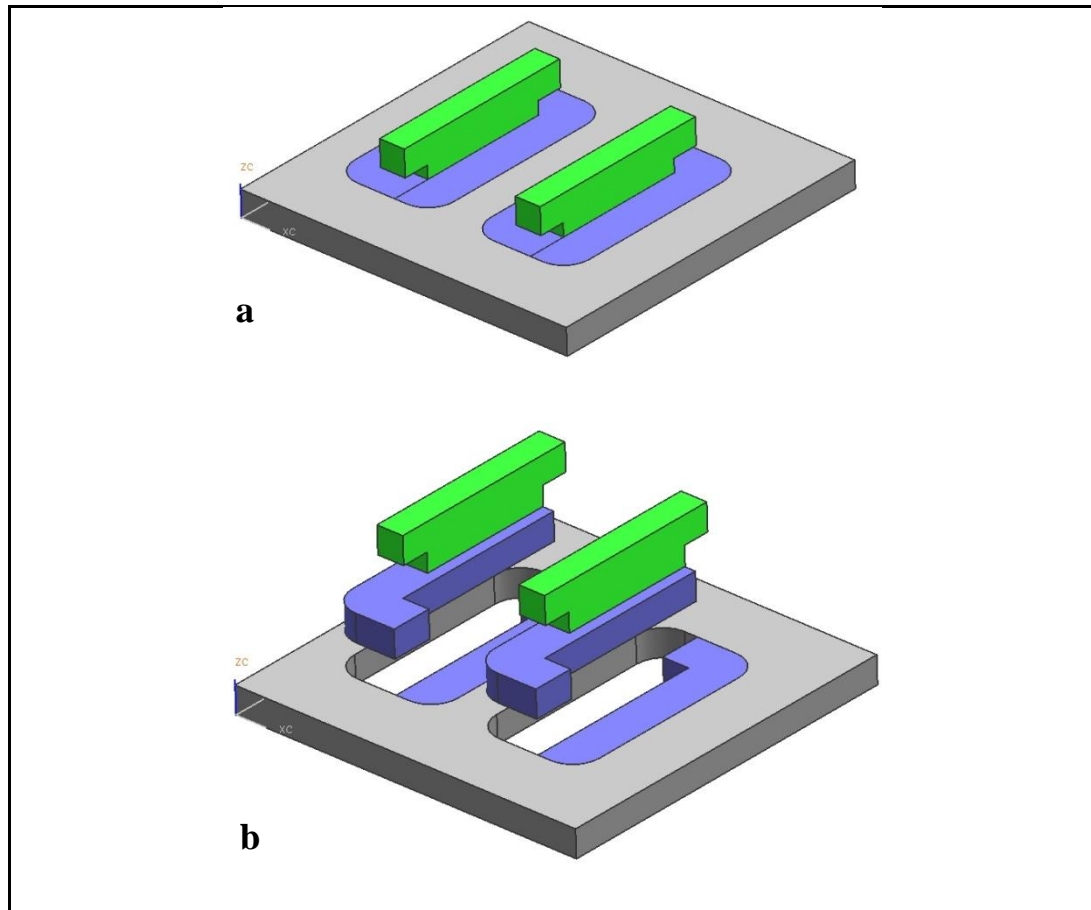


Figure 2.4. Custom made steel mold for hot pressing bone plate constructs: (a) assembled, (b) disassembled view.

Mechanical testing of the samples was done according to directives of American Society for Testing and Materials (ASTM) for each sample type. Young's Modulus values were calculated from the force-displacement data obtained in the tests. All the specimens were kept at room temperature in a desiccator to prevent absorption of humidity.

Mechanical testing of the polymer and polymer/HAP composite fibers were done on a MT-LQ (Stable Micro Systems, UK) model materials tester with a 250 kg load cell installed. Tensile tests of fibers obtained by wet spinning were done according to ASTM D3379-75 (Standard test method for tensile strength and

Young's Modulus for high-modulus single-filament materials). Crosshead speed was 0.2 mm/min and gage length 2 cm. Each sample was tested at least 5 times and the data averaged.

For tensile tests of fibers obtained by sub-melting temperature extrusion and by capillary rheometer, tensile tests were done on 5 cm long samples according to ASTM D3039M-00 (Standard test method for tensile properties of plastics) in the same mechanical tester. Gage length was 2 cm and test speed was 2 mm/min. Each sample was tested at least 5 times and averaged.

Compressive tests of polymeric plates were done according to the ASTM D 695M-91 (Standard test method for compressive properties of rigid plastics) using the same test device on 25x10x3 mm³ samples. Crosshead speed was 1.3 cm/min. Each sample was tested twice and averaged.

2.7. Microscopic Characterization

2.7.1. Scanning Electron Microscopy

Examination of the samples was done with Scanning Electron Microscope (SEM, 400F model Field Emission SEM, Quanta Inc., USA). Samples were fixed on SEM stubs with a double sided carbon tape (EMS, USA) and they were coated with 5 – 20 nm thick layer of Gold/Palladium by sputtering.

2.7.2. Transmission Electron Microscopy

HAP nanocrystals were visualized with Transmission Electron Microscopy (TEM, 100CX model TEM, Jeol Inc., Japan). A small amount of HAP powder was dispersed in ethanol and ultrasonicated to prevent agglomeration. Then a few droplets of the suspension were added on the carbon coated copper holey TEM grids and air dried.

2.7.3. Confocal Laser Scanning Microscopy

A confocal laser scanning microscope (model TCS SPE, Leica, Germany) was used to obtain fluorescent images of tissue cultures.

2.8. Chemical Characterization

2.8.1. Attenuated Total Reflectance - Fourier Transform Infrared Spectrometry (ATR-FTIR) of LA Coated HAP

LA coated HAP samples were evaluated with an FTIR (model 4100, Jasco, Japan) to determine the efficiency of LA coating.

2.8.2. Elemental Analysis of LA Coated HAP

Elemental analysis studies of LA coated HAP were done in order to determine the carbon and hydrogen content on the HAP nanocrystal surfaces with a CHNS device (model 932, Leco, USA).

2.9. *In Situ* Degradation Studies

Pure PLLA fiber and PLLA – HAP composite fibers (ca. 60 mg each) were dried in vacuum oven at 80 °C until constant weight is obtained and fibers were put in phosphate buffered saline (PBS, 10 mL, 0.1 M, 0.1 M NaCl, pH 7.4) solutions for 1 day, 2, 4, and 6 weeks in an orbital shaker (37 °C, 50 rpm). At the end of each time interval, the composite fibers were removed, gently washed with distilled water, dried in vacuum oven until constant weight.

The PLLA – HAP composite fibers and pure PLLA fibers (ca. 60 mg each) were also incubated in 10 mL ultrapure water for the same time intervals in an orbital shaker (37°C, 50 rpm) in order to determine pH changes due to soluble degradation products. At the end of each time interval, pH of the solutions was

measured with pH meter (Eutech Cyberscan pH510, Thermo Fisher scientific, USA).

2.10. *In Vitro* Evaluation of Composite Fibers

Composite fibers were evaluated for their effect on proliferation, spreading, and differentiation of rat bone marrow derived mesencymal stem cells.

2.10.1. Production of Polymeric Plates for *In Vitro* Evaluation

PLLA or PLLA-HAP composite fibers were used to produce constructs in order for evaluation of cellular response to the materials. Polymer or composite fibers were aligned side by side and sprayed with chloroform which slightly dissolves PLLA and helps the adjacent fibers to stick to each other to create an impermeable surface. By this way, ca. 1 cm² planar polymeric samples were produced (Figure 2.5).

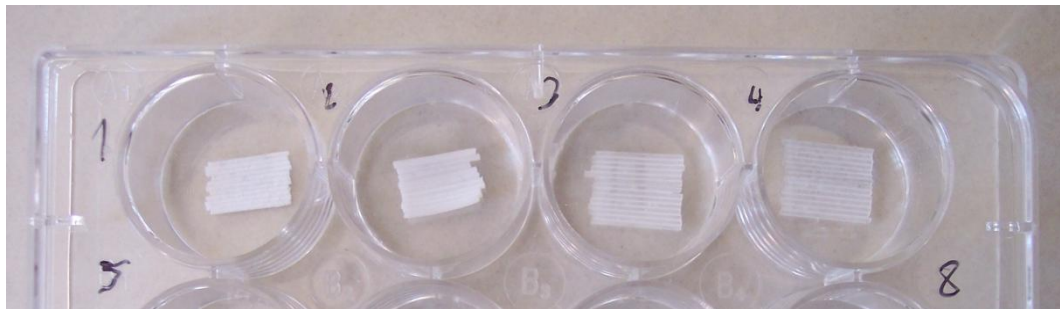


Figure 2.5. Polymeric plates produced from PLLA –HAP composite fibers during *in vitro* testing.

2.10.2. Isolation of Rat Mesenchymal Osteoprogenitor Cells

Isolation of mesenchymal osteoprogenitor cells (MSCs) was done according to Kose *et al.*, (2003). After euthanizing 6 week old, approximately 150 g Sprague-Dawley rats with diethyl ether inhalation, femurs and tibia were excised and marrow cavities were flushed out with primary medium (DMEM with 20% fetal calf serum (FCS), 1 $\mu\text{g}/\text{mL}$ amphotericin B against fungi and yeast contaminations, 100 units/mL penicillin and 100 $\mu\text{g}/\text{mL}$ streptomycin against bacterial contamination) injection. Medium with cells was centrifuged (3000 rpm, 5 min) and pellet was resuspended with the same medium, which was plated in T-75 flasks (one femoral flush per flask) and incubated in 5% CO_2 atmosphere for 2 days. Then, flasks containing hematopoietic and other cells were repeatedly washed with PBS (10 mM, pH 7.2) and the medium was refreshed every other day.

2.10.3. Seeding Rat Mesenchymal Osteoprogenitor Cells on Polymeric Plates

When cells reached ca. 80% confluency, they were lifted from the flask by trypsinization (0.05% trypsin at 37°C for 5 min, followed by addition of FCS containing medium for inactivation of trypsin) and following centrifugation (3000 rpm, 5 min), cells were resuspended in complete medium (primary DMEM supplemented with 10 mM β -glycerophosphate, 50 $\mu\text{g}/\text{mL}$ l-ascorbic acid and 10 nm dexamethasone). After a cell count using hemocytometer, a calculated volume of suspension (50 μL) containing 2.5×10^5 cells were seeded on each construct that was placed in 6-well plates. The cells were grown in complete medium for 1, 2, and 3 weeks. Medium was refreshed every other day.

2.10.4. Determination of Cell Proliferation

Viable cell number during *in vitro* incubations was assessed using Alamar Blue assay. At each time point, the medium in the wells was discarded and the wells were washed with sterile PBS to remove any remaining medium. Then Alamar Blue solution (10% in colorless DMEM, 1.5 mL) was added to the wells and

incubated at 37°C and 5% CO₂ for 1 h. After 1 h, 200 µL of the incubation solution was transferred to a 96 well plate and absorbance was determined at 570 and 595 nm with a plate reader spectrophotometrically (Molecular Devices, USA). The test medium in the wells was then discarded, washed with sterile PBS, fresh primary medium was added to the wells and the incubation was continued. All experiments were carried out in duplicates.

Alamar Blue assay incorporates an oxidation-reduction (redox) indicator that changes color in response to chemical reduction of growth medium resulting from the metabolic activity of the cells. Reduction related to metabolic activity (directly related to cell number) causes the redox indicator to change its color from that of oxidized form (blue) to that of the reduced form (red).

The absorbance values were recorded at 570 nm and 595 nm correspond to the absorption spectra of the reduced and oxidized forms of Alamar Blue, respectively. Since there is considerable overlap in these spectra, the following equation is used for the calculation of percent reduction of Alamar Blue:

$$\text{Reduction (\%)} = \frac{(\epsilon_{\text{OX}})_{\lambda_2} \times A_{\lambda_1} - (\epsilon_{\text{OX}})_{\lambda_1} \times A_{\lambda_2}}{(\epsilon_{\text{RED}})_{\lambda_1} \times A'_{\lambda_2} - (\epsilon_{\text{RED}})_{\lambda_2} \times A'_{\lambda_1}} \times 100$$

where;

ϵ_{OX} = molar extinction coefficient of Alamar Blue oxidized form (Blue)

ϵ_{RED} = molar extinction coefficient of Alamar Blue reduced form (Red)

A = absorbance of test wells

A' = absorbance of negative control wells

λ_1 = 570 nm

λ_2 = 595 nm

To correlate the reduction (%) with the viable cell number, a calibration curve of known cell numbers versus reduction (%) was constructed (Appendix A).

2.10.5. Microscopic examination of the Bone Plates in the *In Vitro* Medium

At the end of 3 days of incubation, cell seeded plates were rinsed with PBS (pH 7.4) in order to remove the media and fixed with 4% p-formaldehyde in PBS for 30 min at room temperature. The samples were then treated with Triton X-100 (0.1%) for 5 min to permeabilize the cell membranes. After washing with PBS, samples were incubated at 37 °C for 30 min in BSA-PBS (1%) solution before staining to prevent non-specific binding. After washing with 0.1% BSA in PBS, the plates were stained with FITC-labeled phalloidin (1:100 dilution of the stock) for 1 h at 37°C for actin filaments. After several washes with PBS to remove the unbound dye, samples were further treated with 1/3000 diluted DAPI for 4 min at room temperature for staining the nuclei. Afterwards the samples were washed with PBS and the samples were studied with the confocal laser scanning microscope (CLSM, TCS SPE, Leica, Germany) with a 488 nm laser for FITC-phalloidin and 358 nm light for DAPI. The obtained images were overlaid one on another to visualize both actin filaments and cellular nuclei simultaneously.

CHAPTER 3

RESULTS AND DISCUSSION

3.1. Synthesis of HAP Nanorods

3.1.1. Method 1: Synthesis of HAP Nanofibers in Simulated Body Fluid

According to Wang *et al.* (2006), HAP nanorods with 50 – 100 nm length and 3 – 5 nm diameter form with a reaction between CaCl_2 and K_2HPO_4 in a simulated body fluid environment at 37°C at uncontrolled pH. However, the suggested procedures yielded plate-like structures with ca. 10 μm length and 5 μm width (Figure 3.1a). Several synthesis parameters conditions, including temperature and time, were changed but neither of these resulted in products of desired nano dimensions. Prolonging the incubation time to 3 days (from 24 h) resulted in similar but larger structures. Increasing the reaction temperature to 50°C (from 37°C) resulted in rods with 40 – 50 μm length and 3 – 5 μm diameter (Figure 3.1b).

3.1.2. Method 2: Production of HAP Nanorods by Recrystallization

In the literature, HAP nanorods (20 nm x 100-400 nm) were reported to form by first dissolving commercial HAP and then recrystallizing it under appropriate conditions (Chen *et al.*, 2005). The parameters (incubation time, temperature, and pH) were given as a range instead of exact values, therefore, optimization of the reaction parameters was studied.

Although nanorods structures were obtained in each reaction, they were found to have agglomerated. For example, reaction for 3 days at 50°C and pH 7.0 resulted in ca. 250 nm nanorods which seemed connected to each other with plate-like structures (Figure 3.2a); while the reaction for 7 days at 75°C and pH 8.0 produced ca. 300 nm or shorter nanorods that were all fused (Figure 3.2b). Therefore, individual nanorods were not obtained even after applying combinations of different reaction parameters.

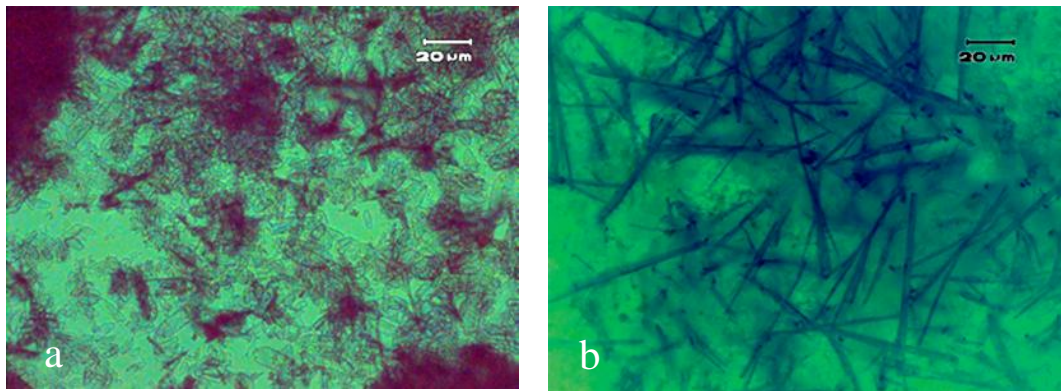


Figure 3.1. Light microscopy images of HAP molecules obtained under different conditions. a) t: 24 h, T: 37°C, pH: uncontrolled b) t: 24 h, T: 50°C, pH: uncontrolled.

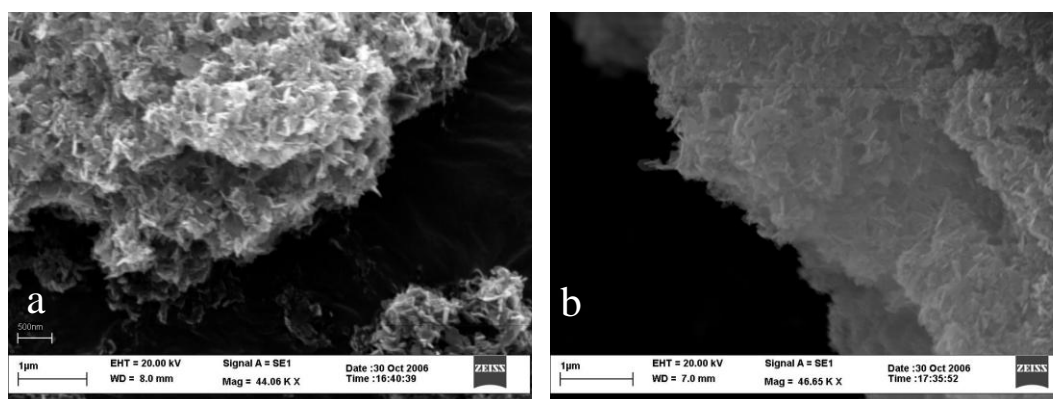


Figure 3.2. Scanning Electron Microscope (SEM) images of HAP crystals obtained by varying some conditions of the procedure of Chen *et al.*, 2005. a) t: 3 days, T: 50°C, pH: 7.0; x44,060, b) t: 7 days, T: 75°C, pH: 8.0; x46,650. Scale bars: 1 μm .

3.1.3. Method 3: Preparation of Nanograde Osteoapatite-Like Rods

In another article in the literature, HAP nanorods that are like those in bones (osteoapatite) with 15 – 150 nm length and ca. 20 nm diameters were reported (Yubao *et al.*, 1994). HAP nanorods were obtained (Figure 3.3 and 3.4). Several types of HAP structures were produced with slight variations in the procedure. Figure 3.3a appears as a network of fibrous structures and these particles were obtained after incubation of calcium and phosphate mixture at room temperature (RT) and pH 11 for 2 h (Figure 3.3a). Incubation of the same at 70°C and pH 11 for 2 h resulted in a granular structure with no appreciable aspect ratio and dimensions were ca. 50 nm (Figure 3.3b).

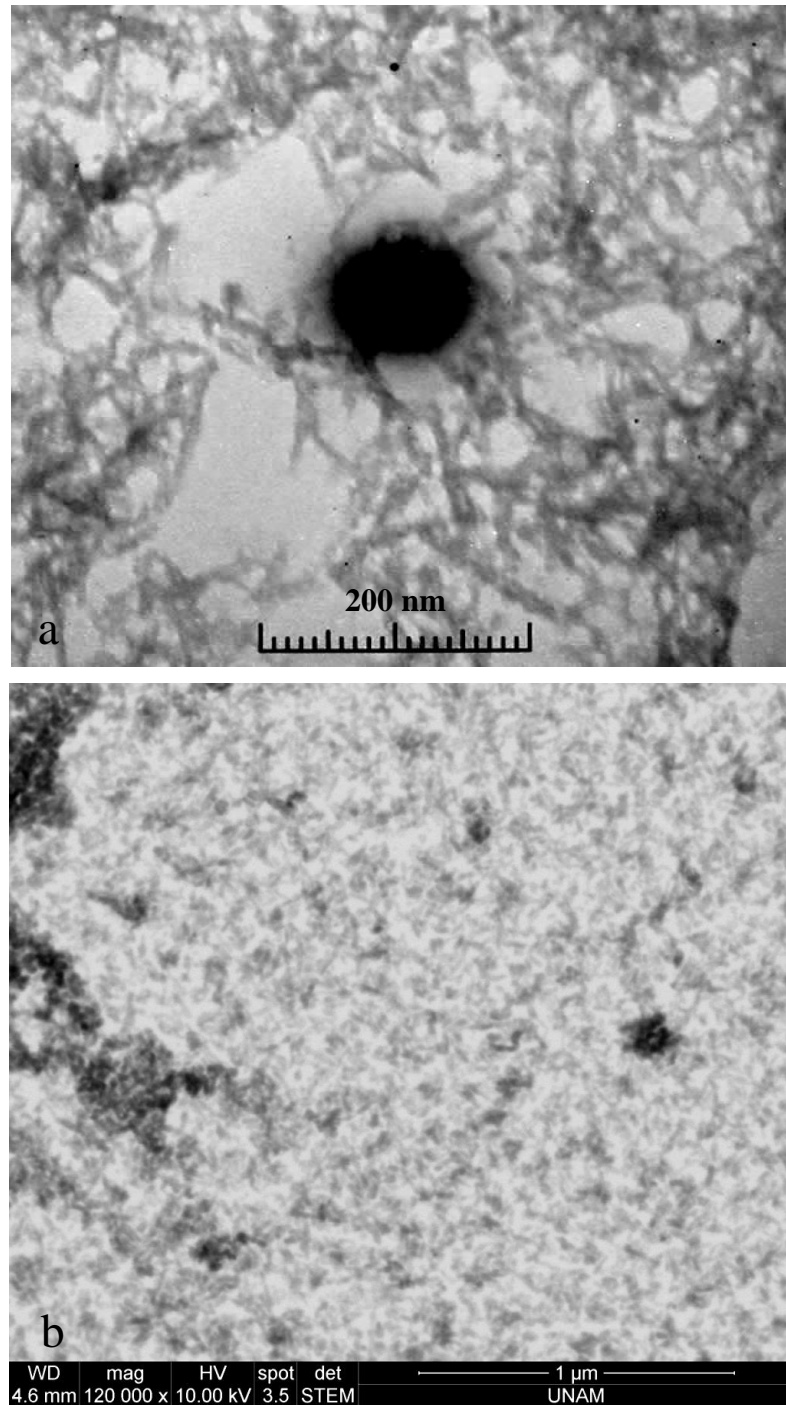


Figure 3.3. Electron microscopy images of HAP nanoparticles obtained with the procedure adapted from Yubao *et al.*, 1994. Particles obtained after incubation at a) T: RT, pH: 11, t: 2 h (TEM (Transmission Electron Microscope) image, x100,000), b) T: 70°C, pH: 11, t:2 h (S-TEM (Scanning-Transmission mode in SEM) image, scale bar: 1 μm, x120,000).

The third type, which was suitable for our purposes was obtained after treating the grains previously obtained in 70°C incubation for a further 2 h at 140°C. Nanorods having a proper aspect ratio, 50 – 150 nm in length and 5 – 20 nm in diameters were obtained (Figure 3.4a and 3.4b). It was possible to disperse in ethanol by ultrasonication without significant aggregate formation.

Energy dispersive X-ray spectroscopy (EDS or EDX) results showed that the obtained nanorods have a Ca/P ratio of 1.56 (Figure 3.5). This value is obtained by dividing the Ca and P atomic contents (shown as At% in the Figure 3.5). This is a so-called “calcium deficient hydroxyapatite”, because when the Ca/P ratio is compared to that of hydroxyapatite’s 1.67 – it is somewhat lower. Even though this calcium phosphate is not hydroxyapatite for convenience, it will be referred to as HAP.

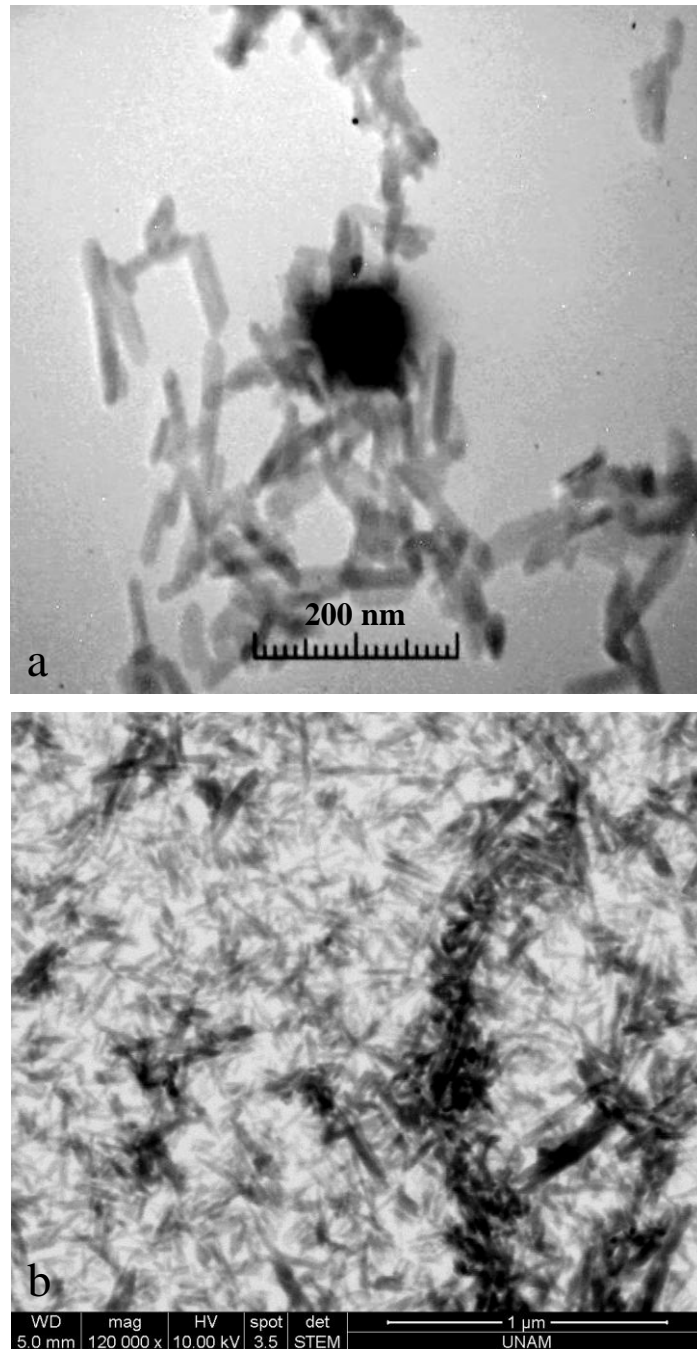
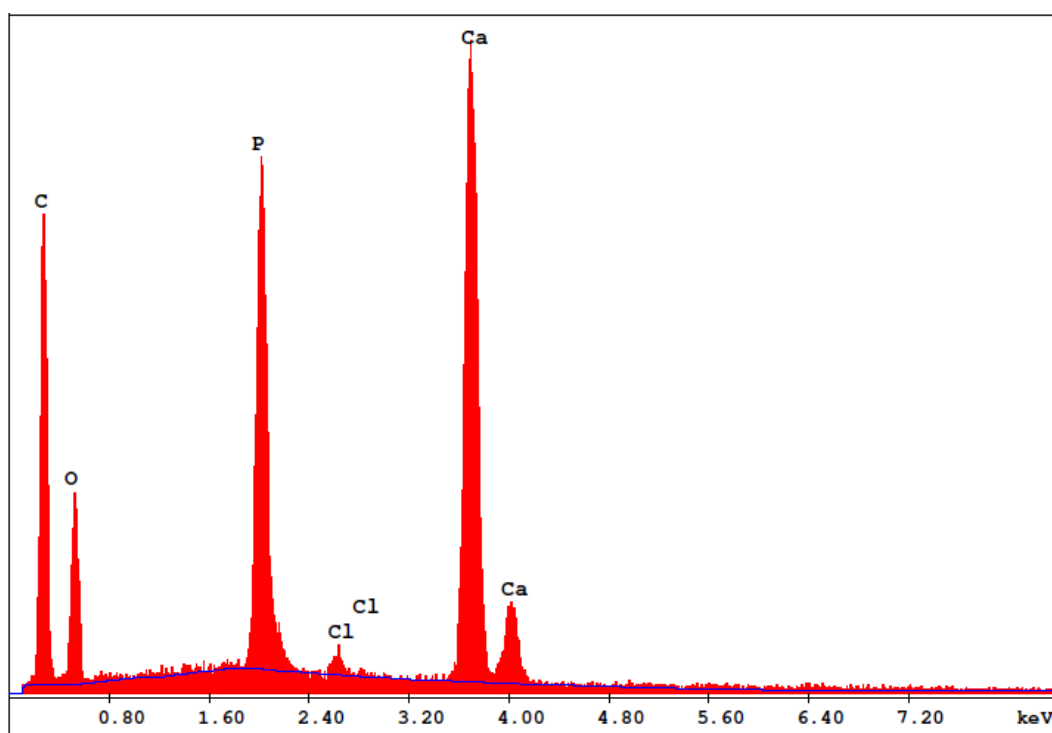


Figure 3.4. Electron microscopy images of hydrothermally synthesized (at 140°C) HAP nanorods. a) TEM image, x100,000, b) S-TEM image, x120,000.



Element	Wt %	At %	K-Ratio	Z	A	F
C K	49.88	66.49	0.1546	1.0278	0.3015	1.0003
O K	20.50	20.52	0.0286	1.0106	0.1382	1.0001
P K	9.66	4.99	0.0830	0.9319	0.9151	1.0070
ClK	0.48	0.22	0.0041	0.9102	0.9286	1.0185
CaK	19.48	7.78	0.1828	0.9394	0.9993	1.0000
Total	100.00	100.00				

Figure 3.5. Energy dispersive X-ray spectroscopy result of the calcium phosphate nanorods obtained after hydrothermal treatment at 140°C.

3.2. Grafting of Lactic Acid on HAP Surface

To improve the chemical compatibility between HAP and PLLA, HAP nanorod surface was modified chemically, by grafting with lactic acid. FTIR spectrum of lactic acid (LA) grafted HAP confirms the presence of LA on the surface of HAP nanorods (Figure 3.6). The FTIR spectrum of HAP shows a band at 1583 cm^{-1} ,

which, in literature (Qiu *et al.*, 2005), is attributed to $-\text{COO}$ vibration in lactate of calcium lactate bonds. The band was not present in the FTIR spectrum of both ungrafted HAP and LA itself.

Surface grafting of LA was also confirmed by comparing carbon and hydrogen contents data (obtained through CH elemental analysis system) for non-grafted HAP nanorods and two separate LA grafted HAP nanorod samples (Table 3.1). The difference between these two LA grafted HAPs is the starting concentrations of LA during the grafting reaction, where LA to HAP ratios (w/w) were 1.2 and 2.2 at the onset of grafting reaction. The results also show that the level of grafting is the same regardless of the starting composition.

The proposed mechanism for grafting of LA onto HAP by loss of the $-\text{OH}$ group from HAP, loss of one $-\text{H}$ group from LA and association of Ca^+ and LA^- , releasing a H_2O molecule. For 5 calcium atoms present in simple unit of HAP molecule ($\text{Ca}_5(\text{PO}_4)_3(\text{OH})$), there is only one hydroxyl group. Therefore, association of only one LA is possible with each HAP unit.

It is seen in Table 3.1 that the 2.12% (w/w) C represents that a fraction of 5.24 % (w/w) LA, is present in LA-grafted HAP. Theoretically, in order to have 1 LA molecule to be bound to one HAP unit, the weight ratio of LA had to be 15.5 % (w/w). So this result indicates that a LA grafting efficiency of 33% was achieved.

In another batch of experiment where LA to HAP starting ratio in the grafting reaction was increased from 1.2:1 to 2.2:1, the carbon weight percent did not raise at all (still 2.12%, w/w). Therefore, 15.5% was also found to be the maximum grafting efficiency that could be obtained under these reaction conditions.

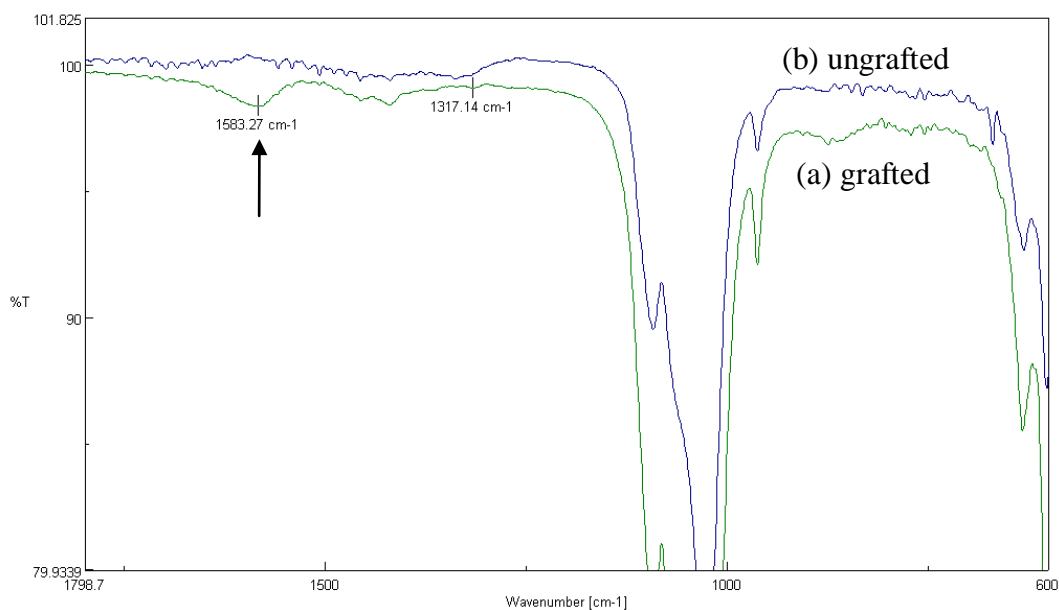


Figure 3.6. ATR-FTIR spectra of lactic acid surface grafted (a) and non-grafted (b) HAP nanoparticles. Arrow indicates the peak for -COO vibration that would be found in calcium lactate molecule.

Table 3.1. Elemental analysis results of non-grafted and LA grafted HAP samples with different LA to HAP starting ratios.

LA:HAP ratio (w/w)	Composition of HAP (% w/w)	
	C	H
Pristine HAP	0.62	0.70
LA	40.0	6.67
1.2:1	2.12	0.78
2.2:1	2.12	0.77

3.3. Spinnability Tests of Polymers

The spinnability test results showed that, poly(3-hydroxybutyrate-co-3-hydroxyvalerate) (PHBV, 3-hydroxyvalerate content 8%, w/w) would be processed with this melt spinning technique. The melting temperature (T_m) for PHBV is given in the literature as 143 – 160°C in the literature (Ferreira *et al.*, 2003), but the polymer could not be spun at this temperature. Only when the temperature was increased to 202°C, it was possible to produce ca. 60 cm long spins. Poly(L-lactide) (PLLA) was also tested for its spinnability. No spinning occurs around the T_m of PLLA (173 -178°C, Bronzino, 2006) but when the temperature was raised to 245°C, spins longer than 3 m without break could be obtained. Therefore, PLLA was also shown to be processable with melt spinning technique.

3.4. Production of Polymer – HAP Nanorod Composite Fibers

3.4.1. Melt Spinning of Polymers

After the spinnability tests, a custom-made melt spinning system –originally designed for textile fiber production using standard commercial polymers– was evaluated for its suitability for the production of PHBV or PLLA fibers, or their composite fibers containing HAP. The production temperatures were varied from 143°C to 202°C for PHBV and from 173°C to 245°C for PLLA.

Even though nitrogen gas atmosphere was supplied (to prevent thermal degradation by eliminating oxygen from the system), the trials with both polymers resulted in charred polymers because of insufficient control of temperature and/or low intra-barrel pressure. No spinning through the spinnerets could be achieved. There may be several possible reason for the failure: The melt spinning system was originally designed to process commercial engineering polymers, such as polyethylene, polyamide, and the temperature and pressure controls of the system were not precise and stable. The fluctuation in these processing parameters could

be a possible reason for the inability to spin and the degradation of these temperature sensitive, biodegradable polymers. Another possible reason would be the insufficient priming of the system with the polymers. Biodegradable polymers are much more expensive compared to the commercial, high volume polymers like polyethylene or polypropylene and melt spinning tests were done with only 3-4 g of polymer which might not be sufficient for the ram to apply adequate pressure on the molten polymer to push it through the spinnerets. In conclusion, for use of this technique with biodegradable polymers, the above mentioned points have to be considered. This method was abandoned.

3.4.2. Wet Spinning of Polymers

3.4.2.1. Wet Spinning of PHBV

Using the parameters in Table 3.2, PHBV fibers with 60 to 120 μm diameters were obtained (Figure 3.7). The table shows the effect of polymer solution concentration and injection rate on fiber diameters. No real correlation between the parameters and fiber thickness were observed. The fibers produced did not have sufficient strength for mechanical evaluation. This technique was also abandoned for the production of PHBV based reinforced fibers to be used in implants with high mechanical demands.

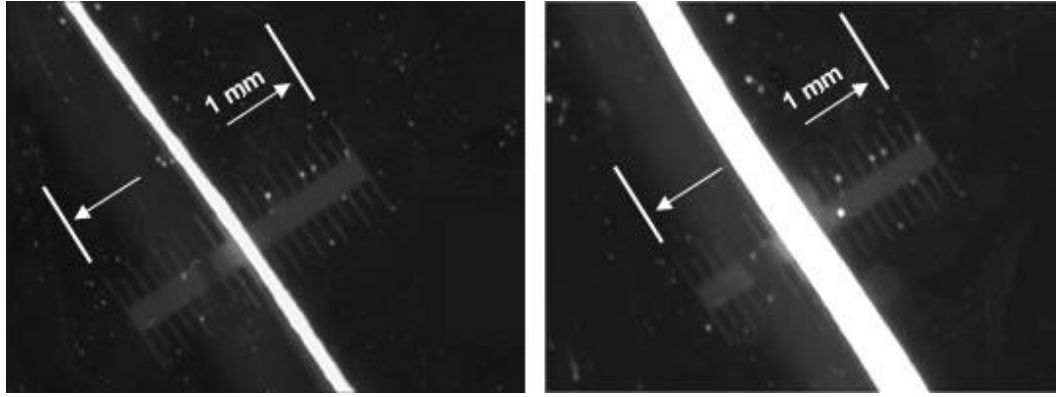


Figure 3.7. Stereomicrographs showing the effect of injection rate on PHBV fiber diameter. a) concentration: 0.15 g/mL, injected rate: 5 $\mu\text{L}/\text{min}$. b) concentration: 0.15 g/mL, injection rate: 200 $\mu\text{L}/\text{min}$. The scale bar below the fibers is 1 mm long.

3.4.2.2. Wet Spinning of PLLA

PLLA was also wet-spun using concentrations and injection rates, and fibers with 40 - 120 μm diameters were obtained (Table 3.3). The most concentrated solution that could be injected was found to be 0.1 g/mL in chloroform. Higher concentrations were too viscous to be injectable. Effects of these parameters on fiber diameter are shown in Table 3.3.

After PLLA wet spinning experiments, it was seen that all PLLA fibers had much better mechanical properties (Table 3.3) compared to PHBV fibers because at least PLLA fibers could be tensile tested. They were tested with the mechanical test machine according to ASTM D3379-75 test standard.

Table 3.2. Effect of injection rate, PHBV concentration and HAP nanorod contents on wet spun fiber diameter (n=5).

Polymer concentration (g/mL) and content	Injection rate ($\mu\text{L}/\text{min}$)	Fiber diameter (μm)
0.1 / PHBV	5	70
0.1 / PHBV	10	120
0.1 / PHBV	20	70
0.1 / PHBV	50	100
0.1 / PHBV	100	70
0.1 / PHBV	200	70
0.1 / PHBV	500	120
0.15 / PHBV	5	60
0.15 / PHBV	10	70
0.15 / PHBV	20	65
0.15 / PHBV	50	100
0.15 / PHBV	100	100
0.15 / PHBV	200	120
0.1 / PHBV + 10% (w/w) HAP	20	70
0.1 / PHBV + 10% (w/w) HAP	50	70
0.1 / PHBV + 10% (w/w) HAP	75	70
0.1 / PHBV + 20% (w/w) HAP	5	70
0.1 / PHBV + 20% (w/w) HAP	10	70
0.1 / PHBV + 20% (w/w) HAP	50	70
0.1 / PHBV + 20% (w/w) HAP	100	80

For pure PLLA polymer, best tensile properties were observed with 0.1 g/mL pure PLLA (50 μ L/min injection rate), which showed an Ultimate Tensile Strength (UTS) of 45 MPa and a Young's Modulus of 1.13 GPa. For PLLA - HAP composites, the best result was obtained with 5% HAP content (100 μ L/min injection rate). UTS was 30 MPa and Young's Modulus was 2.0 GPa for this composite. The introduction of HAP into the composites almost doubled the Young's Modulus values of pure PLLA (from 1.13 GPa to 2.0 GPa) but the UTS of the composite was decreased by 1/3 (from 45 MPa to 30 MPa).

Thus, these values are not close to those of cortical bones such as human femur – one of the strongest materials in the body (with UTS of 135 MPa and Young's Modulus of 17 GPa, in longitudinal direction, Reilly and Burstein, 1975). These show that in its current wet spun fiber form, the composite has almost 35% of the UTS and 12% of the Young's Modulus values of the compact bone. The composite designed from the wet spun fibers can find use as a reinforcement in the production of bone plates to be used in low weight bearing bones, such as femoral cancellous bone (UTS: 6 MPa, Young's Modulus: 0.5 GPa, Pietrzak *et al.*, 2006) or spongy bone (maximum compressive strength: 1.3 – 12 MPa, Young's Modulus: 0.17 – 0.5 GPa, Evans, 1969), or intervertebral fusion devices (vertebrae compressive strength 6.2 MPa or 3 MPa for 20–40 or 60–80 years old persons, respectively, Mathey *et al.*, 1993).

3.4.2. Extrusion of Polymers at Sub-Melting Temperatures

In the extrusion of PHBV with a custom made extruder to obtain fibers, the optimum temperature was found to be 150°C in order to obtain a smooth and continuous extrudate. Initially a die with an orifice of 2 mm diameter and 1 cm path length was tested. However, this die produced curvy and inhomogeneous fibers that were not suitable for mechanical testing.

Table 3.3. Effect of injection rate, PLLA concentrations, and HAP nanorod content on wet spun fiber diameter (n=5).

Polymer concentration (g/mL) - content	Injection rate ($\mu\text{L}/\text{min}$)	Fiber diameter (μm)	UTS (MPa)	Young's Modulus (GPa)
0.05 / PLLA	50	40	44	*
0.05 / PLLA	100	57	57	*
0.1 / PLLA	50	100	45	1.13
0.1 / PLLA	100	100	47	0.95
0.05 / PLLA + 10% (w/w) HAP nanorods	100	100	39	0.78
0.05 / PLLA + 10% (w/w) HAP nanorods	200	85	18	0.31
0.1 / PLLA + 5% (w/w) HAP nanorods	100	120	30	2.00
0.1 / PLLA + 10% (w/w) HAP nanorods	100	120	23	0.50

*: Young's Modulus values not calculated due to absence of a linear elastic region in the stress-strain plots.

Therefore, the design was changed to increase the path length to 3 cm, while the diameter of the orifice stayed the same (2 mm). This design eliminated both the problems, and straight and uniform extrudes with ca. 2 mm diameter were produced.

With this method, pure PHBV rods and PHBV-HAP composite fibers with 10% (w/w) HAP from three different sources (synthesized HAP nanorods, commercial

amorphous HAP nanoparticles, and commercial HAP microrods were incorporated into different composite rods) were produced.

The SEM images of longitudinal sections of PHBV – HAP composites produced with the same approach are shown in Figure 3.8. Synthesized HAP nanorods (sHAP) within the composites showed a general tendency to align parallel to the extrusion axis (Figure 3.8 a). The bulk of the material was solid polymer without voids or pores. On the other hand, commercial HAP nano-microrods with heterogenous size distribution (nmHAP) did not show any alignment with the extrusion axis (Figure 3.8 b). This may be due to the presence of a large amount of particles with irregular shapes and a small fraction with the fiber shape, which might have interfered with the flow of the extruding polymer and prevented alignment. This may also be the reason of the large numbers of voids observed in the bulk material.

Stereomicrographs of PHBV and PHBV – HAP composites containing sHAP and pHAP revealed very smooth surfaces without any cracks on the surface or voids within the bulk (Figure 3.9). However, the nmHAP were seen to have deep surface cracks (Figure 3.9 d). These microcracks easily propagated even under manual stress and failed, thus preventing proper and reliable mechanical testing. Conversely, UTS and Young's Modulus of PHBV or its composites obtained with both commercial and synthesized nano HAPs were stronger due to the absence of these cracks in the structure. Addition of both nano HAPs to the fiber structure increased the Young's Modulus by more than 60%. While composites with pHAP did not cause a change in the UTS, sHAP composites decreased the UTS value ca. 19%. The mechanical properties of extruded composites and the polymers are collectively presented in Table 3.4.

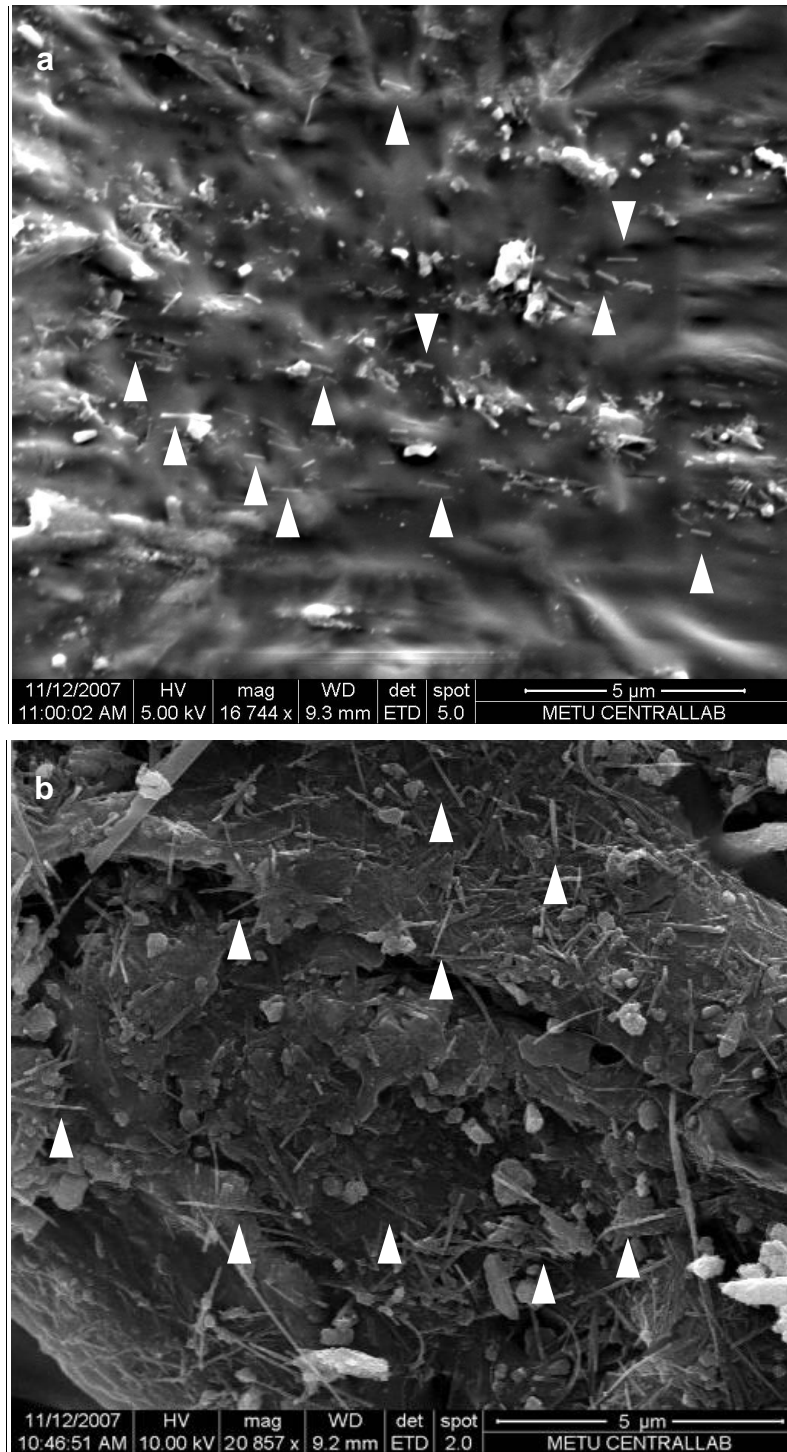


Figure 3.8. SEM micrographs of longitudinal sections of PHBV-HAP composites produced by extrusion at sub-melting temperatures. (a) Composites produced with sHAP (arrowheads). (b) Composites produced with nmHAP (arrowheads).

Table 3.4. Tensile properties of PHBV – HAP composites. (n=5).

	UTS (MPa)	Young's Modulus (GPa)
PHBV	34.6 ± 2.5	1.11 ± 0.09
PHBV – 10%(w/w) sHAP	28.1 ± 1.9	1.61 ± 0.08
PHBV – 10%(w/w) pHAP	37.1 ± 2.1	1.67 ± 0.13
PHBV – 10%(w/w) nmHAP	n/a	n/a
Human femur *	121	17.2

* Park, 1979.

3.4.3. Composite Fiber Production with Capillary Rheometer

3.4.3.1. PHBV – HAP Composite Fiber Production with Capillary Rheometer

During the spinnability test conducted as a preliminary step for melt spinning experiments, the first PHBV spins were obtained at temperatures ca. 195°C. Around this temperature, however, the polymer had started to degrade and lost its strength. Therefore, extrusion trials were started at 160°C with gradual increases. At 165°C, the PHBV started to come out continuously but considerable surface roughness. It is reported that melt flow instabilities are associated commonly with such rough surfaces. In order to correct this, the temperature was increased further until 175°C, where the mobility of the polymer chains was sufficiently high and the polymer started to come out of the die, free from the control of piston pressure. So, this was the ceiling point for any shear application, and temperature was again started to be gradually decreased for optimization. Eventually the best processing conditions were determined to be 4 mm/min piston speed at 168°C, giving a smooth surfaced fibrous product with 0.36 mm diameter. Under these conditions, the load cell showed force values as high as 800 – 850 N. Ability to achieve continuous material production (without break) is a significant advantage (Figure 3.10).

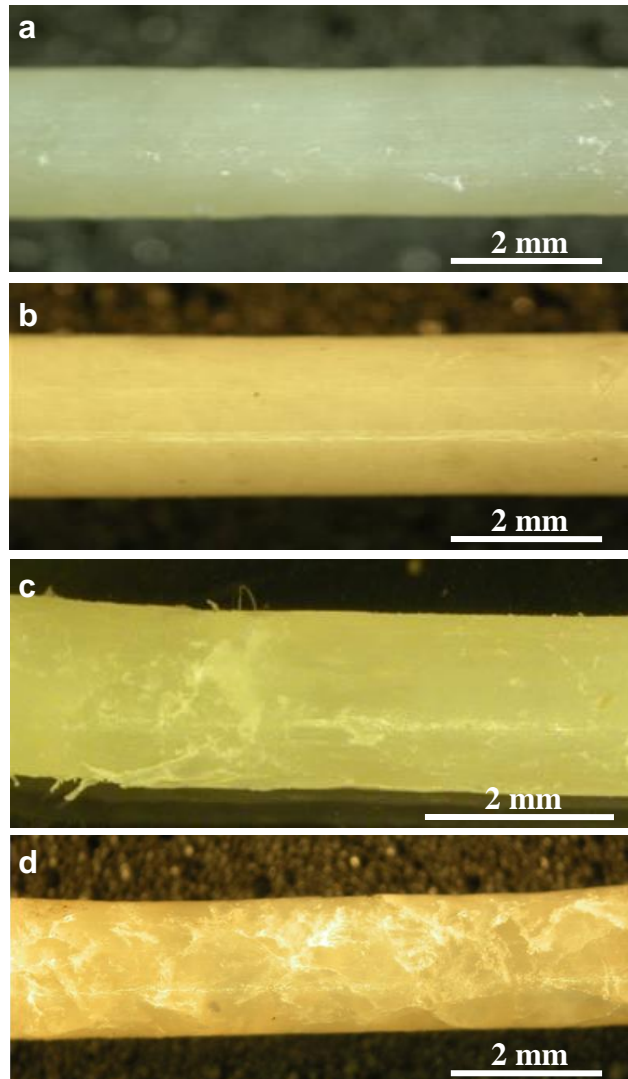


Figure 3.9. PHBV and PHBV – HAP composite rods extruded at sub-melting temperatures. (a) PHBV, (b) PHBV-10% synthesized HAP nanorod (sHAP) composite, (c) PHBV-10% commercial, amorphous HAP nanoparticle (pHAP) composite, (d) PHBV-10% commercial HAP nano-microrod (nmHAP) composite.

Mechanical test results of the PHBV filaments produced under the above conditions were undesirably low. Ultimate Tensile Strength (UTS) was 46 MPa and Young's Modulus was 203 MPa. The reason for this was oxidation and subsequent degradation as was evident from the light-brown color of the product, in contrast to the white color of the unprocessed polymer. Thus, the processibility of this batch and type of PHBV was found to be inadequate for the targeted use and was abandoned.



Figure 3.10. A ca. 2 m long continuous PHBV filament produced with capillary rheometer. Fiber diameter is 33 μm , scale bar is 2 cm.

3.4.3.2. PLLA – HAP Composite Fiber Production with Capillary Rheometer

Melting temperature of PLLA is given to be between 173 to 178°C in the literature (Bronzino, 2006). PLLA has ca. 33% crystallinity, which is higher than that of PHBV and this causes it to be processible at temperatures higher than that of

PHBV. This was also evident from the previous observations with the spinnability test, in which PLLA gave spins at temperatures around 245°C.

Capillary rheometer was also employed in the formation of fibers using PLLA. Optimum processing temperature and rate for PLLA was determined in this instrument. The optimization was started at 160°C with gradually increasing the temperature while the free flow of the polymer is achieved at 200°C. First continuous product formation was at 210°C but with a rough surface. Smooth and continuous product was obtained at 235°C with 6 mm/min piston speed. Under these conditions, the load cell showed a force of around 825 N. These conditions were selected as the processing conditions from this point onwards. As a results, continuous fibers with diameters between 0.65 mm to 0.85 mm were obtained.

Synthesized HAP nanorods (sHAP) as is or grafted with LA (LA-sHAP), and commercial amorphous HAP nanoparticles (pHAP) were used to produce different composite fibers using capillary rheometer. Addition of any of this HAPs caused a decrease in the optimum processing temperature earlier determined. It was found that HAP content of the mixture was inversely related to the optimum processing temperature; decreasing from 235°C for pure PLLA to as low as 180°C for 50% HAP content. This can be explained by the fact that presence of HAP among the macromolecules decreases the extent of their association causing an increase in the flow of the material.

In order to determine the tensile properties of the PLLA – HAP composites, tests were carried out using the mechanical tester. The results are presented in Figures 3.11 and 3.12. As shown in Figure 3.11, composites with all HAP types and contents showed lower UTS values than the PLLA-only fibers. The presence of filler materials (the HAP nanoparticles) within a polymer matrix act as plasticizers in the macro structure and increase processibility by decreasing the glass transition temperature (T_g) of polymers. In general, presence of fillers decreases mechanical strength values (Roeder *et al.*, 2008) and this is also valid for the results obtained

in this study. Increasing the HAP content of each HAP type resulted in a gradual decrease in UTS.

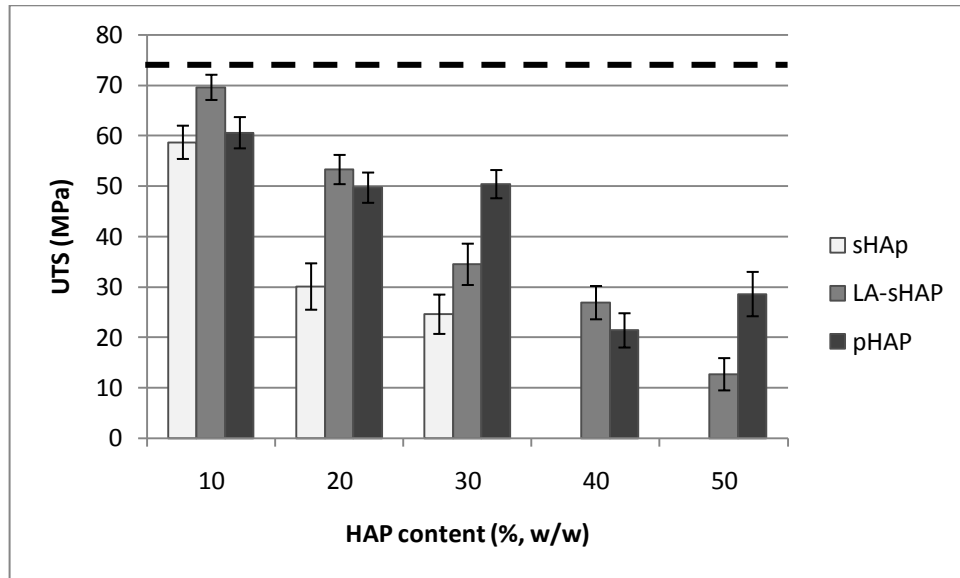


Figure 3.11. UTS values of PLLA-HAP composite fibers prepared with capillary rheometer. Dashed line represents UTS value of PLLA-only fibers (73.9 ± 5.9 MPa). (n=5).

Unlike the UTS values, Young's Modulus values appear to present maximum values at around 30% loading (Figure 3.12). The sHAP nanorod containing composites have the optimum composition somewhat earlier (at 10%). Ceramic particles are much stiffer (have higher Young's Modulus values) than polymers and they resist deformation up to a higher extent than the polymer itself. This is the reason for addition of HAP particles into the polymers to produce stiffer composites. In theory, for increasing the tensile mechanical properties by conduction of this higher stiffness to the whole composite fiber is only possible in the case that polymer and HAP particles do have some sort of chemical

association. This situation is evident from the observation that composites containing LA grafted HAP nanorods have higher Young's Modulus values compared to those composites containing non-grafted types of the same HAP nanorods (only except the 10% HAP loaded composites) (Figure 3.12). Therefore, compatibility between PLLA and HAP nanorods increases with chemical grafting of HAP with LA.

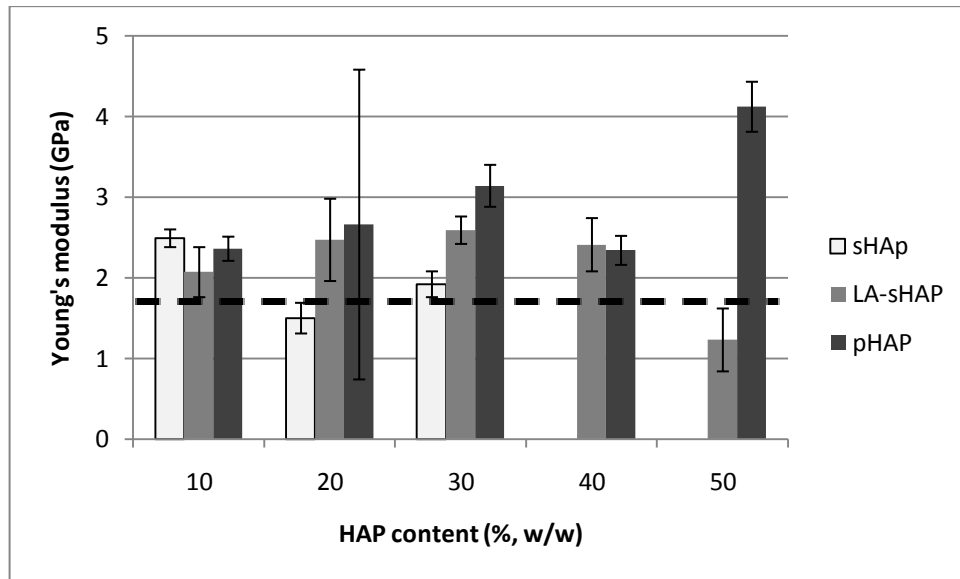


Figure 3.12. Young's Modulus values of PLLA-HAP composite fibers prepared with capillary rheometer. Dashed line represents Young's Modulus value of PLLA-only fibers (1.75 ± 0.04 GPa). (n=5).

Although the 4.12 GPa value for 50% pHAP appears to be an anomaly, these composites with amorphous HAP particles had higher values than the ones with both non-grafted and LA grafted HAP nanorods at each weight ratio tried. This is probably due to the fact that amorphous HAP particles used in the composites had rough and irregular surfaces (Figure 3.14 c). Hydroxyapatite powder with such

rough surfaces can help mechanical interlocking between polymer molecules in the bulk and improve tensile properties (Cheang and Khor, 2003). This is not observed with fillers with smooth surfaces, as is the HAP nanorods synthesized and used in this study (Figures 3.14 a and b).

UTS value of the produced pure PLLA fibers were close to other results in the literature. Weir et al. (2004) produced PLLA (Resomer L210) rods of 2 mm diameters with extrusion and a following annealing. The resulting rods had UTS of 64.3 MPa and Young's Modulus of 0.67 GPa. Lewitus *et al.* (2006) produced PLLA films (0.1 mm thickness) by extrusion and obtained UTS of up to 57 MPa and Young's Modulus of up to 1.79 GPa.

Orientation of polymer molecules within the bulk has a strong influence on mechanical properties. For example, the tensile strength of polypropylene could increase more than 10 times after orientation (Nadella et al., 1978). Based on this knowledge, Yu *et al.*, (2008) prepared polylactide films of 0.16 – 0.70 mm thickness and 5 mm width in order to see the effect of die-drawing (0 – 200 cm/min) on the tensile properties of polylactide. They obtained drawn polylactide sheets with UTS values of 45 – 56 MPa and Young's Modulus values of 2.3 – 2.9 GPa. These results showed that tensile properties of polylactides did not increase significantly and they are comparable our results.

When comparing the tensile properties of polymers, it should be borne in mind that dimensions (thickness or diameter) of the test samples may cause great variation on the results (even though obtained stress values are divided to the cross-sectional area of the specific sample) (Dyl'kov, 1966). Therefore, it may not be possible to directly compare results obtained with the same polymeric material for different geometries.

In Figure 3.13, UTS and Young's Modulus values were plotted against the composite's lactide coated HAP nanorod content and an opposite trend is observed between these two. Increasing the fraction of any type of HAP in the composites

decreased the UTS values. This is expected since presence of HAP particles between the polymer macromolecules decreases the polymers' crystallinity, and therefore, its mechanical strength.

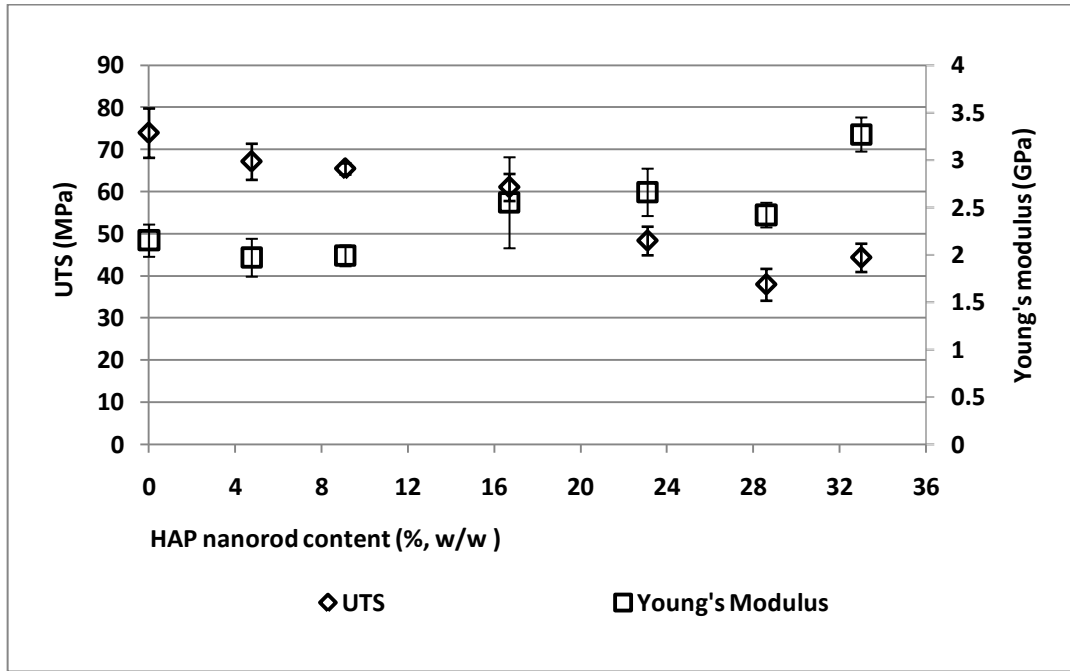


Figure 3.13. The variation of ultimate tensile strength and Young's Modulus values of the PLLA composite fibers with changing content of LA grafted HAP nanorods. (n=5).

This trend, the decrease of UTS with increasing HAP content was less severe in composites containing LA grafted HAP nanorods compared to the ones containing non-grafted HAP (Figure 3.11). This supports the expectation that presence of molecular association between PLLA and LA that is chemically grafted onto HAP particles. The 40% and 50% non-grafted HAP containing composites were very fragile and easily crumbled during handling them. However, composites containing the same amount of LA grafted HAP were much stronger and could be

handled much better. UTS values of the composites containing commercial amorphous HAP nanoparticles were mostly lower than those of LA grafted HAP. Eventually at higher loadings they seem to perform better.

3.4.3.3. SEM Investigation of the HAP Nanoparticles

Micrographs of non-coated synthesized HAP loaded nanorods (sHAP), LA coated synthesized HAP nanorods (LA-sHAP), and commercial amorphous HAP nanoparticles (pHAP) are shown in Figure 3.14. As observed in these figures, synthesized HAP particles (Figure 3.14. a and b) have rod shapes that would be appropriate for alignment of them within polymer matrices. Particle size and shape show great homogeneity. Both have very smooth surfaces without any bulky surface structures to interfere with their mobility within extruding polymer. On the other hand, the commercially obtained pHAP particles have very rough surfaces and inhomogeneous particle size distribution (Figure 3.14. c.)

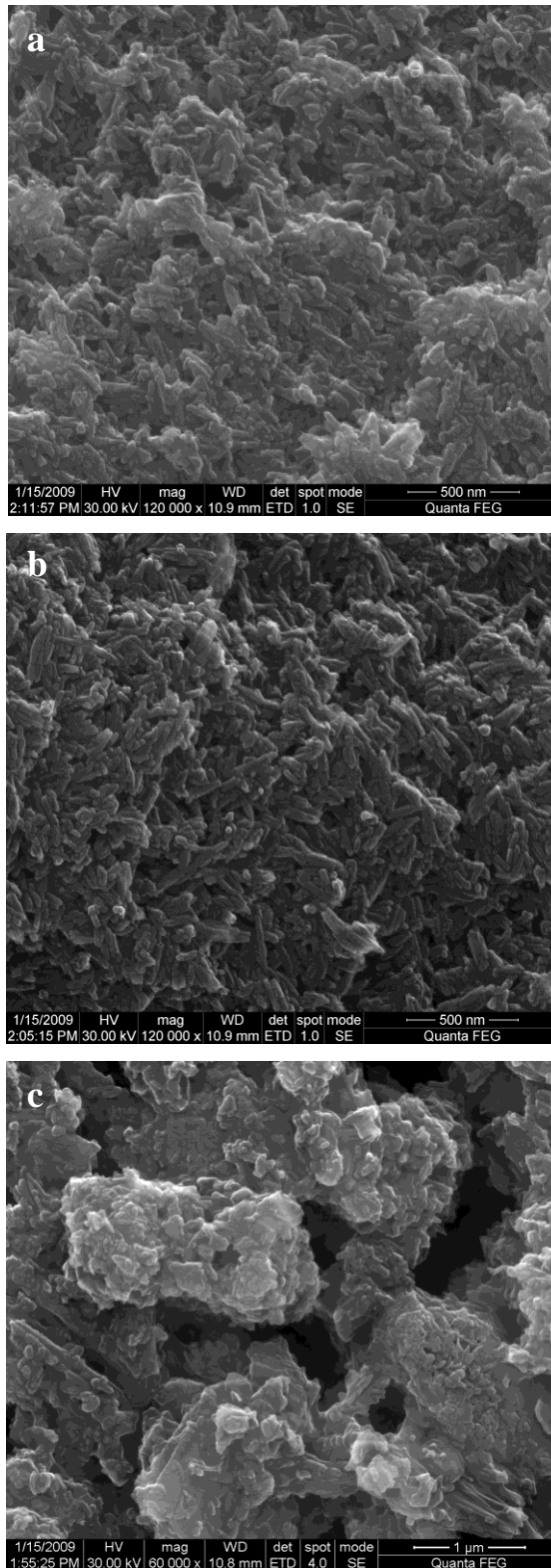


Figure 3.14. SEM micrographs of HAP particles. (a) sHAP, (b) LA-sHAP, and (c) pHAP.

3.4.3.4. SEM Investigation of the Produced PLLA-sHAP Nanocomposite Fibers

Scanning electron microscopy studies of the produced PLLA – HAP composites were done in order to see the distribution and positioning of the HAP nanorods within the polymer bulk. For SEM studies, the nanocomposite fibers were dipped in liquid nitrogen and then fractured to prevent bending and flow that would change the internal structure. Figure 3.15 shows SEM image of the cross-section of nanocomposite fiber that contains 10% LA-sHAP. In this figure, nanorod loaded composites have a homogeneous interior with no voids or gaps. In the figure, “D” denotes the areas deformed polymer regions after high magnification, instead of inherent cracks within the structure. The amorphous particle loaded one (Figure 3.16), on the other hand, shows large particles and distinct gaps between them implying that in the in vivo application this group will behave unpredictably and fail. In Fig 3.15b, the LA-sHAP nanorods are seen to be oriented perpendicular to axis of the rod and besides they do not appear to be aligned.

A similar observation is also made in the Figure 13.17 where the SEM of the longitudinal-section of a composite fiber containing 40% (w/w) non-grafted HAP nanorods is presented. A detailed examination of the figure reveals that, most of the HAP nanorods lie in the same direction with the long axis of the fiber, although they are not 100% parallel to the flow direction. Therefore, it appears that HAP nanoparticles can be aligned, up to a certain extent, parallel to the extrusion axis of composite fiber produced with the capillary rheometer.

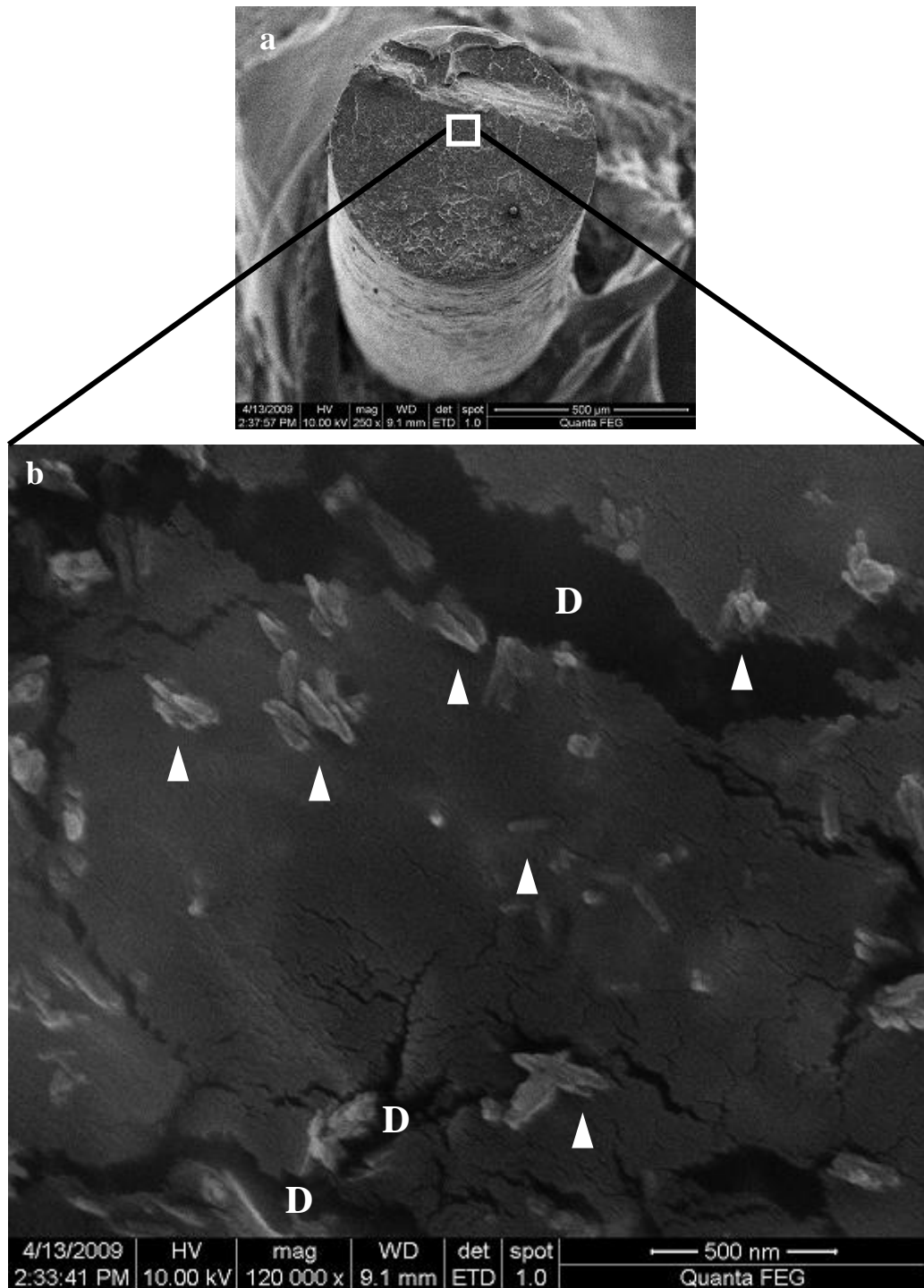


Figure 3.15. SEM image of the cross-section of nanocomposite fiber containing 10% LA-sHAP nanorods. (a) x250, and (b) a portion of (a), x120,000. Arrowheads show some of the HAP nanorods. D: Regions deformed due to high magnification of SEM, obtained with extensive electron beam bombardment.

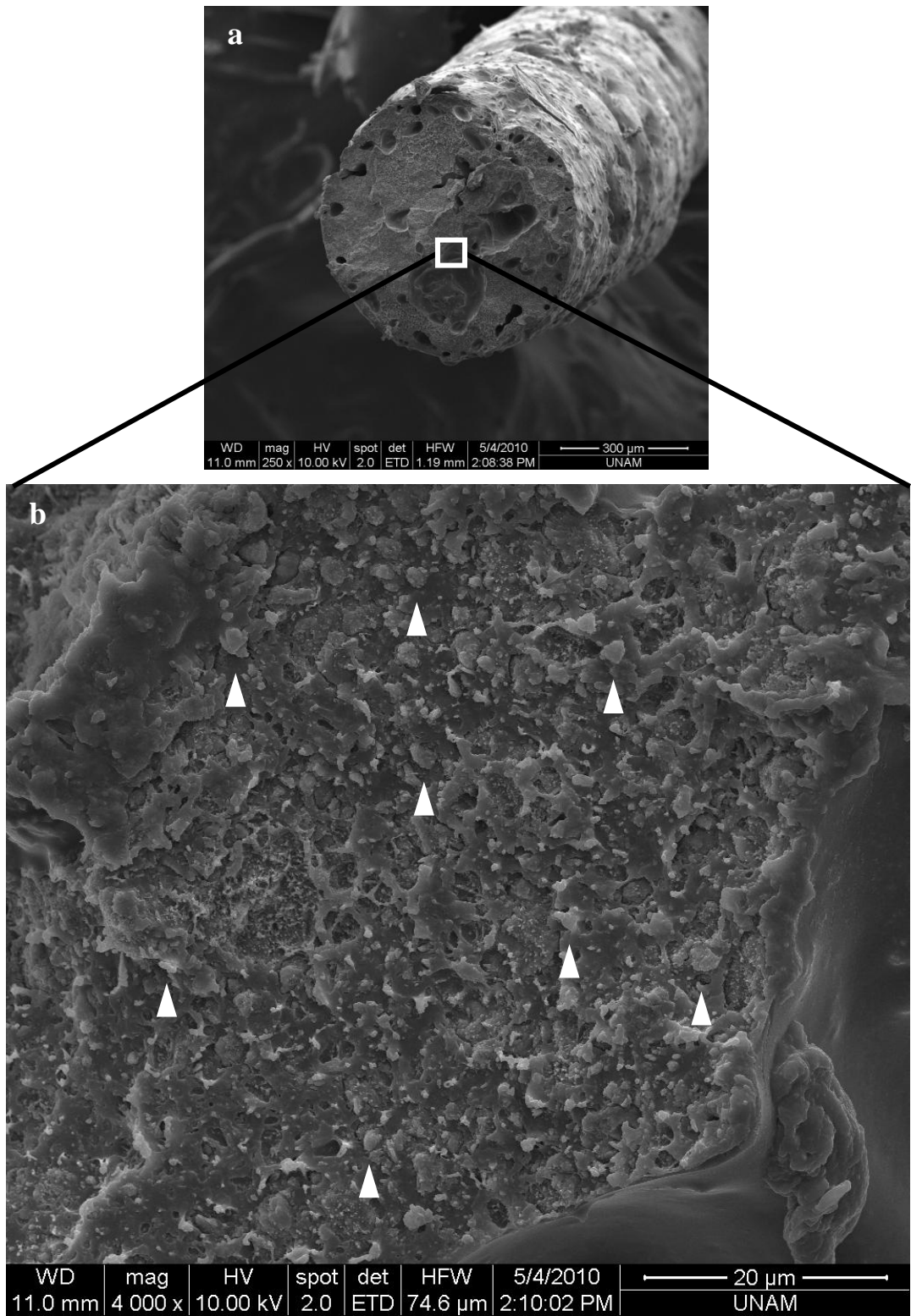


Figure 3.16. SEM image of the cross-section of nanocomposite fiber containing 40% pHAP nanoparticles. (a) x250, and (b) a portion of a, x4000, (c) x60000 magnification of the same location. Arrowheads show some pHAP nanoparticles.

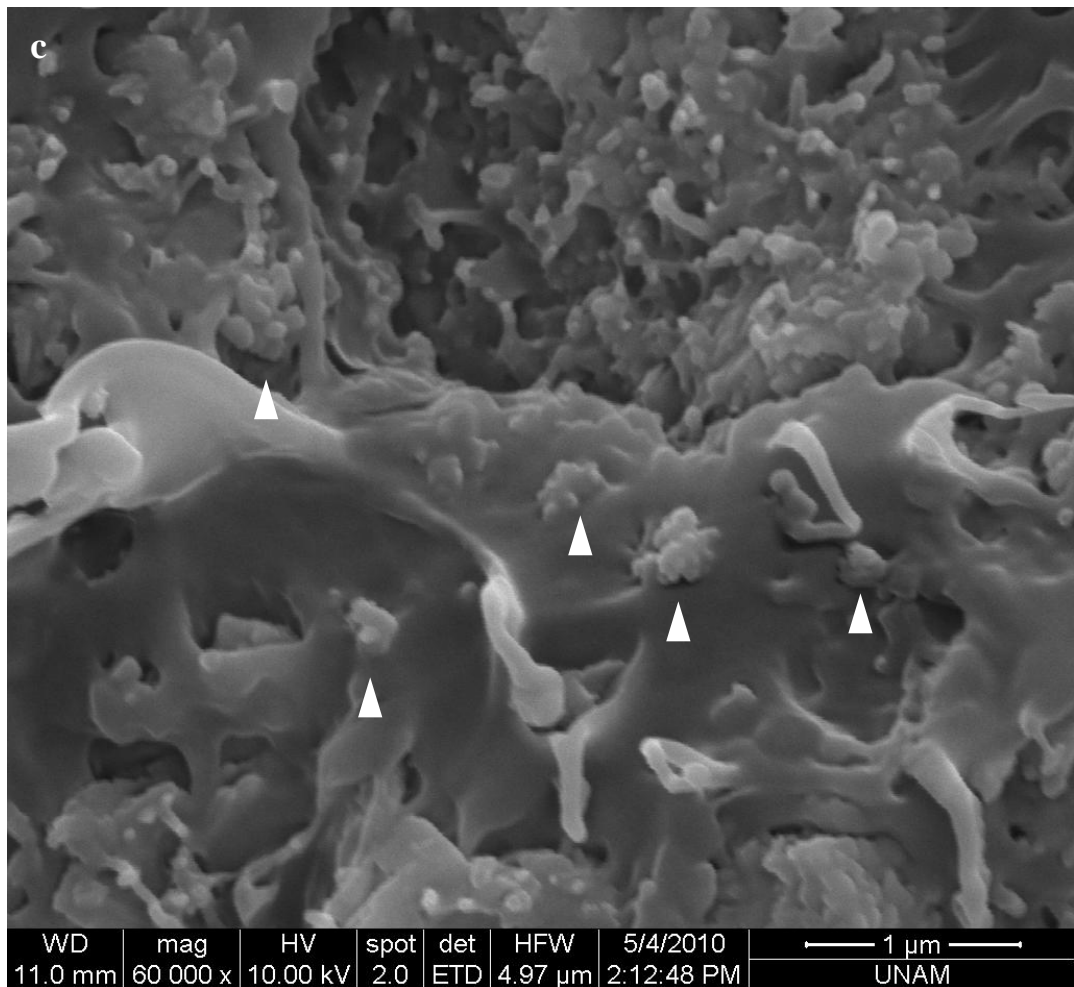


Figure 3.16 (continued). SEM image of the cross-section of nanocomposite fiber containing 40% pHAP nanoparticles. (a) x250, and (b) a portion of a, x4000, (c) x60000 magnification of the same location. Arrowheads show some of the pHAP nanoparticles.

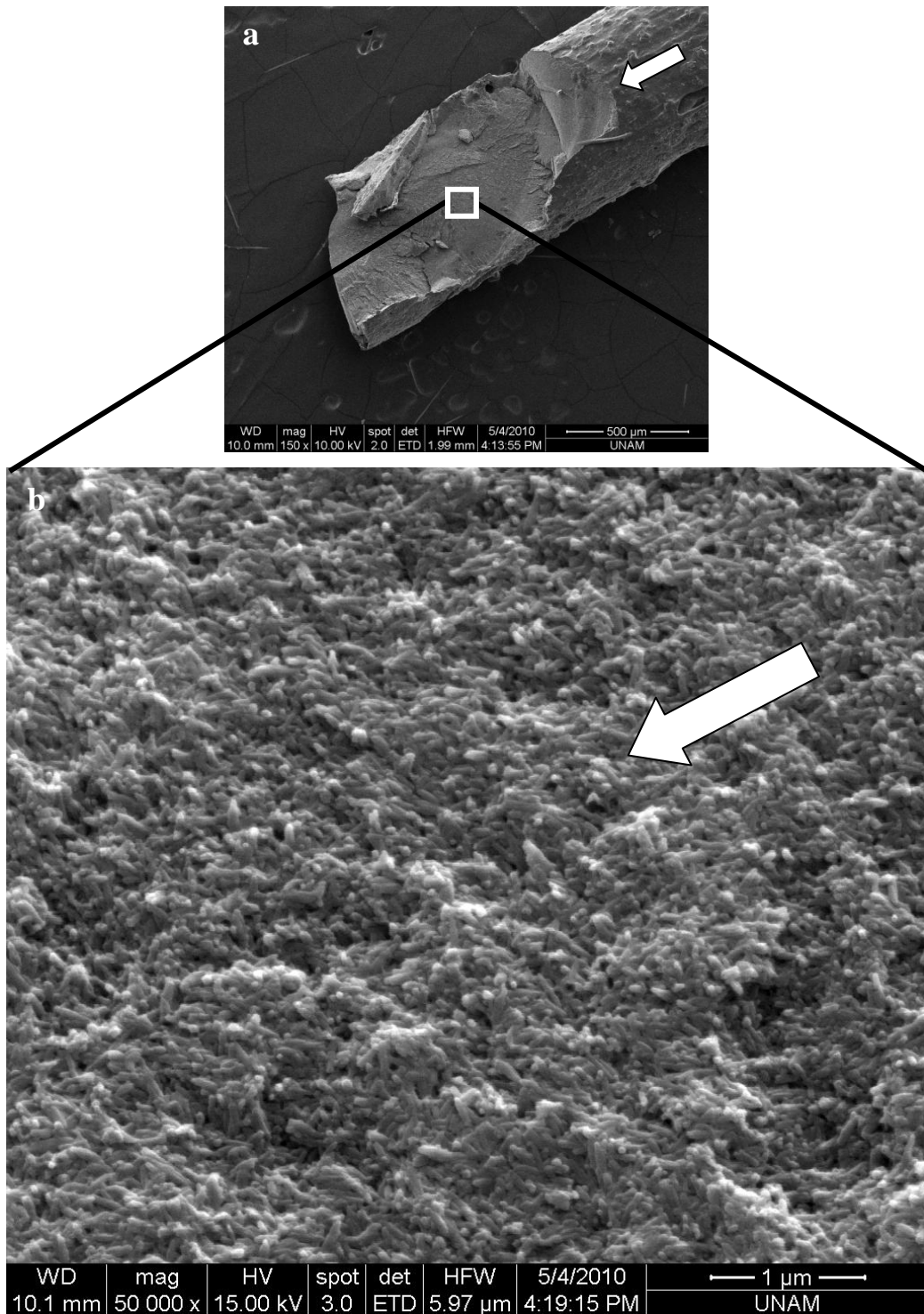


Figure 3.17. SEM of longitudinal section of nanocomposite fiber containing 40% non-grafted HAP nanorods. The certain location in (a) was magnified x150, (b) x50,000 and (c) x100,000. Arrows show extrusion axis.

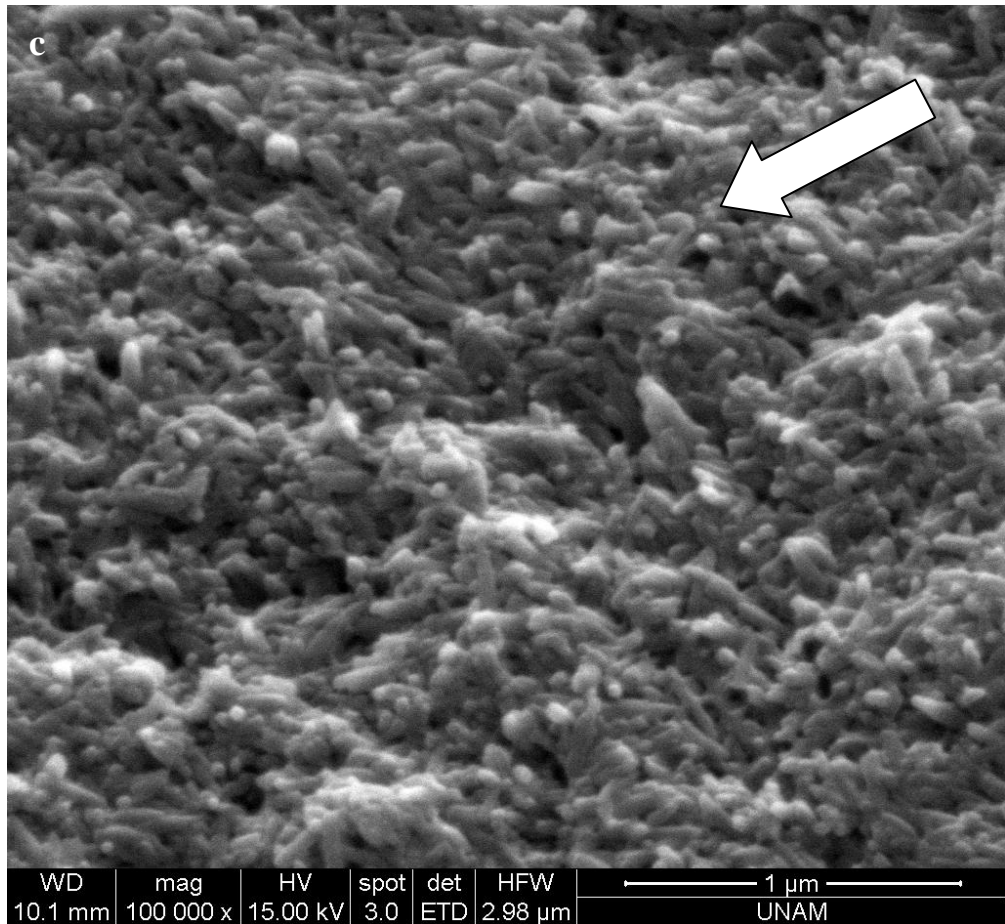


Figure 3.17 (continued). SEM of longitudinal section of nanocomposite fiber containing 40% non-grafted HAP nanorods. The certain location in (a) was magnified x150, (b) x50,000 and (c) x100,000. Arrows show extrusion axis.

3.5. In situ degradation of PLLA – HAP composite fibers

The produced composite fibers are planned to be used in the reinforcement of a biodegradable bone plate system, and therefore, they must be biodegradable. Their *in situ* biodegradation behavior was evaluated in phosphate buffer, to simulate the body fluids. Change of pH in ultra pure water was also investigated.

The changes in pH in the incubation medium (ultra pure water) during 42 days of *in situ* degradation are shown on Figure 3.18. The initial pH of ultra pure water was 6.93 and as seen in the graph, there are significant deviations from this value in pure PLLA or in composites containing 10% (w/w) and 20% (w/w) HAP of any type. However, composites with 40% (w/w) HAP content caused significant decrease in pH.

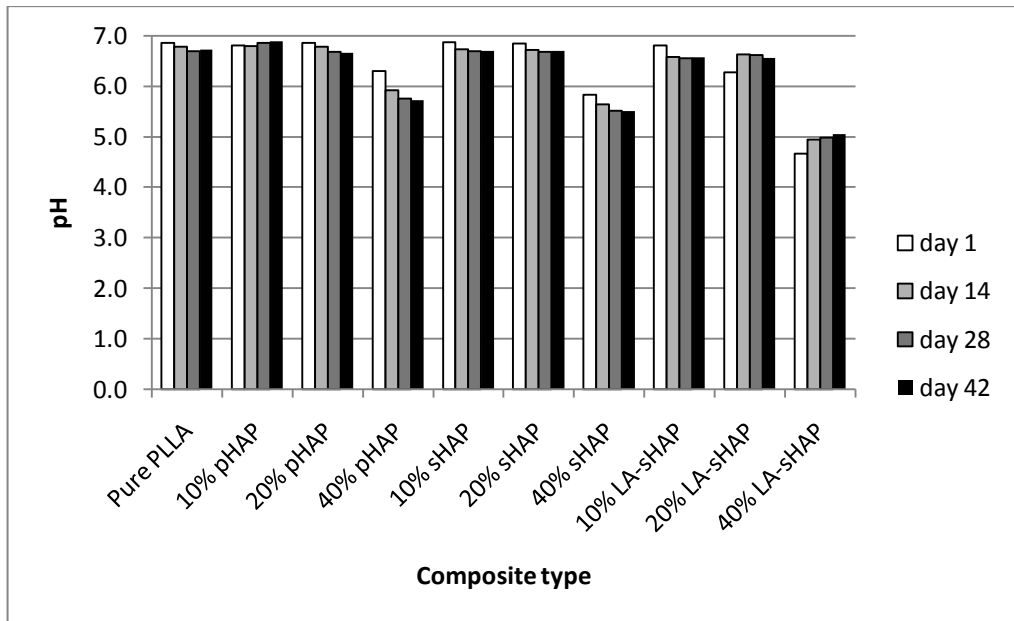


Figure 3.18. pH change in ultra pure water incubation medium during 42 days of *in situ* degradation. pHA_p: commercial amorphous HAP nanoparticles; sHAP: non-grafted synthesized HAP nanorods; LA-sHAP: lactic acid grafted synthesized HAP nanorods.

Being hydrophilic in nature, HAP crystals absorb water. In a polymer – HAP composite, HAP crystals within the polymer structure speed up transfer of water from the surrounding medium into the polymer bulk, compared to a hydrophobic

pure polymer material, like PLLA. Since hydrolysis is the main degradation mechanism for PLLA, such a situation would further speed up the degradation of PLLA – HAP composites.

Therefore, the highest pH drop observed in composites containing the highest HAP ratio in the test (40%, w/w) should be a result of water drawing activity of HAP into the polymer bulk, which caused more hydrolysis in the polymer backbone and release of lactic acid monomer. The most significant pH drop was observed with composite containing 40% (w/w) LA grafted HAP, which is probably also affected by the release of lactic acid grafts on the HAP crystals.

Weight loss (% loss of the original weight) of pure PLLA or composites fibers were also monitored in 0.1 M phosphate buffered saline (PBS) *in situ* for the duration of 42 days (according to ASTM standard F1635: Standard Test Method for in vitro degradation testing). The results are shown in Figure 3.19. As expected, the weight loss increases by the incubation time for composites with HAP of any type. Pure PLLA fibers and composite fibers containing 10% (w/w) HAP of all types did not show a significant weight loss for the complete test duration. This was detectable but very limited for the composite fibers with 20% (w/w) HAP of any sort. Although there is significant weight loss (ca. 2-3%) in composite fibers containing 40% (w/w) of all types of HAP, while the most distinct weight loss was seen in composite fibers with 40% (w/w) LA-sHAP. This is in accordance with the occurrence of the most significant pH loss with this composite type. Therefore, presence of higher amounts of HAP within composite facilitates the degradation. Also, lactic acid grafting of the HAP nanorods further speeds up the process. It was noticed that the composite fibers containing 40% (w/w) LA grafted HAP nanorods left very small particles behind at the bottom of the test tube containing the degradation solution. Also, these fibers leave small quantities of powder remnants on fingers if they were rubbed. This must be an indication of the presence of loose surface particles on these composite fibers and it might have an effect on the high rate of the observed weight loss in these samples. No such behavior was observed on any other composite fibers.

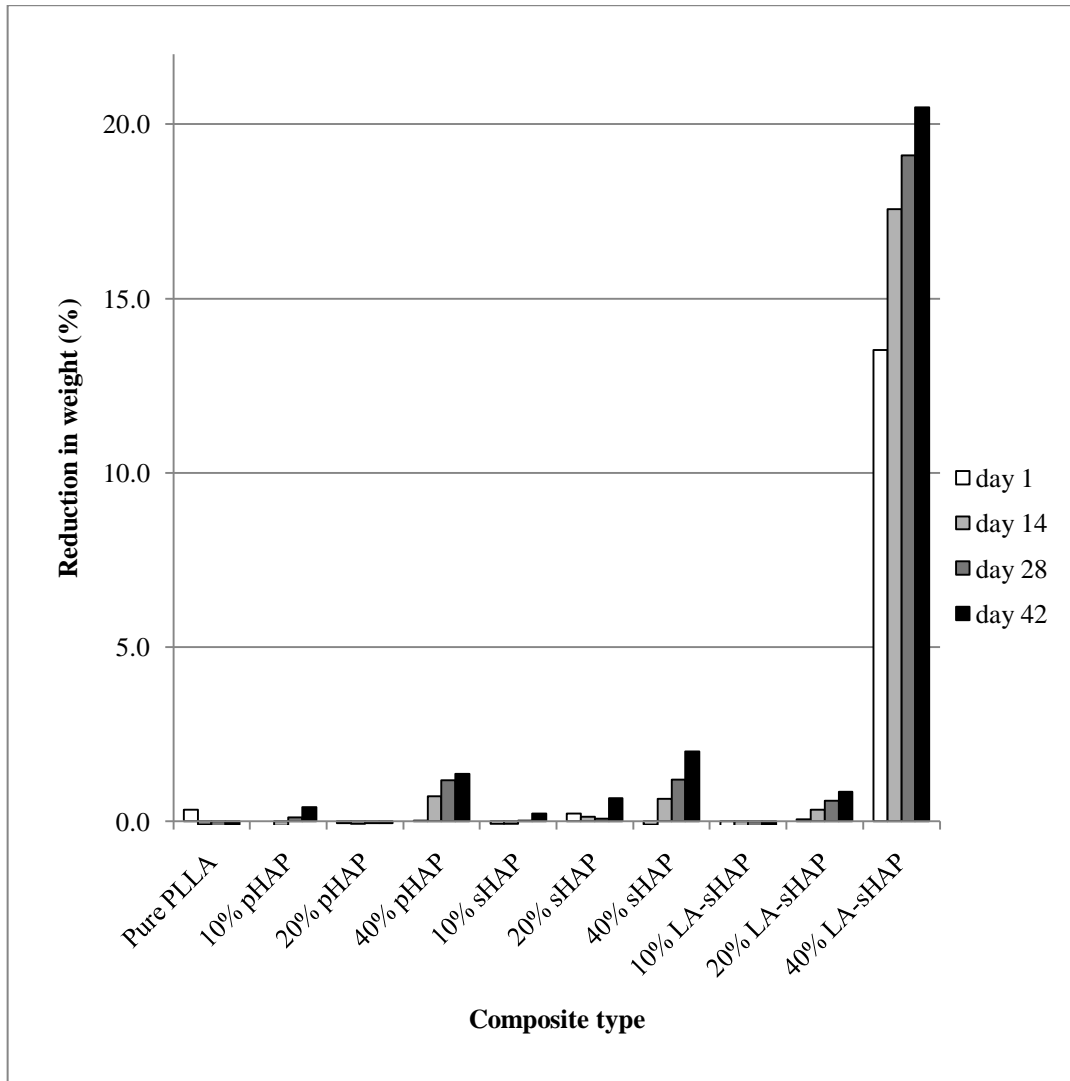


Figure 3.19. Reduction (%) in weights of composites in PBS during 42 days of *in situ* incubation. pHAp: commercial amorphous HAP nanoparticles; sHAP: non-grafted synthesized HAP nanorods; laHAP: lactic acid grafted synthesized HAP nanorods.

3.6. Production of Fiber Reinforced PLLA Bone Plates

Possibility of use of the produced PLLA – HAP composite fibers as reinforcement in bone plate production was investigated within the study. For this, plates were

produced using compression molding with a hot press with the help of a custom-design heated block with a mold having inner dimensions of 50 mm x10 mm x 3 mm. PLLA powder was put in the mold and after heat and pressure application, PLLA bone plates were obtained in dimensions of the mold. In some of the plates, pure PLLA or PLLA-HAP composite fibers were sandwiched so as to obtain one or two layers of 8 fibers (50 mm lengths) buried within the plate for reinforcement. In these reinforcement experiments, 30% HAP containing composite fibers were used based on the observation that this ratio showed the best mechanical properties.

A plate with one layer of 8 such composite rods is seen in Figure 3.20.

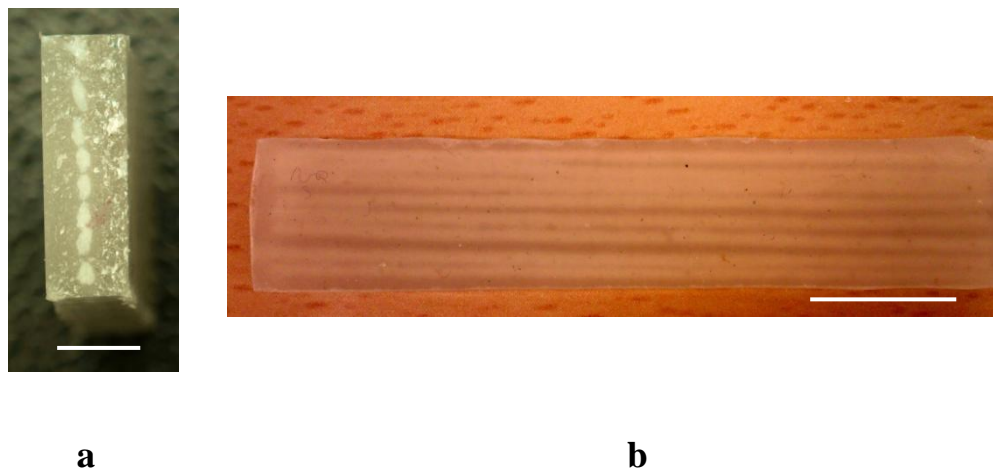


Figure 3.20. PLLA bone plate reinforced with 8 PLLA-HAP composite fibers. a) Cross sectional view (scale bar: 3 mm), b) top view (scale bar: 1 cm).

The bone plates obtained were cut using a circular electrical saw into two to yield $25 \times 10 \times 3 \text{ mm}^3$ samples for compression testing. The mechanical properties of these plates are shown in Table 3.5. From the Table 3.5 a, it is seen that incorporation of

composite rods affected slightly the Young's Modulus values where the highest increase were observed with the plates containing non-grafted HAP (sHAP) nanorods with a ca. 4% increase in the value (from 1.26 GPa of non-reinforced plate to 1.31 GPa of plate reinforced with 16x nHAP fibers). In a similar way, UTS values were also very slightly affected by the incorporation of composite fibers. Unexpectedly, incorporation of LA grafted HAP (LA-sHAP) containing composite fibers into the plates decreased the UTS values significantly from ca. 109.8 MPa to ca. 63.1 MPa and 76.4 MPa with 8x or 16x fiber addition, respectively. This seemed to be a result of the fact that the surface of 30% LA grafted HAP containing composite fibers were somehow loose, just as in the case with composite fibers containing 40% of the same HAP species. Indeed, during compressive testing, the plates were seen to delaminate significantly in parallel to the long axis, starting from the point where the plate touches the mechanical tester's clamps. Such a delamination did not occur in the case of composites containing other types of HAPs.

Table 3.5. Mechanical properties of PLLA bone plates prepared with PLLA or PLLA-HAP composite fibers a) Young's Modulus, b) UTS.

(a) Sample	Young's Modulus (GPa)		
	No fiber	8x fibers	16x fibers
Plate without fiber reinforcement	1.26±0.04		
30% pHAP fiber reinforced		1.25±0.07	1.08±0.11
30% sHAP fiber reinforced		1.30±0.03	1.31±0.05
30% LA-sHAP fiber reinforced		1.23±0.06	1.21±0.04

(b) Sample	UTS (MPa)		
	No fiber	8x fibers	16x fibers
Plate without fiber reinforcement	109.8±6.1		
30% pHAP fiber reinforced		100.0±15.6	109.1±6.9
30% sHAP fiber reinforced		108.6±3.4	110.3±6.6
30% LA-sHAP fiber reinforced		63.1±14.4	76.4±18.0

3.7. *In Vitro* Evaluation of the Composite Fibers

Suitability of the produced composite fibers as a biocompatible implant was evaluated using rat bone marrow mesenchymal stem cells (MSC). During a course of 14 days, MSC proliferation was monitored for all the constructs prepared using PLLA or PLLA – HAP composite fibers. As seen in Figure 3.21, the cell numbers increased from day 7 to day 14 on all the construct types produced and tested. Despite the fact that minimum increase in the cell numbers was observed on the constructs produced from PLLA-only fibers, slightly lower than 20%, this is still in correlation with the literature that polymers belonging to the PLA family do support osteoblast proliferation (Ishaug *et al.*, 1996).

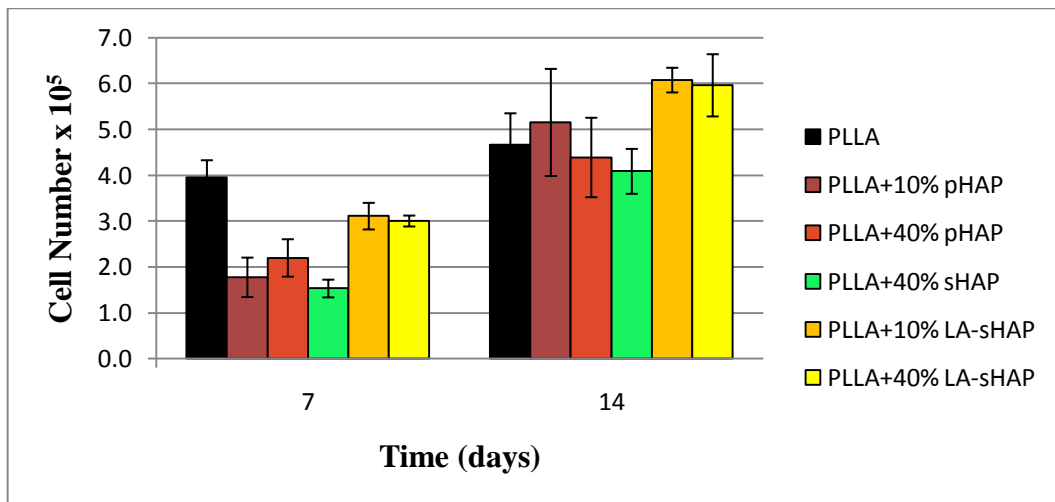


Figure 3.21. MSC proliferation on PLLA – HAP constructs (n=2).

In all the other constructs, there were some type of HAP within the structure and all of these supported a minimum 2-fold increase in cell numbers. The increase did not depend strictly on HAP content in the constructs so that presence of HAP seemed to be enough to enhance cell growth. Again, this is in agreement with the

literature where the presence of HAP molecules on the materials surfaces provides highly favorable attachment site to bone tissue cells (Ducheyne and Qiu, 1999).

Therefore, all the produced constructs were found to be favorable for attachment of osteoblasts, the bone synthesizing cells of the body. This property is a further advantage in terms of attraction of these cells to the injury site whenever the bone is fixed with a bone plate made of the materials studied in this work.

In order to determine the cell behavior and to qualitatively monitor cell attachment and spreading of cells on the constructs, samples were fixed 3 day after seeding and stained with FITC-labelled phalloidin and DAPI staining (Figure 3.22 a-d). It was observed that the cells attach well on the fiber surfaces of the scaffolds regardless of fiber type, PLLA or PLLA – HAP composite fibers. This is evident from the observation that cells showed very well elongated cytoskeletons in all types of fibers.

Spreading of cells on a support material provides information about the compatibility between the cell and the material. If chemical and/or physical properties of the material surface favor cellular attachment, then cells spread on the surface, maximizing the interaction with the material. Conversely, cells minimize contact with a non-favorable surface either by stretching over gaps or taking a spherical shape.

SEM micrographs revealed that 3 days after seeding, cells spread well on composite fibers containing any type of HAP, in any polymer to HAP ratio tested (Figures 3.24 - 3.26). Especially in Figure 3.25, direct contact of cellular protrusions on a HAP nanorod-rich region of the composite fiber is apparent. The nanorod-shaped HAP crystals were visible in the SEM (denoted as H) and their chemical identity was proven by EDS. In contrast to HAP containing composite fibers, both spread and normal cells were observed on HAP-free PLLA fiber/plates (Figure 3.23). This is in agreement with the cell proliferation studies which showed the minimum increase in cell numbers with HAP-free PLLA fibers/plates.

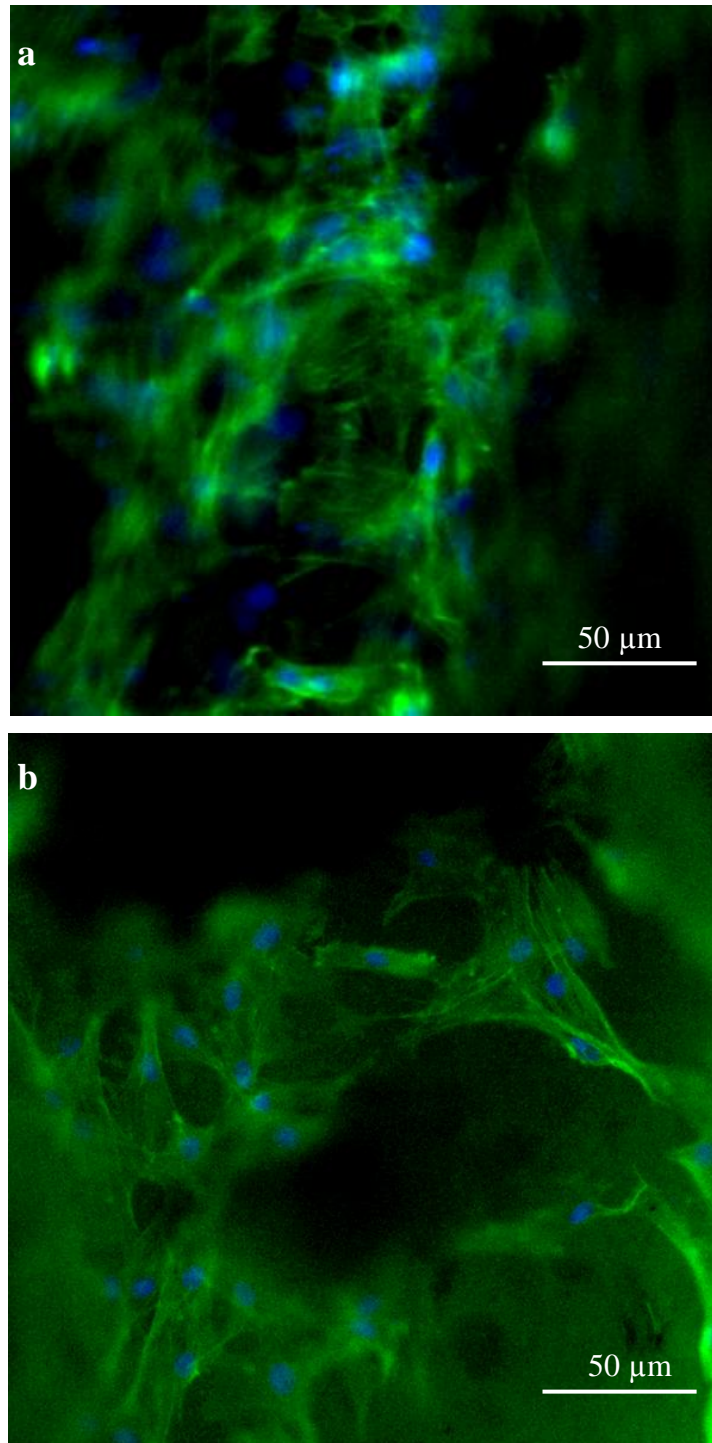


Figure 3.22. FITC-phalloidin for cytoskeleton (green) and DAPI for nucleus (blue) staining of cell after 3 days of seeding. Cells seeded on polymer/composite fibers produced from (a) PLLA, x10, (b) PLLA – 40% nmHAP, x10, (c) PLLA – 40% sHAP, x20, and (d) PLLA – 40% LA-sHAP, x10.

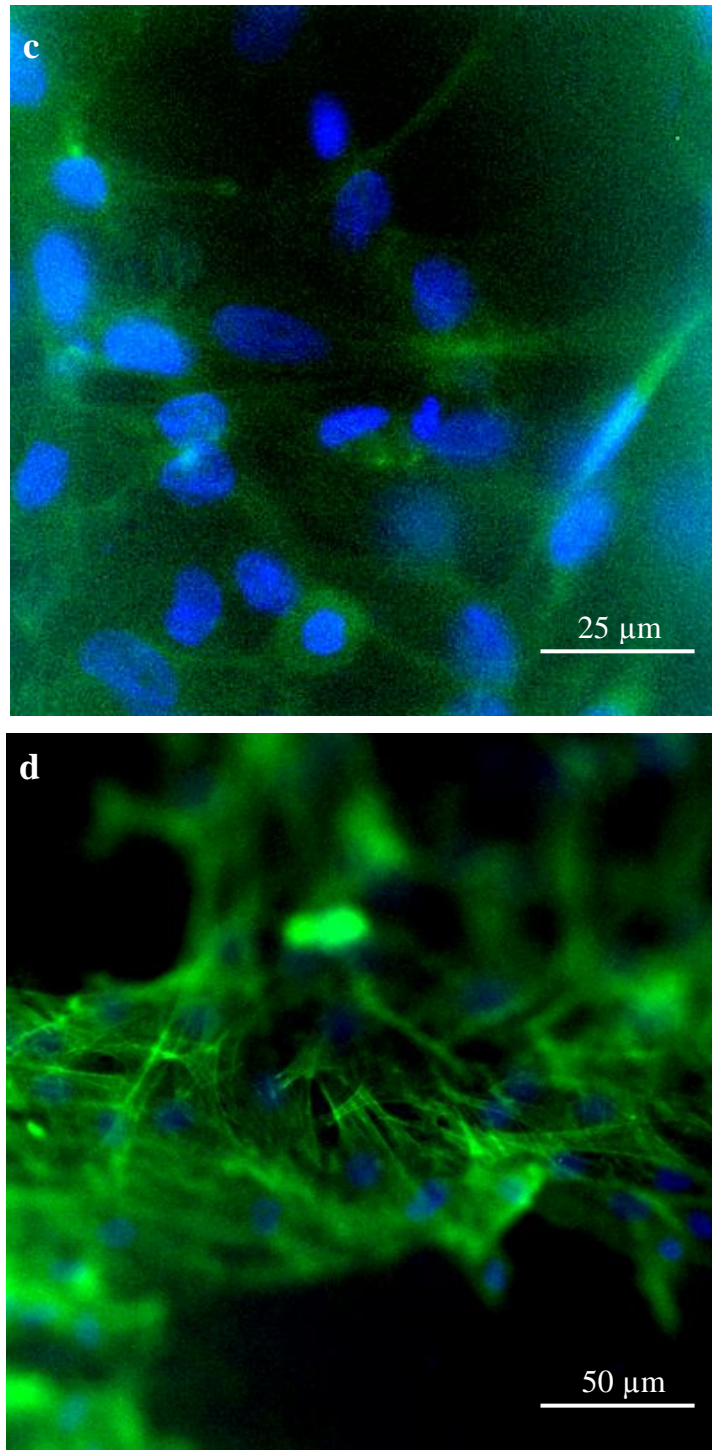


Figure 3.22 (continued). FITC-phalloidin for cytoskeleton (green) and DAPI for nucleus (blue) staining of cell after 3 days of seeding. Cells seeded on polymer/composite fibers produced from (a) PLLA, x10, (b) PLLA – 40% nmHAP, x10, (c) PLLA – 40% sHAP, x20, and (d) PLLA – 40% LA-sHAP, x10.

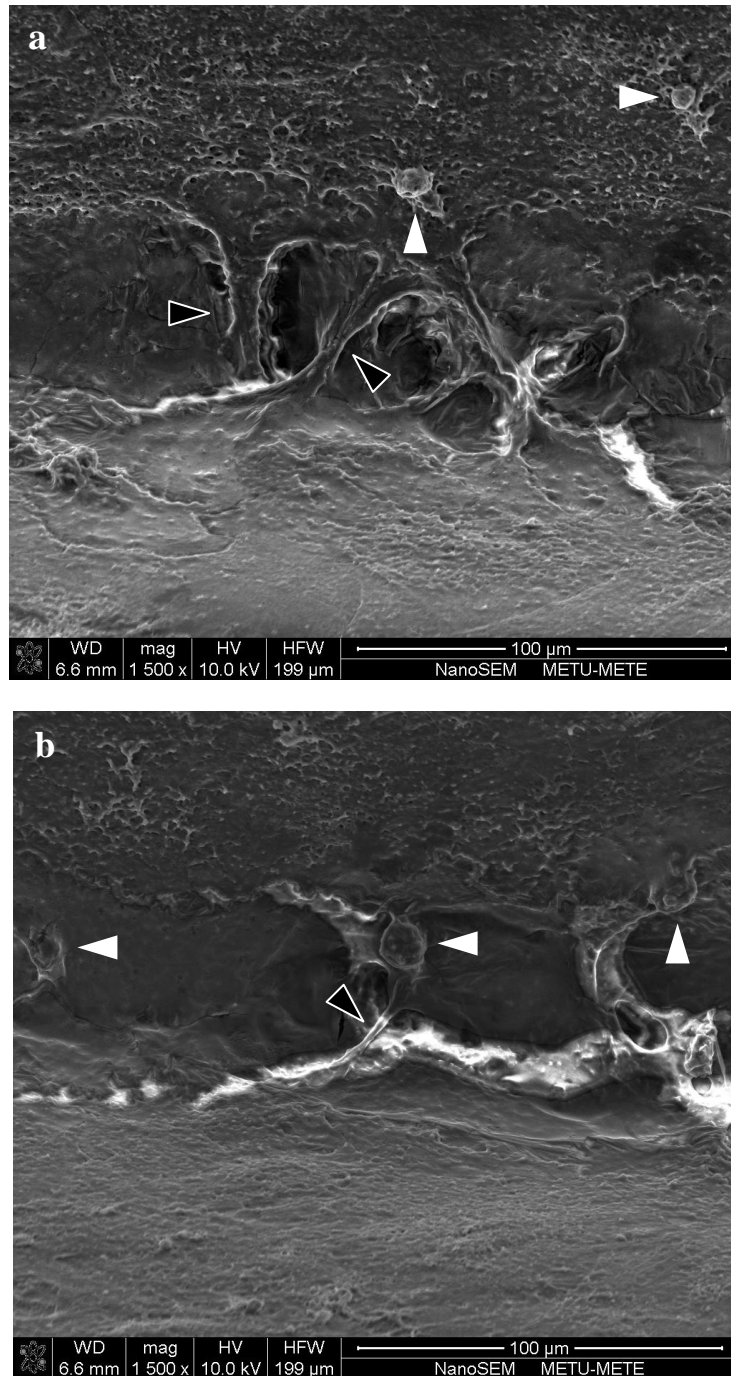


Figure 3.23. SEM micrographs of cells on PLLA fibers after 3 days of seeding. a and b shows two different regions on the same plate. White arrowheads show cells not spreaded. Black arrowheads show well spreaded cells. (both images x1500).

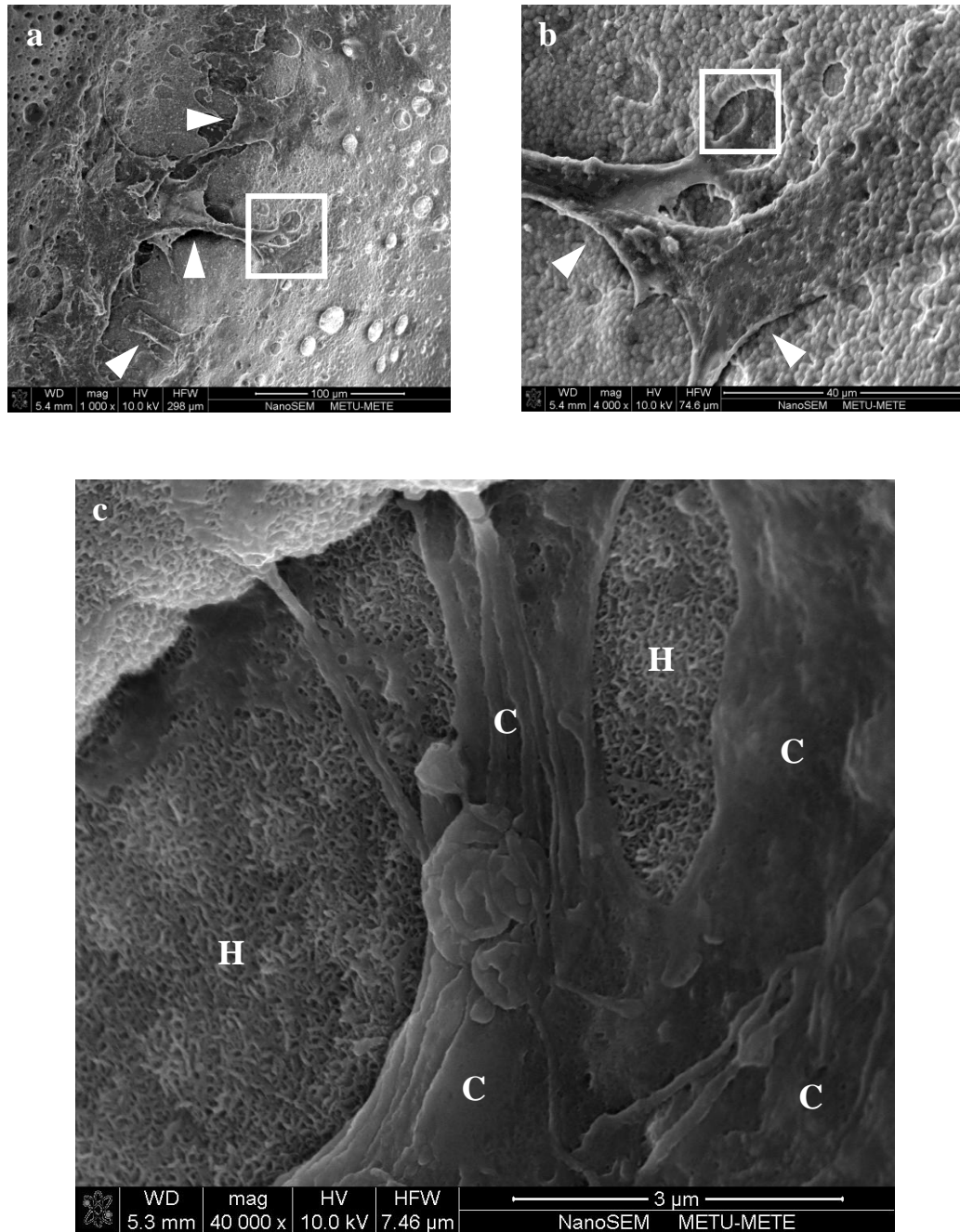


Figure 3.24. SEM micrographs of cells on 10% sHAP – PLLA fibers after 3 days of seeding. b and c shows higher magnified versions of the regions encircled with squares in a and b, respectively. Arrowheads show well spreaded cells, H: sHAP nanorods, C: parts of a cell. a) x1,500, b) x4,000, c) x40,000.

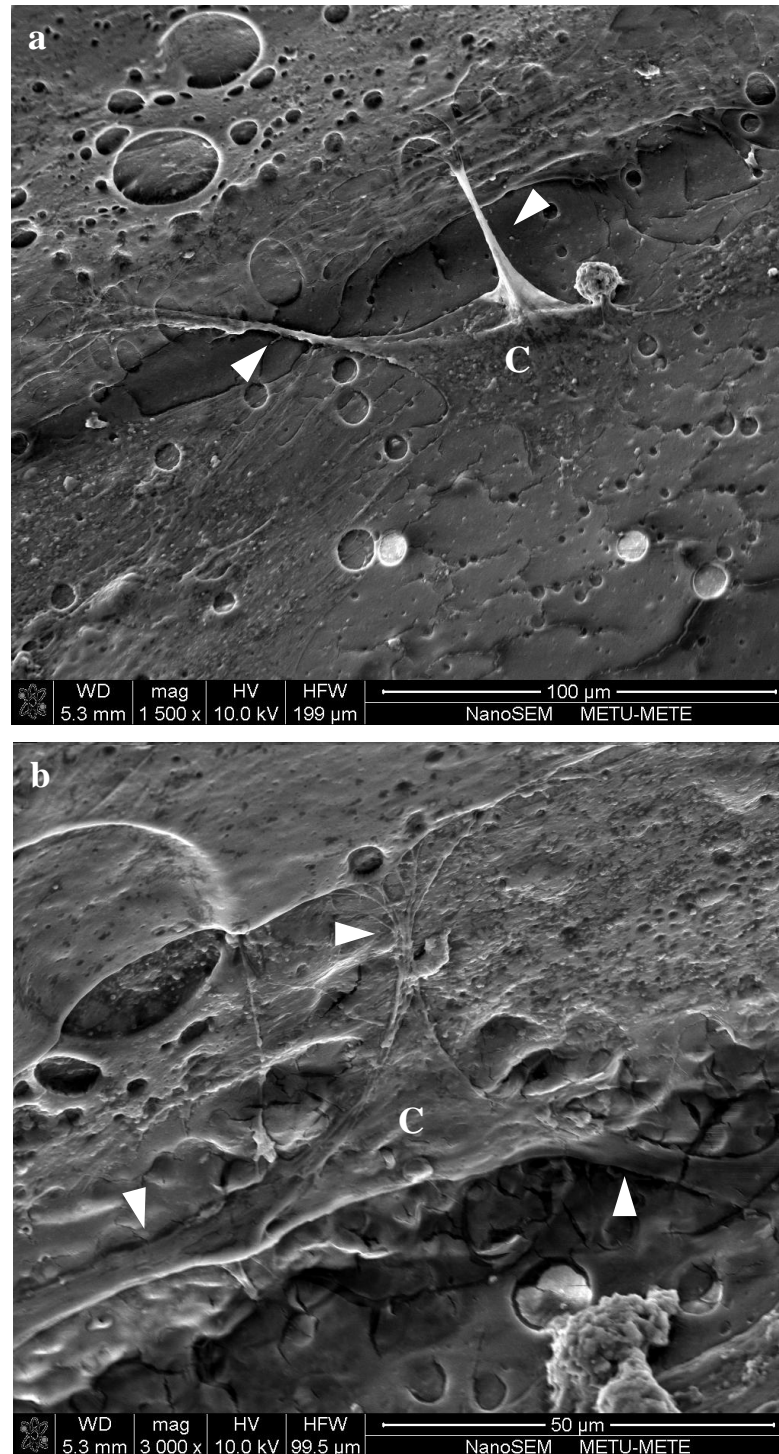


Figure 3.25. SEM micrographs of cells on 10% LA-sHAP – PLLA fibers after 3 days of seeding. a and b shows two different regions on the same plate. Arrowheads show protrusions of a well spreaded cell (C). a) x1,500, b) x3,000.

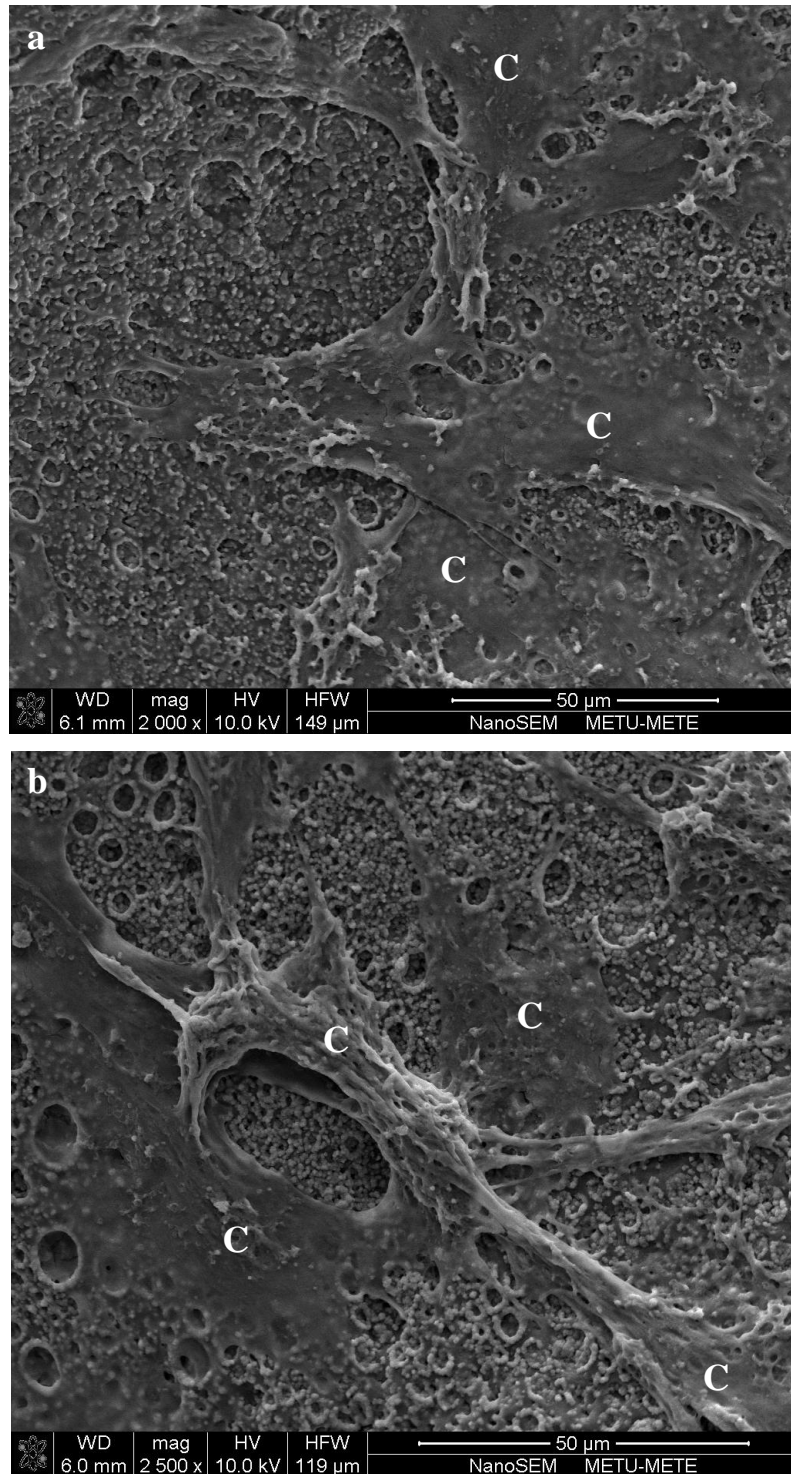


Figure 3.26. SEM micrographs of cells on 10% pHAP – PLLA fibers after 3 days of seeding. a and b shows two different regions on the same plate. C: well spreaded cell. a) x2,000, b) x2,500.

CHAPTER 4

CONCLUSIONS

Diaphyseal fractures are fractures that are through the shaft of long bone. These are common fracture patterns of the long bones, and the usual strategy to treat them is to fix the fracture site with non-degradable metallic bone plate in order to restrain movement of the fractured fragments. Bone plate transfers the compression force between bone fragments to support the body and protect the fracture area with proper alignment of the fragments throughout healing process. Elastic modulus of human cortical bone is in the range of 15–26 GPa, however, that of metals are 5 to 10 times higher than this value. This material modulus mismatch leads to a phenomenon known as "stress-shielding effect" - in which the metal plates provoke the decrease of bone mineral mass and occasionally cause bone refracture after the plate removal, which is a necessity as metals are not degradable in the body.

In this study, biodegradable polymer (PHBV or PLLA) – hydroxyapatite nanocomposite fibers were produced for use as reinforcements in polymeric bone plates and PLLA was found to have better mechanical properties and selected as the appropriate polymer for bone plate applications.

Hydroxyapatite nanorods with lengths of 50 – 150 nm and diameters of 5 – 20 nm were synthesized and used in the composites with the inspiration from the hydroxyapatite nanocrystals present in bones structure. The synthesized hydroxyapatite nanorods were aligned parallel to the long axis of the produced

composite fiber with the hypothesis that this longitudinal alignment could increase tensile and compressive properties of the fibers.

To achieve this, several solution and melt polymer based extrusion and injection methods were evaluated. Use of a simple extrusion technique with capillary rheometer for production of the composite fibers was found to be a successful approach in that composites produced with this instrument showed a degree of alignment of hydroxyapatite nanorods towards the longitudinal axis of composite fibers. The fibers produced with this method showed the best mechanical properties obtained throughout the study. Incorporation of 50% (w/w) hydroxyapatite nanoparticles increased the Young's Modulus value of pure polymeric fiber ca. 2.35 times (from 1.75 GPa to 4.12 GPa). The optimum hydroxyapatite loading was found to be 30% (w/w) that help increase of Young's Modulus value (from 1.75 GPa of pure polymeric fiber to 3.14 GPa) without sacrificing the ultimate tensile strength of the final composite (from 73.9 MPa of pure polymeric fiber to 50.4 MPa).

Furthermore, it was seen that chemically grafting these hydroxyapatites with lactic acid monomers of the bulk polymer PLLA in the composite had positive effects on mechanical properties of the composites loaded with these.

Effect of alignment on compressive strength could not be evaluated directly, due to the fiber geometry of the obtained composites, which was necessary for the alignment of HAP nanorods. As an indirect approach, these fibers were impregnated into polymeric plates so that long axis of both plates and fiber are parallel to each other. The fiber impregnated plates were compression tested along their long axis and up to 4% increase in the Young's Modulus was obtained, without any decrease in compressive strength. Even though the increase in Young's Modulus was not high (due to the low content of fibers in the final plates, up to ca. 16% w/w), this approach holds true in an effort for production biodegradable polymeric bone plates, of which the compressive mechanical values are designed to be close to that of cortical bones.

Degradation of obtained fibers resulted in composite fibers (except 40% composite HAP) that could maintain their mechanical properties for up to six weeks during degradation studies.

Biological compatibility of fibers was validated *in vitro* and it was observed that they provided a good attachment surface for osteoblasts. This is an advantage in that fractured bones fixed with such constructs could facilitate the attraction of bone forming osteoblasts into the defect area.

Future work:

Although the obtained enhancement in mechanical values was not dramatic in the final construct, increasing the content of these composite fibers within the final product would have the potential to reinforce any polymeric material to be used in hard tissue repair. As a next step, HAP nanorod lengths and number of composite fibers within the polymeric bone plates should be optimized to maximize the mechanical properties of the final plates.

REFERENCES

Alan BF, Elrod BF, McGuire DA, Paulos LE. Preliminary results of an absorbable interference screw. *Arthroscopy: The Journal of Arthroscopic & Related Surgery* 1995;11(5):537-548.

Allori AC, Sillon AM, Warren SM. Biological Basis of Bone Formation, Remodeling, and Repair- Part I: Biochemical Signaling Molecules. *Tissue Eng Part B* 2008;14(3):259-273.

Ananta Ortho Systems Pvt. Ltd., India. Accessed on 04-07-2010. Distal Radius with locked plating. www.indiamart.com/anantaortho/orthopedic-instruments.html.

Bakos D, Soldan B, Hernandez-Fuentes. Hydroxyapatite-collagen-hyaluronic acid composite. *Biomaterials* 1999;20:191-195.

Basmanav FB, Kose GT, Hasirci V. Sequential growth factor delivery from complexed microspheres for bone tissue engineering. *Biomaterials* 2008;29(32):4195-4202.

Bayston R, Nuradeen B, Ashraf W, Freeman BJC. Antibiotics for the eradication of *Propionibacterium acnes* biofilms in surgical infection. *J. Antimicrob Chemother* 2007;60:1298-1301.

Bell RB, Kindsfater CS. The use of biodegradable plates and screws to stabilize facial fractures. *J Oral Maxillofac Surg* 2006;64:31-9.

Bhardwaj R, Mohanty A, Drzal LT, Pourboghraat F, Misra M. Renewable Resource-Based Green Composites from Recycled Cellulose Fiber and Poly(3-hydroxybutyrate-co-3-hydroxyvalerate) Bioplastic. *Biomacromol* 2006;7:2044-2051.

Bohner M. Calcium orthophosphates in medicine: from ceramics to calcium phosphate cements. *Injury* 2000;31(4):D37-47.

Bronzino JD. *Biomedical engineering fundamentals*, CRC Press, 2006, pp40-13.

Brown SA, Mayor MB. The biocompatibility of materials for internal fixation of fractures. *Journal of Biomedical Materials Research* 1978;12:67-82.

Buckwalter JA, Glimcher MJ, Cooper RR, Recker R. Bone biology - Part II: Formation, form, modeling, remodeling, and regulation of cell function. *J Bone Joint Surg* 1995;77-A:1276-1283.

Burchardt H and Enneking WF. Transplantation of bone. *Surg Clin North Am* 1978;58:403-427.

Burg K.J.L., Porter S. and Kellam J.F. (2000) Biomaterial developments for bone tissue engineering. *Biomaterials* 21: 2347-2359.

Celsum Technologies, UK. Accessed on 04-07-2010. Eta 2100 Extrusion Rheometer System. <http://www.celsum.com/eta2100.htm>.

Chang MC, Ikoma T, Kikuchi M, Tanaka J. Preparation of a porous hydroxyapatite/collagen nanocomposite using glutaraldehyde as a crosslinkage agent. *J Mater Sci Lett* 2001;20:1199-1201.

Cheang P and Khor KA. Effect of particulate morphology on the tensile behaviour of polymer-hydroxyapatite composites. *Materials science and engineering A* 2003;345(1-2):47-54.

Chen H, Clarkson BH, Sun K, Mansfield J. Self-assembly of synthetic hydroxyapatite nanorods into an enamel prism-like structure. *J. Colloid and Interface Science* 2005;288:97-103.

Cheung LK, Chow LK, and Chiu WK. A randomized controlled trial of resorbable versus titanium fixation for orthognathic surgery. *Oral and maxillofacial surgery* 2004;98(4):386-97.

Chu TMG, Warden SJ, Turner CH, Stewart RL. Segmental bone regeneration using a load-bearing biodegradable carrier of bone morphogenetic protein-2. *Biomaterials* 2007;28(3): 459-467.

Cnet news. New surgical bone screw biodegrades in two years. Accessed on 15-06-2010. http://news.cnet.com/8301-27083_3-10461572-247.html?tag=mncol;title.

Coskun S, Korkusuz F, Hasirci V. Hydroxyapatite reinforced poly(3-hydroxybutyrate) and poly(3-hydroxybutyrate-co-3-hydroxyvalerate) based degradable composite bone plate. *J Biomater Sci, Polymer Edition* 2005;16(12):1485-1502.

Currey JD, Brear K, Zioupos P. The effects of aging and changes in mineral content in degrading the toughness of human femora. *J Biomech* 1996;29:257-260.

Danilchenko SN, Koropov AV, Protsenko IY, Sulkio-Cleff B, and Sukhodub LF. Thermal behavior of biogenic apatite crystals in bone: An X-ray diffraction study. *Cryst. Res. Technol* 2006;41(3):268–75.

D'Antonio, JA , Sutton, K. Ceramic materials as bearing surfaces for total hip arthroplasty. *J Am Acad Orthop Surg* 2009;17(2):63-68.

De Jonge LT, Leeuwenburgh SCG, Wolke JGC, Jansen JA. Organic-Inorganic Surface Modifications for Titanium Implant Surfaces. *Pharmaceut Res* 2008;25 (10):2357-2369.

Ducheyne P, Qiu Q. Bioactive ceramics: The effect of surface reactivity on bone formation and bone cell function. *Biomaterials* 1999;20:2287-303.

El-Rahman SSA. Neuropathology of aluminum toxicity in rats (glutamate and GABA impairment). *Pharmacol Res* 2003;47(3):189-94.

Emedicine. Middle Third Forearm Fractures: eMedicine Orthopedic Surgery. Accessed on 26-04-2010. <http://emedicine.medscape.com/article/1239870-overview>.

Emery DFG, Clarke HJ, Glover M. L. J. *Bone Joint Sug.* 1997;79(2):240.

Eppley, BL, Morales, L, Wood R, Pensler J, Goldstein J, Havlik RJ, Habal M, Losken A, Williams JK, Burstein F, Rozzelle A, Sadove AM. Resorbable PLLA-PGA Plate and Screw Fixation in Pediatric Craniofacial Surgery: Clinical Experience in 1883 Patients. *Plastic & Reconstructive Surgery* 2004;114(4):850-6.

Evans FG. The Mechanical properties of bone. *Artificial limbs* 1969; 13(1):37-48.

Ferreira BMP, Zavaglia CAC, Duek EAR. Thermal, morphologic and mechanical characterization of poly (L-lactic acid) / poly (hydroxybutyrate-co-hydroxyvalerate) blends. *Brazilian Journal of Biomedical Engineering* 2003;19(1):21-27.

Ficai A, Andronescu E, Trandafir V, Ghitulica C, Voicu G, ECollagen/hydroxyapatite composite obtained by electric field orientation. *Mater Lett* 2010;64(4):541-544.

Fleck C, Eifler D. Corrosion, fatigue and corrosion fatigue behaviour of metal implant materials, especially titanium alloys. *Int J Fatig* 2010;32(6):929-935.

Fujihara K, Teo K, Gopal R, Loh PL, Ganesh VK, Ramakrishna S, Foong KWC and Chew CL. Fibrous composite materials in dentistry and orthopaedics: review and applications. *Composites Science and Technology* 2004;64(6):775-88.

Fukada E and Ando Y. Piezoelectric properties of poly b-hydroxybutyrate and copolymers of b-hydroxybutyrate and b-hydroxyvalerate. *Int J Biol Macromol* 1986; 8:361-6.

Fukuda A. and Itabashi M. Simplified compression bending test method for advanced composites. *Composites: Part A* 1999;30:249–256.

Furukawa T, Matsusue Y, Yasunaga T, Shikinami Y, Okuno M, Nakamura T. Biodegradation behavior of ultra-high-strength hydroxyapatite/poly (L-lactide) composite rods for internal fixation of bone fractures. *Biomaterials* 2000;21:889-98.

General Principles of Internal Fixation: emedicine clinical procedures. Accessed on 04-07-2010. <http://emedicine.medscape.com/article/1269987-overview>.

Gu X, Zheng Y, Zhong S, Xi T, Wang J, Wang W. Corrosion of, and cellular responses to Mg–Zn–Ca bulk metallic glasses. *Biomaterials* 2009; doi:10.1016/j.biomaterials.2009.11.015.

Gu X, Zheng Y. A review on magnesium alloys as biodegradable materials. *Front Mater Sci China* 2010;4(2):111-115.

Hankermeyer CR ,Tjeerdema RS Polyhydroxybutyrate: plastic made and degraded by microorganisms. *Rev Environ Contam Toxicol.*1999;159:1-24.

Hänzi, AC, Gerber I, Schinhammer M, Löffler JF, Uggowitzer PJ. On the in vitro and in vivo degradation performance and biological response of new biodegradable Mg-Y-Zn alloys. *Acta Biomater* 2009; doi:10.1016/j.actbio.2009.10.008.

Hasirci V, Lewandrowski KU, Bondre SP, Gresser JD, Trantolo DJ, Wise DL. High strength bioresorbable bone plates: preparation, mechanical properties and in vitro analysis. *Biomed Mater Eng* 2000;10:19-29.

Hasirci V. and Yucel D. (2008) Polymers used in tissue engineering. In *Encyclopedia of Biomaterials and Biomedical engineering*, 2nd Edition. Edited by Wnek G.E. and Bowlin G.L. Informa Healthcare, USA.

Hauschka PV, Mavrakos AE, Iafrazi MD, Doleman SE, Klagsbrun M. Growth Factors in Bone Matrix. *J Biol Chem* 1986;261(27):12665-12674.

Hukins DWL. Bone stiffness explained by the liquid crystal model for the collagen fibril. *Journal of Theoretical Biology* 1978;71(4):661-667.

Hutchens SA, Benson RS, Evans BR, Rawn CJ, O'Neill H. A resorbable calcium-deficient hydroxyapatite hydrogel composite for osseous regeneration. *Cellulose* 2009;16:887-898.

Ishaug SL, Payne RG, Yaszemski MJ, Aufdemorte TB, Bizios R, Mikos AG. Osteoblast Migration on Poly(α -hydroxy esters). *Biotech Bioeng* 1996;50:443-451.

Jain R, Podworny N, Hupel TM, Weinberg J, Schemitsch EH. Influence of plate design on cortical bone perfusion and fracture healing in canine segmental tibial fractures. *J Orthop Trauma* 1999;13:178–86.

Jeil Medical Corporation, Korea. Accessed on 04-07-2010. Leforte System. http://jeilmed.en.ec21.com/GC00673860/CA01767811/Leforte_System.html.

Ji B, Gao H. Mechanical properties of nanostructure of biological materials. *Jornal of the Mechanics and Physics of Solids* 2004;52:1963-70.

Kalfas IH. Principles of bone healing. *Neurosurg Focus* 2001;10(4):1-4.

Katz J.L. (1996) Orthopedic applications. In *Biomaterials science, An introduction to materials in medicine*. Edited by Ratner B.D., Hoffmann A.S., Schoen F.J. and Lemons J.E. Academic Press.

Lewitus D, McCarthy S, Ophir A, Kenig S. The Effect of Nanoclays on the Properties of PLLA-modified Polymers Part 1: Mechanical and Thermal Properties. *J Polym Environ* 2006;14:171–177.

Keading C, Farr J, Kavanaugh T, Pedroza A. A prospective randomized comparison of bioabsorbable and titanium anterior cruciate ligament interference screws. *Arthroscopy* 2005;21(2):147–51.

Kikuchi M, Itoh S, Ichinose S, Shinomiya K, Tanaka J. Self organization mechanism in a bone-like hydroxyapatite/collagen nanocomposite synthesized in vitro and its biological reaction in vivo. *Biomaterials* 2001;22:1705-1711.

Kim YK, Yeo HH, Lim SC. Tissue response to titanium plates: a transmitted electron microscopic study. *J Oral Maxillofac Surg* 1997;55:322-326.

Konan S, Haddad FS. A clinical review of bioabsorbable interference screws and their adverse effects in anterior cruciate ligament reconstruction surgery. *The Knee* 2009;16:6-13.

Koosha F, Muller RH, Davis SS. Polyhydroxybutyrate as a drug carrier. *Crit Rev Therap Drug Carr Sys* 1989;6:117–30.

Kose GT, Kenar H, Hasirci N, Hasirci V. Macroporous poly (3-hydroxybutyrate-co-3-hydroxyvalerate) matrices for bone tissue engineering. *Biomaterials* 2003;24(11):1949–1958.

Kose GT, Korkusuz F, Ozkul A, Soysal Y, Ozdemir T, Yildiz C, Hasirci V. Tissue engineered cartilage on collagen and PHBV matrices. *Biomaterials* 2005;26:5187-97.

Ku C-H, Pioletti DP, Browne M, Gregson PJ. Effect of different Ti-6Al-4V surface treatments on osteoblasts behaviour. *Biomaterials* 2002;23(6):1447-54.

Laurencin C.T., Ambrosio A.M.A., Borden M.D. and Cooper J.A. (1999) Tissue engineering: Orthopedic applications. *Annual Reviews Biomedical Engineering* 01: 19-46.

Lee H.B., Khang G. and Lee J.H. (2003) Polymeric Biomaterials. In *Biomaterials: Principles and applications*. Edited by Park J.B. and Bronzino J.D. CRC Press.

LeGeros RZ. Calcium Phosphate-Based Osteoinductive Materials. *Chem Rev* 2008;108:4742-4753.

Li Z, Gu X, Lou S, Zheng Y. The development of binary Mg-Ca alloys for use as biodegradable materials within bone. *Biomaterials* 2008;29(10):1329-44.

Liao SS, Cui FZ, Zhang W, Feng QL. Hierarchically Biomimetic Bone Scaffold Materials: Nano-HA/Collagen/PLA Composite. *Biomed Mater Res Part B: Appl Biomater* 2004;69B:158-165.

Lim T.Y., Poh C.K. and Wang W. (2009) Poly (lactic-co-glycolic acid) as a controlled release delivery device. *Journal of materials science-materials in medicine*. 20: 1669-1675.

Ma CB, Francis K, Towers J, Irrgang J, Fu FH, Harner CH. Hamstring anterior cruciate ligament reconstruction: a comparison of bioabsorbable interference screw and endobutton-post fixation. *Arthroscopy* 2004;20(2):122-8.

Macarini L., Milillo P., Mocci A., Vinci R. and Ettorre G. C. (2008) Poly-L-lactic acid - hydroxyapatite (PLLA-HA) bioabsorbable interference screws for tibial graft fixation in anterior cruciate ligament (ACL) reconstruction surgery: MR evaluation of osteointegration and degradation features. *Radiologica Medica*, 113: 1185-1197.

Mathey M, Meier C, Luscher P, Mayer J, Wintermantel E and Koch B, A new intervertebral disc replacing biomaterial: open porous, hydroxyapatite filled polymethylmethacrylate, *Biomed Eng Appl Basis Comm* 1993;5(3):18-23.

Mathieu LM, Bourban PE, Manson J-AE. Processing of homogeneous ceramic/polymer blends for bioresorbable composites. *Compos Sci Technol* 2006;66(11-12):1606-1614.

McBride ED. Absorbable metal in bone surgery. *J Am Med Assoc* 1938;111:2464–7.

Meisenberg G, Simmons WH. *Principles of Medical Biochemistry* 2006, 2nd ed. St. Louis, Missouri, Mosby Inc.

Middleton J.C. and Tipton A.J. Synthetic biodegradable polymers as orthopedic devices. *Biomaterials* 2000;21:2335-2346.

Mine Y, Makihira S, Nikawa H, Murata H, Hosokawa R, Hiyama A and Mimura S. Impact of titanium ions on osteoblast-, osteoclast- and gingival epithelial-like cells. *J Prosthodont Res* 2010;54:1-6.

Mohanty AK, Misra M, Drzal LT. *Natural Fibers, Biopolymers and Biocomposites*, CRC Press, 2005, pp599-600.

Moon SM, Ingalthalika A, Highsmith JM, Vaccaro AR. Biomechanical rigidity of an all-polyetheretherketone anterior thoracolumbar spinal reconstruction construct: an in vitro corpectomy model. *Spine J* 2009;9(4):330-335.

Murugan R and Ramakrishna S Development of nanocomposites for bone grafting. *Composites Science and Technology* 2005;65:2385-406.

Murugan R, Ramakrishna S. Aqueous mediated synthesis of bioresorbable nanocrystalline hydroxyapatite. *Journal of Crystal Growth* 2005;274:209-213.

Nadella PH, Spruiell EJ, White LJ. Drawing and annealing of polypropylene fibers: Structural changes and mechanical properties. *J. Appl Polym Sci* 1978;18:3121.

Nagels J, StokdijkM, Rozing PM. Stress shielding and bone resorption in shoulder arthroplasty. *J Shoulder Elbow Surg* 2003;12:35-39.

Navarro M, Michiardi A, Castano O, Planell JA. Biomaterials in orthopaedics. *R Soc Interface* 2008;5:1137-1158.

Niinomi M. Metallic biomaterials. *J Artif Organs* 2008;11:105–110.

Paavolainen P, Karaharju E, Slatis P, Ahonen J, Holmstrom T. Effect of rigid plate fixation on structure and mineral content of cortical bone. *Clin Orthop Relat Res* 1978;136:287-293.

Park J. and Lakes R.S. (2007) *Biomaterials, An Introduction*. 3rd Edition. Park JB. *Biomaterials, an introduction*. Plenum Press, NY, 1979, pp105-109.

Park S-H., Llinas A., Goel V.K. and Keller J. C. (2003) Hard tissue replacements. In *Biomaterials: Principles and applications*. Edited by Park J.B. and Bronzino J.D. CRC Press.

Pietrzak WS, Lessek TP and Perns SV. A bioabsorbable fixation implant for use in proximal interphalangeal joint (hammer toe) arthrodesis: biomechanical testing in a synthetic bone substrate. *J foot ankle surg* 2006;45(5):288-294.

Pouton CW, Akhtar S. Biosynthetic polyhydroxyalkanoates and their potential in drug delivery. *Adv drug del rev* 1996;18:133–62.

Qiu X, Hong Z, Hu J, Chen I, Chen x, and Jing X. Hydroxyapatite surface modified by L-lactic acid and its subsequent grafting polymerization of L-lactide. *Biomacromolecules* 2005;6:1193-1199.

Ramakrishna S, mayer J, Wintermantel E, Leong KM. Biomedical application of polymer-composite material: a review. *Compos sci technol* 2001;61:1189-1224.

Ramay HRR and Zhang M. Biphasic calcium phosphate nanocomposite porous scaffolds for load-bearing bone tissue engineering. *Biomaterials* 2004;25:5171-5180.

Reilly DT and Burstein AH. The elastic and ultimate properties of compact bone tissue. *J. Biomechanics* 1975;8:393-405.

Rho JY, Kuhn-Spearing L, Zioupos P. Mechanical properties and the hierarchical structure of bone. *Medical Engineering & Physics* 1998;20:92-102.

Rizzi SC, Heath DJ, Coombes AGA, Bock N, Textor M, Downes S. Biodegradable polymer/hydroxyapatite composites: Surface analysis and initial attachment of human osteoblasts. *J Biomed Mater Res.* 2001;55:475-486.

Roeder RK, Converse GL, Kane RJ, Yue W. Hydroxyapatite-reinforced polymer biocomposites for synthetic bone substitutes. *JOM* 2008;60(3):38–45.

Ruhe P.Q., Hedberg E.L., and Padron N.T.(2005) Biocompatibility and degradation of poly(DL-lactic-co-glycolic acid)/calcium phosphate cement composites. *Journal of biomedical materials research part a.* 74A: 533-544.

Sabir M.I., Xu X. and Li L. (2009) A review on biodegradable polymeric materials for bone tissue engineering applications. *Journal of Materials Science* 44: 5713-5724.

Sasaki CT, Marotta JC, Lowlicht RA, Ross DA, Johnson M. Efficacy of resorbable plates for reduction and stabilization of laryngeal fractures. *Ann Otol Rhinol Laryngol* 2003;112(9 Pt 1):745-750.

Science Museum, UK. Accessed on 04-07-2010. Bone plate to repair fractures. <http://www.sciencemuseum.org.uk/broughttolife/objects/display.aspx?id=5826>

Skrtic D, Antonucci JM, Eanes ED. Amorphous calcium phosphate-based bioactive polymeric composites for mineralized tissue regeneration. *J Res Natl Inst Stand Technol* 2003;108:167-182.

Song G, Atrens A. Understanding magnesium corrosion-a framework for improved alloy performance. *Adv Eng Mater* 2003;5(12):837-858.

Staiger MP, Pietak AM, Huadmai J, Dias G. Magnesium and its alloys as orthopedic biomaterials: A review. *Biomaterials* 2006;27:1728-1734.

Steele DG and Bramblett CA. *The Anatomy and biology of the human skeleton*. Texas A&M University Press, TX, 1998, pp4.

Suchanek WL, Yoshimura M. Processing and properties of hydroxyapatite-based biomaterials for use as hard tissue replacement implants. *J Mater Res* 1998;13:94-117.

Sun ZL, Wataha JC, Hanks CT. Effects of metal ions on osteoblast-like cell metabolism and differentiation. *Journal of Biomedical Materials Research* 1997; 34:29-37.

Sutherland D and Bostrom M. *Grafts and Bone Graft Substitutes, from Bone regeneration and Repair: Biology and Clinical Applications*. Ed. Lieberman JB and Friedlaender GE. Humana Press, USA, 2005, pp133-156.

Synthes Corp., USA, Synthes North America-Products. Accessed on 04-07-2010. <http://us.synthes.com/Products/Biomaterials/Resorbable+Fixation/>.

Tapiero H, Tew KD. Trace elements in human physiology and pathology: zinc and metallothioneins. *Biomed Pharmacother* 2003;57(9):399-411.

Thomas MV, Puleo DA, Al-Sabbagh M. Bioactive glass three decades on. *J Long-Term Eff Med* 2005;15(6):585-597.

Thomson RC, Ak S, Yaszemski MJ, Mikos AG. *Principles of tissue engineering*. Academic Press, NY. 2000, pp251.

Uthoff H.K., Poitras P. and Backman D.S. (2006) Internal plate fixation of fractures: short history and recent developments. *Journal of Orthopedics Science*, 11: 118-126.

Uthoff HK, Poitras P, and Backman DS. Internal plate fixation of fractures: short history and recent developments. *J Orthop Sci* 2006;11:118-26.

Vaccaro AR, Venger BH, Kelleher PM, Singh K, Carrino JA, Albert T, Hilibrand A. Use of a bioabsorbable anterior cervical plate in the treatment of cervical degenerative and traumatic disk disruption. *Orthopedics* 2002;25(10):1191-1199.

Visser S.A., Hergenrother R.W. and Cooper S.L. Polymers. In Biomaterials science, An introduction to materials in medicine. Edited by Ratner B.D., Hoffmann A.S., Schoen F.J. and Lemons J.E. Academic Press, 1996.

Wang F, Li MS, Lu YP, Qi YX, Lui YX. Synthesis and microstructure of hydroxyapatite nanofibers synthesized at 37°C. *Materials Chemistry and Physics* 2006;95:145-149.

Webster TJ., Nanophase ceramics as improved bone tissue engineering materials. *Am Ceramic Soc. Bull.* 2003;82(6):1-8.

Weiner S and Wagner HD. The material bone: Structure-mechanical function relations. *Annu. Rev. Mater. Sci.* 1998. 28:271-98.

Weiner S and, Traub W. Bone structure: from angstroms to microns. *FASEB* 1992;6:879-85.

Weir NA, Buchanan FJ, Orr JF, Dickson GR. Degradation of poly-L-lactide. Part 1: in vitro and in vivo physiological temperature degradation. *Proc Institut Mech Eng, Part H: Journal of Engineering in Medicine* 2004;218(5):307-319.

Witte F, Kaese V, Haferkamp H, Switzer E, Meyer-Lindenberg A, Wirtha CJ, Windhagen H. In vivo corrosion of four magnesium alloys and the associated bone response. *Biomaterials* 2005;26:3557-3563.

Wolff J. The Law of Bone Remodelling. Originally published in 1892, translated to english by Maquet P, Furlong R. Berlin: Springer-Verlag, 1986.

Wood GD. Inion biodegradable plates: The first century. *British Journal of Oral and Maxillofacial Surgery* 2006;44:38-41.

Wu C, Sassa K, Iwai K, Asai S. Unidirectionally oriented hydroxyapatite/collagen composite fabricated by using a high magnetic field. *Mater Lett* 2007;61:1567-1571.

Xu LP, Yu GN, Zhang E, Pan F, Yang K. In vivo corrosion behavior of Mg-Mn-Zn alloy for bone implant application. *J Biomed Mater Res A* 2007;83A(3):703-711.

Yang W, Zhang P, Liu J, Xue Y. Effect of long-term intake of Y³⁺ in drinking water on gene expression in brains of rats. *J Rare Earth* 2006;24(3):369-73.

Yaremchuk MJ, Posnick JC. Resolving controversies related to plate and screw fixation in the growing craniofacial skeleton. *J Craniofac Surg* 1995;6:525-538.

Yaszemski MJ, Payne RF, Hayes WC, Lander R, Mikos AG. Evolution of bone transplantation: molecular, cellular and tissue strategies to engineer human bone. *Biomaterials* 1996;17:175-185.

Yerit KC, Enislidis G, Schopper C, Turhani D, Wanschitz F, Wagner A, Watzinger F, Ewers R. Fixation of mandibular fractures with biodegradable plates and screws. *Oral and maxillofacial surgery* 2002;94(3):294-300.

Yilgor P, Tuzlakoglu K, Reis RL, Hasirci N, Hasirci V. Incorporation of a sequential BMP-2/BMP-7 delivery system into chitosan-based scaffolds for bone tissue engineering. *Biomaterials* 2009;30(21):3551-3559.

Yu L, Liu H, Xie F, Chen L, Li X. Effect of annealing and orientation on microstructures and mechanical properties of polylactic acid. *Polymer Engineering and Science* 2008;48(4):634-641.

Yubao L, De Wijn J, Klein CPAT, Van Der Meer S. Preparation and characterization of nanograde osteoapatite-like rod crystals. *Journal of Materials Science: Materials in Medicine* 1995;5:252-255.

Yumiko N, Yukari T, Yasuhide T, Tadashi S, Yoshio I. Differences in behavior among the chlorides of seven rare earth elements administered intravenously to rats. *Fundam Appl Toxicol* 1997;37:106-116.

Zberg B, Uggowitzer PJ, and Löffler JF. MgZnCa glasses without clinically observable hydrogen evolution for biodegradable implants. *Nature Materials* 2009;8:887-891.

Zhang H, Yang G, Wang X, Shao H, Hu X. Study on the melt-spinnability of poly(L-lactic acid). *Polym eng sci* 2009; 49: 2315-2319.

Zhang S, Zhang X, Zhao C, Li J, Song Y, Xie C, Tao H, Zhang Y, He Y, Jiang Y, Bian Y. Research on an Mg–Zn alloy as a degradable biomaterial. *Acta Biomater* 2009: doi:10.1016/j.actbio.2009.06.028.

APPENDIX A

CALIBRATION CURVE FOR CELL NUMBER DETERMINATION

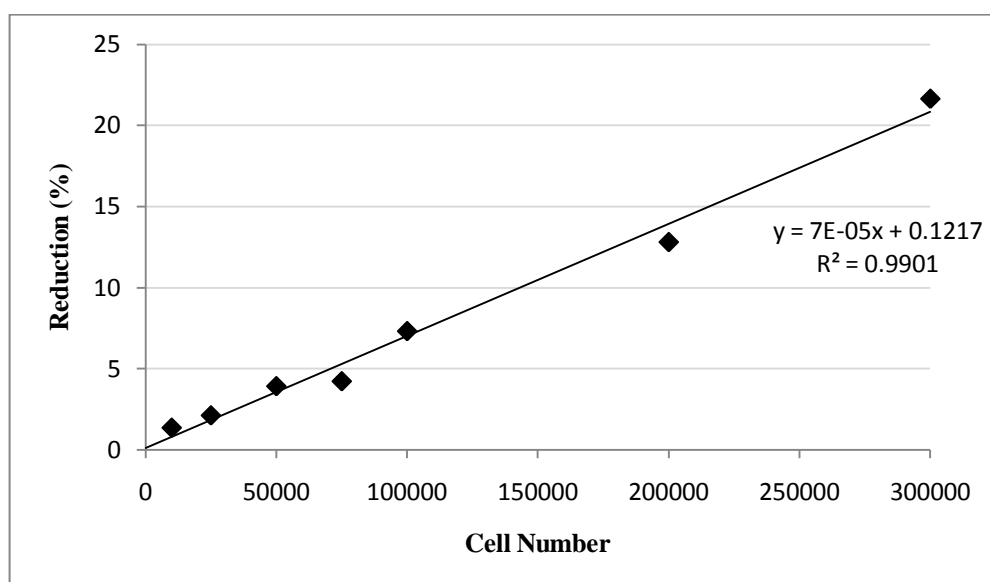


Figure A.1. Calibration curve of rat bone marrow mesenchymal stem cells for Alamar Blue Assay.

CURRICULUM VITAE

PERSONAL INFORMATION

Surname, Name: Aydın, Erkin

Nationality: Turkish

Date and Place of Birth: 01 January 1978, Ankara

Marital Status: Married with a son.

e-mail: erkin.aydin.1@gmail.com

EDUCATION

Degree	Institution	Year of Graduation
M.Sc.	METU Biochemistry	2002
B.S.	METU Biology	1999
High School	Kuşadası Kaya Aldoğan Lisesi	1994

WORK EXPERIENCE

Year	Place	Enrollment
2000-2010	METU Department of Food Engineering	Research Assistant
2000-July- August	Akıncı Clinical Biochemistry Laboratory	Biologist
1998 July	Ankara Numune Hospital	Intern Student

FOREIGN LANGUAGES

Advanced English

PUBLICATIONS

1. Shokouhi, B, Coban C, Hasirci V, Aydin E, Dhanasingh A, Shi N, Koyama S, Akira S, Zenke M, Sechi AS. The role of multiple toll-like receptor signalling cascades on interactions between biomedical polymers and dendritic cells. *Biomaterials* 2010;31(22):5759-5771.
2. Hasirci V, Vrana E, Zorlutuna P, Ndreu A, Yilgor P, Basmanav B, and Aydin E. Nanobiomaterials: a review of the existing science and technology, and new approaches. *J. Biomater. Sci. Polymer Edn.* 2006;17(11):1241-1268.